Title	全二重無線ネットワークのための効率的な協調中継媒体アクセス制御フレームワーク
Author(s)	KHUN, AUNG THURA PHYO
Citation	
Issue Date	2023-06
Type	Thesis or Dissertation
Text version	ETD
URL	http://hdl.handle.net/10119/18703
Rights	
Description	Supervisor:リム 勇仁, 先端科学技術研究科, 博士

Doctoral Dissertation

Efficient Cooperative Relaying Medium Access Control Framework for Full-duplex Wireless Networks

KHUN Aung Thura Phyo

Supervisor: LIM Yuto

Graduate School of Advanced Science and Technology
Japan Advanced Institute of Science and Technology
[Information Science]

June, 2023

Efficient Cooperative Relaying Medium Access Control Framework for Full-duplex Wireless Networks

by

KHUN Aung Thura Phyo

submitted to
Japan Advanced Institute of Science and Technology
in partial fulfillment of the requirements
for the degree of

Doctor of Philosophy

Supervisor: LIM Yuto

School of Information Science

Division of Advanced Science and Technology

Japan Advanced Institute of Science and Technology

June, 2023

Abstract

Fifth-generation (5G) mobile communication system has been commercialized worldwide. Now, academia and industrial research organizations are moving forward to investigate the next mobile communication system, i.e., beyond 5G or six-generation (6G). Besides, 6G is also expected to play a central role in the Internet society changing from an Information Society 4.0 to a Super-smart Society 5.0. The progress of technology and the development of society in the communication environment is bringing the explosive growth of mobile devices and traffic connections. As a result, the capacity demand becomes a potential problem for efficient and effective communication in the future wireless network due to the limited wireless spectrum resources. To meet these requirements, the 6G is expected to support massive connectivity with extremely high data rate/capacity low latency, and high reliability. 3GPP Release 18 also investigates the possibility of performing uplink and downlink transmission simultaneously within the available TDD band in order to use the flexible spectrum. As one of the potential research interests in 6G, the full-duplex (FD) system with the characteristics of simultaneous data transmission and reception over a single channel has gained attention because of its ability to efficiently utilize the spectrum. This dissertation investigates the potential benefit of the FD system in providing efficient and effective communication through multihop wireless transmission and addressing the capacity demand of the future wireless network.

In this dissertation, the target problem of capacity demand for efficient and effective communication is approached by focusing on the three key issues of inefficient network capacity, ineffective transmit power control and inefficacious resource allocation in the multihop wireless network environment. Extensive research has been done in FD systems with or without the relaying strategy, focusing on simultaneous transmission to increase transmission capacity. However, more research work is still required consideration to truly achieve the potential benefit of the FD system. This dissertation investigates different approaches to the FD system to achieve efficient data communication for future wireless networks. The efficient and effective communication in this dissertation refers to communication with optimum transmission capacity, low interference, and high resource utilization, even in a dense network environment.

This dissertation develops a cooperative relaying medium access control (coreMAC) framework for the FD wireless networks. The coreMAC framework is conceptualized from the cooperative communication strategies, i.e., transmission strategy, relaying strategy, and allocation strategy. The proposed framework provides efficient communication through three schemes: a mixture of concurrent and sequential transmission (MCST) scheme, optimal achievable transmission capacity (OATC) scheme, and channel interference balancing allocation (CIBA) scheme.

The MCST scheme is designed for transmission capacity optimization in multihop wireless networks. MCST is the first transmission scheme to support the combination of both sequential and concurrent transmissions in a single timeslot in terms of spatial reuse mechanism. MCST scheme is proposed as the capacity management module to address the issue of inefficient network capacity management in the wireless network. Besides, an FD medium access control (MAC) protocol is proposed as FD-MCST to assist the MCST scheme.

As the second scheme, the OATC scheme is proposed to extend the MCST scheme to minimize interference and optimize transmission capacity. The OATC scheme is conceptualized by considering the temporal reuse mechanism with the MCST scheme and the spatial reuse mechanism with the TPC technique. The proposed OATC scheme acts as a power management module to address the second issue of ineffective transmit power control for effective communication.

Then, the CIBA scheme is designed to investigate the FD transmission capacity through interference mitigation via channel allocation in the multi-channel multihop wireless networks. The CIBA scheme reduces the interference by allocating nearby transmissions into different sub-channels and optimizes the transmission capacity. In this way, CIBA works as the resource management module and represents the possible solution to the inefficacious resource allocation management of future wireless networks.

The performance of the proposed three schemes of the coreMAC framework is evaluated through numerical simulations written in MATLAB programming with different simulation scenarios. The performance evaluation is mainly compared in terms of the achievable network capacity, throughput, transmission overhead, and total interference power of existing MAC protocols. The numerical simulation results can be summarized

as follows:

- The FD-MCST achieves 1.7 times and nearly two times improvement in achievable network capacity and achievable throughput, respectively, compared to existing MAC protocols in FD wireless networks.
- The OATC scheme shows a higher achievable network capacity with minimum interference power and around 56% improvement in achievable throughput.
- The multi-channel allocation scheme reduces the total interference power and optimizes the achievable network capacity compared to the single-channel allocation scheme in the FD wireless networks. Furthermore, in the multi-channel multihop wireless networks, the CIBA scheme accomplishes lower total interference power and higher achievable network capacity than the fixed multi-channel allocation schemes.

In this dissertation, the framework is proposed in the data link layer of the TCP/IP protocol. Through the three schemes, the proposed framework results in higher transmission capacity, higher achievable network capacity, higher achievable throughput, and lower achievable transmission latency and overhead. Furthermore, the proposed framework accomplishes lower transmission latency and higher achievable throughput that affect the transport layer protocol performance, which will benefit the quality of service for specified applications such as auto-driving cars and unmanned aerial vehicles.

Keywords: Capacity optimization, Interference mitigation, Interference-aware channel allocation, Cooperative communication strategies, Full-duplex system

Acknowledgement

Foremost, I would like to express my deepest gratitude to my supervisor, Associate Professor **LIM Yuto** for his invaluable guidance. His sincerity and supervision have deeply inspired me a lot, his supervision gives me lots of motivation and his high generosity was a big help to make my enjoyable time in Japan, especially at JAIST. Additionally, this endeavor would not have been possible without the generous support from Professor **TAN Yasuo**, the respectful second supervisor, and the defense examiner.

I would like to extend my sincere thanks to Professor **KANEKO Mineo**, the advisor for the Internship, for his invaluable patience and guidance. Besides, I am also thankful to Dr. **SHAN Lin**, supervisor of the Internship, for his kindness during the Internship at the Wireless Network Research Center, Wireless Systems Laboratory, National Institute of Information and Communications Technology (NICT), Japan.

Words cannot express my gratitude to my defense examiners, Professor **BEURAN Razvan Florin**, Dr. **KUCERA Stepan** and Professor **OKADA Hiraku**. I could not have undertaken this PhD journey without their support. What is more, I'm extremely grateful to the generous support from IUCHI Asia Students Memorial Foundation and Doctoral Research Fellow (DRF), who financed my education. Their support helped me a lot to continue my research.

I am also grateful to my classmates, lab mates, and researchers from TAN Laboratory and WiSE Laboratory (LIM Laboratory), for their kind support and sharing in collaboration meetings. With their friendliness, my life in JAIST was fun every day. Then, I would like to thank unknown significant others (USO) who help me directly and/or indirectly to complete my study.

Last but not least, I would be remiss in not mentioning my family for their belief and letting me find my own self in education.

Contents

List of Figures

List of Tables

List of Abbreviations

1G First-generation mobile communication system

5G Fifth-generation mobile communication system

6G Sixth-generation mobile communication system

ACK Acknowledgement

ADC Analog-to-Digital Converter

AI Artificial Intelligence

ANS LoRa Answer

BRF Basic Relaying Flow

CAGR Compound Annual Growth Rate

CCI Co-Channel Interference

CIBA Channel Interference Balancing Allocation

coreMAC Cooperative Relaying Medium Access Control

CSI Channel State Information

CSMA Carrier-Sense Multiple Access

CSMA/CA Carrier-Sense Multiple Access with Collision Avoidance

CSMA/LoRa LoRAWAN MAC based on the CSMA mechanism

CT Concurrent Transmission

CTPC Consensus Transmit Power Control

CTS Clear-To-Send

D Destination

D2D Device-to-device

dB Decibel

DCF Distributed Coordination Function

DIFS DCF Interframe Space

DTPC Distributed Transmit Power Control

EB Exabytes

eMBB Enhanced Mobile Broadband

FCTS Full-duplex Clear-to-Send

FD Full-duplex

FD-DMAC FD Distributed MAC

FD-MCST FD MAC protocol with MCST scheme

FDD Frequency Division Duplexing

FMMC Fault Management Framework based on the Markov Chain

FRM Frame

HD Half-duplex

IoT Internet-of-Things

IP Internet Protocol

ITU International Telecommunication Union

IUI Inter-User Interference

JAIST Japan Advanced Institute of Science and Technology

LACK LoRaWAN Acknowledgement

LAN Local Area Network

LCTS LoRaWAN Clear-to-Send

LLC Logical Link Control

LoRaWAN LoRa Wide Area Network

LRTS LoRaWAN Request-to-Send

LSTS LoRaWAN Set-to-Send

M2M Machine-to-Machine

MAC Medium Access Control

MCST Mixture of Concurrent and Sequential Transmission

MCST/LoRa MCST over LoRa network

MIMO Multiple-Input and Multiple-Output

mMCST/LoRa Modified MCST over LoRa network

mMTC Massive Machine Type Communications

OATC Optimal Achievable Transmission Capacity

R Relay

RD Relay-Destination

RFD Relay FD

RHD Relay HD

RTS Request-To-Send

RTS/FCTS Request-to-Send/Full-duplex Clear-to-Send

S Source

SACA SR Alternating Channel Allocation

SI Self-interference

SIC Successive Interference Cancellation

SIFS Short Interframe Space

SINR Signal-to-Interference-plus-Noise Ratio

SNR Signal-to-Noise Ratio

SPCA SR Pairing Channel Allocation

SR Source-Relay

ST Sequential Transmission

STCA SR Transmitting Channel Allocation

STS Set-To-Send

TCP Transmission Control Protocol

TDD Time Division Duplexing

TDMA Time Division Multiple Access

TPC Transmit Power Control

UAV Unmanned Aerial Vehicle

URLLC Ultra Reliable Low-Latency Communications

WLAN Wireless Local Area Network

List of Definitions

Achievable network capacity (C_a) is the summation of the transmission capacity of every single basic relaying flow transmission in the network.

Achievable throughput (S_a) is the average value of the total number of successfully transferred data in a second by a transmitting node in the network.

Achievable transmission latency (L_a) is the average summation of the transmission delay and propagation delay of a BRF transmission from the source node to the destination node.

Achievable transmission overhead (O_a) is the average value of the overhead that is required to successfully carry out a transmission without considering the retransmission for any collision scenario in the network.

Average transmitter-to-receiver distance (d_{tr}) is the average distance between the transmitting node and receiving node and is computed by averaging the distance from the transmitting node and receiving node of every ongoing transmission.

Basic Relaying Flow is a combination of source-relay transmission and relay-destination transmission of a single relaying transmission flow in which a source node communicates to a destination node with the help of a relay node in the multihop wireless network.

Channel Interference Balancing Allocation is a cooperative channel allocation management scheme that switches the channel allocation to balance the total interference power of the sub-channels over many concurrent transmissions.

Concurrent Transmission is a type of transmission mode in which multiple transmissions occur concurrently rather than sequentially during the overlapping period.

Full-duplex is a type of communication system in which the nodes can perform transmission and reception simultaneously over a single frequency channel.

Half-duplex is a communication system in which the wireless nodes can perform either transmission or reception in non-overlapping timeslots over a single frequency channel of time-division duplexing or the same timeslot over a different frequency channel of frequency-division duplexing.

Inter-User Interference that is also known as co-channel interference or cross-link interference, is the interference from other transmitting nodes that are operating concurrently over the same frequency channel in the network.

Mixture of Concurrent and Sequential Transmission is a cooperative transmission scheme operated over the basic relaying flow transmission through cooperative communication strategies and optimizes the transmission capacity according to the time fraction.

Optimal Achievable Transmission Capacity is a cooperative transmit power control scheme for efficient transmission with high network capacity, low interference power, and power consumption through the temporal and spatial reuse mechanisms.

Saturation throughput (S) is the number of data transmitted during a specific time divided by the time of that period.

Self-interference is the signal disturbed from its own transmitting antenna on the receiving antenna of an FD-enabled wireless node.

Sequential Transmission is a type of transmission mode in which several transmissions are performed sequentially in non-overlapping timeslots.

Set-To-Send (STS) is a newly defined control frame in FD MAC protocol with a mixture of concurrent and sequential transmission scheme. The STS control frame is broadcasted by the relay node for sharing the MCST information of time fraction and transmission control to instruct the sequential transmission to proceed.

Time fraction (τ) is the elapsed time for performing the concurrent transmissions in the mixture of concurrent and sequential transmission scheme.

Total interference power is the total amount of the interference power caused to the successful transmission from other concurrent ongoing transmissions in the whole network.

Transmission capacity (C) is the capacity of a basic relaying flow in the network through the specific transmission scheme.

Transmission energy consumption (E_a) is the average summation of the total energy consumed for transmitting both the control and DATA frame from the source node to the destination node.

Transmit Power Control is a technique used to adjust the transmit power of a transmitting node for advancing the transmission capacity while mitigating the interference of the transmission.

List of Symbols

The following list describes the symbols that are used within the body of this dissertation:

α Pathloss attenuation constant

β SINR threshold

δ Coefficient associated with the offset value of pathloss

η_j Noise level of node j

γ Coefficient associated with the increase of pathloss with frequency

κ Number of floors

$\mathbb{F}$ Set of BRF transmissions

$\mathbb{G}$ Group of transmissions in CIBA algorithm

$\mathbb{K}$ Set of sub-channels

$\mathbb{N}$ Set of nodes in the network

$\mathcal{A}$ Average link rate of all BRF transmissions

$\mathcal{A}(t)$ Average link rate of all BRF transmissions at timeslot t

$\mathcal{C}$ Collision period of transmission

$\mathcal{F}$ Minimum link rate of each BRF transmission

$\mathcal{F}(t)$ Minimum link rate of each BRF transmission at timeslot t

$\mathcal{I}$ Set of interfering nodes

$\mathcal{L}$ Successful period of transmission

$\mathcal{R}$ Transmission control to instruct sequential transmission in MCST scheme

$\mathcal{T}$ Tradeoff threshold of OATC scheme

$\mathcal{T}_{CT}$ Tradeoff threshold of CT with CTPC algorithm

$\mathcal{T}_{MCST}$ Tradeoff threshold of MCST with CTPC algorithm

F Frequency of transmission

n Transition state of transmission

$\mathscr{C}$ Consensus coefficient of CTPC scheme

$\mathscr{G}^*$ Received power of the ongoing transmission

$\mathscr{I}^*$ Interference power of the ongoing transmission

$\mathscr{R}$ Choice transmission rate of OATC with CTPC algorithm

$\mathscr{R}_{CT}$ Choice transmission rate of CT with CTPC algorithm

$\mathscr{R}_{MCST}$ Choice transmission rate of MCST with CTPC algorithm

c Speed of light

K Number of sub-channels

k Index of sub-channel

θ Slot time length

γ_c Collision state

γ_s Success state

τ Time fraction in MCST scheme

τ_{RD} Time fraction in MCST scheme for the condition of RD transmission performs sequential transmission

$\tau_{\mathrm{RD}}(t)$ Time fraction in MCST scheme for the condition of RD transmission performs sequential transmission at timeslot t

τ_{SR} Time fraction in MCST scheme for the condition of SR transmission performs sequential transmission

$\tau_{\mathrm{SR}}(t)$ Time fraction in MCST scheme for the condition of SR transmission performs sequential transmission at timeslot t

B Channel bandwidth

C Transmission capacity of a BRF transmission

c Collision time

C_a Achievable network capacity

C_f Transmission capacity, C of fth BRF transmission

C_{RD} Transmission capacity of a BRF transmission for the condition of RD transmission performs sequential transmission

$C_{\mathrm{RD}}(t)$ Transmission capacity of a BRF transmission for the condition of RD transmission performs sequential transmission at timeslot t

C_{SR} Transmission capacity of a BRF transmission for the condition of SR transmission performs sequential transmission

$C_{\mathrm{SR}}(t)$ Transmission capacity of a BRF transmission for the condition of SR transmission performs sequential transmission at timeslot t

CW Contention window

CW_{max} Maximum contention window

CW_{min} Minimum contention window

d_0 Decorrelation distance

$d_{\mathrm{RD},f}$ Distance between R and D of fth BRF transmission

$d_{\mathrm{SR},f}$ Distance between S and R of fth BRF transmission

d_{ij} Euclidean distance between node i and node j

D_{kj} Interference distance from node k to node j

D_{prop} Propagation delay

D_{tran} Transmission delay

d_{tr} Average transmitter-to-receiver distance

E_a Transmission energy consumption

F Number of BRF transmissions

f Index of BRF transmission

G_{ij} Received power ratio between node i and node j

H Size of MAC header and trailer

I Total interference power

i Transmitting node of ongoing transmission

j Receiving node of ongoing transmission

K Number of simultaneous transmissions

k Interfering node to ongoing transmission

l DATA length

L_a Achievable transmission latency

L_f Latency L of fth BRF transmission

m Maximum number of retransmission stages

N Total number of nodes

n Index of node

n_{c} Node n with sub-channel c allocation

n_{D}^{f} Destination node D of fth BRF transmission

n_{R}^{f} Relay node R of fth BRF transmission

n_{S}^{f} Source node S of fth BRF transmission

O Transmission overhead ratio

O_a Achievable transmission overhead of a BRF transmission

O_f Transmission overhead ratio, O of fth BRF transmission

P Transmit power

p Conditional collision probability

p' Probability of the wireless node observes a collision

P_i Transmit power of node i

p_s Probability of successful transmission

p_{cc} Probability of the transitions of the transmission that a collision state is detected after collision state

P_{CT} Transmit power of CT with CTPC algorithm

$P_i(t)$ Transmit power of node i at timeslot t

P_{max} Transmit power budget

P_{MCST} Transmit power of MCST with CTPC algorithm

p_{sc} Probability of the transitions of the transmission that a collision state is detected after success state

p_t Transmission probability

PL_0^{c} Pathloss under Friis free space model at sub-channel c

PL_{ij}^{c} Channel gain between node i and node j at sub-channel c

PL_0 Pathloss under Friis free space model

PL_F Floor penetration loss factor

PL_{ij} Channel gain between node i and node j

R^{MCST} MCST transmission rate of SR transmission and RD transmission of a BRF transmission

R_RD^{con} Concurrent transmission rate or transmission rate R_RD based on $SINR_\mathrm{RD}$ of RD transmission

$R_\mathrm{RD}^{con}(t)$ Concurrent transmission rate of RD transmission at timeslot t

R_RD^{seq} Sequential transmission rate or transmission rate R_RD based on SNR_RD of RD transmission

$R_\mathrm{RD}^{seq}(t)$ Sequential transmission rate of RD transmission at timeslot t

R_SR^{con} Concurrent transmission rate or transmission rate R_SR based on $SINR_\mathrm{SR}$ of SR transmission

$R_\mathrm{SR}^{con}(t)$ Concurrent transmission rate of SR transmission at timeslot t

R_SR^{seq} Sequential transmission rate or transmission rate R_SR based on SNR_SR of SR transmission

$R_\mathrm{SR}^{seq}(t)$ Sequential transmission rate of SR transmission at timeslot t

R_{base} Basic rate

R_{ij} Transmission rate of transmission from node i to node j

S Saturation throughput of a BRF transmission

S_a Achievable throughput of a BRF transmission

S_f Saturation throughput, S of fth BRF transmission

$SINR_{ij}$ Signal-to-interference-plus-noise-ratio of transmission from node i to node j

SNR_{ij} Signal-to-noise ratio of transmission from node i to node j

t Timeslot

T_o^{CT} Transmission overhead time for concurrent transmission scheme

T_s^{CT} Successful transmission time for concurrent transmission scheme

T_o^{MCST} Transmission overhead time for a mixture of concurrent and sequential transmission scheme

T_s^{MCST} Successful transmission time for a mixture of concurrent and sequential transmission scheme through FD-MCST MAC

T_c Transmission time that faces the collision

T_o Transmission overhead time

T_s Successful transmission time

T_{ACK} Duration of ACK control frame

T_{BK} Time for the initial backoff timer

T_{CTS} Duration of CTS control frame

T_{DIFS} Duration of DIFS

T_{LACK} Duration of LACK control frame set

T_{LCTS} Duration of LCTS control frame set

T_{LRTS} Duration of LRTS control frame set

T_{LSTS} Duration of LSTS control frame set

T_{PHY} Time of physical preamble and header

$T_{preamble}$ Preamble time for synchronization

T_{RTS} Duration of RTS control frame

T_{SIFS} Duration of SIFS

T_{STS} Duration of STS control frame

$T_{timeout}$ Duration for the timeout

TC_{CT} Transmission control set of CT with CTPC algorithm

TC_{MCST} Transmission control set of MCST with CTPC algorithm

W_{ij} Wall attenuation of the transmission from node i to node j

X_{σ} Gaussian random variable with zero mean and standard deviation of σ

X_A Backoff timeslot of node A

X_C Backoff timeslot of node C

Y_{n} Difference in starting time for RTS control frame transmission in the state n

Z_{n} Backoff timeslot a freezing node at the state n

$\mathrm{ACK_{RD}}$ Acknowledgement control frame from destination node to relay node

$\mathrm{ACK_{RS}}$ Acknowledgement control frame from relay node to source node

$\mathrm{CTS_{DR}}$ Clear-to-send control frame from destination node to relay node

$\mathrm{DATA_{RD}}$ DATA from relay node to destination node

$\mathrm{DATA_{SR}}$ DATA from source node to relay node

$\mathrm{LACK_{DR}}$ LoRa ACK control frame set from the destination node to relay node

$\mathrm{LACK_{RS}}$ LoRa ACK control frame set from relay node to source node

$\mathrm{LCTS_{DR}}$ LoRa CTS control frame set from the destination node to relay node

$\mathrm{LRTS_{RD}}$ LoRa RTS control frame set from relay node to destination node

$\mathrm{LRTS_{SR}}$ LoRa RTS control frame set from the source node to relay node

$\mathrm{LSTS_{RS}}$ LoRa STS control frame set from relay node to source node

$\mathrm{RTS_{RD}}$ Request-to-send control frame from relay node to destination node

$\mathrm{RTS_{SR}}$ Request-to-send control frame from source node to relay node

STS_{RS} Set-to-send control frame from relay node to source node

RD^f RD transmission of fth BRF transmission

SR^f SR transmission of fth BRF transmission

Chapter 1

Introduction

The mobile communication system has changed from the first-generation (1G) as the analogue telecommunication standards to the latest fifth-generation (5G) in the Internet-of-Things (IoT) era. This continuous evolution of communication systems has had a great impact on the industry and people's lifestyles in many respects. As the commercial deployment of 5G is well ongoing around the world, both academia and industrial research organizations are turning their attention to the next coming communication system. Since the wireless world never stops growing, it is the perfect time to change the research direction for the new possible mobile communication system beyond 5G or six-generation (6G).

Compared to the previous generation of mobile communication systems, beyond 5G or 6G is expected to enhance what the user needs in not only the data transfer speed but also the connectivity and energy efficiency of the mobile wireless networks. Additionally, the rapid development of communication technology put forward the growth of data traffic and device increasingly and globally. It means that the later communication system is expected to deal with the dense wireless network environment. As one of the research areas of the next-generation mobile communication system, this dissertation explores the full-duplex (FD) system for future wireless networks.

In this chapter, the general introduction of the dissertation is described with the trend of communication systems and the future wireless concept relating to the beyond 5G or 6G. This dissertation focuses on the capacity optimization of future wireless networks through three research problems, i.e., inefficient network capacity, ineffective transmit power control and inefficacious resource allocation scheme. Then, the conceptual framework of the research work is discussed with the three main schemes to solve the mentioned research problems as the main content of the dissertation.

1.1 Niche of Communication Systems

According to the Cisco Annual Internet Report, the amount of global mobile devices and traffic connections is growing faster in various aspects of communication systems. The growth of the devices is predicted to increase from 8.8 billion in 2018 to 13.1 billion by 2023 at a compound annual growth rate (CAGR) of eight percent [1]. As shown in Figure 1.1, the growth of the devices in the machine-to-machine (M2M) communication system is most noticeable, although every category is growing clearly. It means that Internet-of-Things (IoT) services are rapidly popularized and developed through various smart devices, sensor networks, and the IoT system. Besides, as illustrated in Figure 1.2, the global mobile traffic connection is expected to increase up to 81 times in ten years from 62 exabytes [EB] per month in 2020 to 5016 EB per month in 2030 [2]. Furthermore, with the purpose of providing a better comfortable and sustainable life to all people's lives, shifting from Information Society 4.0 to Super-smart Society 5.0 is also a big hot topic in today's Internet society [3]. Therefore, the researchers put effort into the next mobile

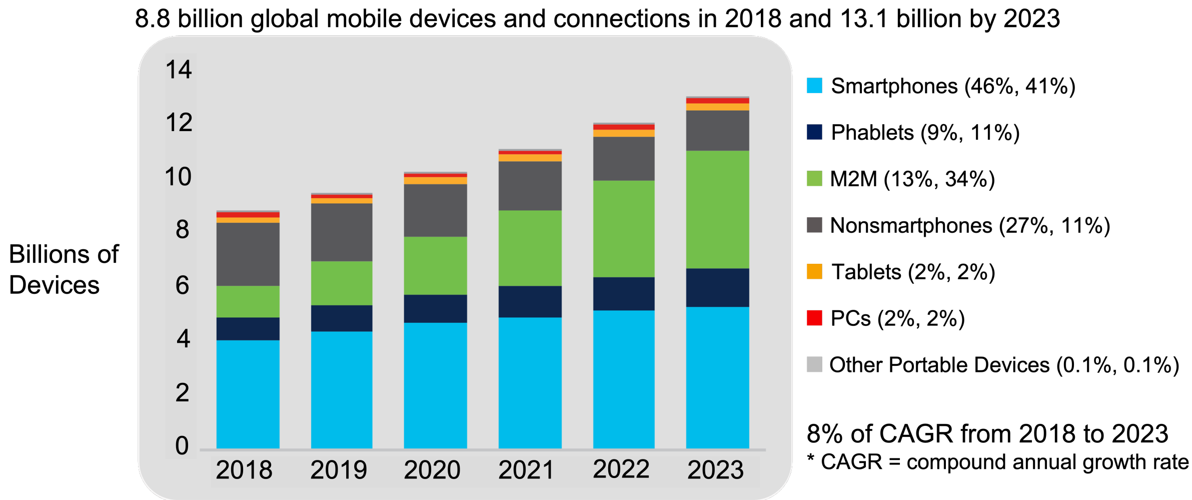

Figure 1.1: Global mobile device and connection growth from Cisco Annual Internet Report, 2018-2023 [1]

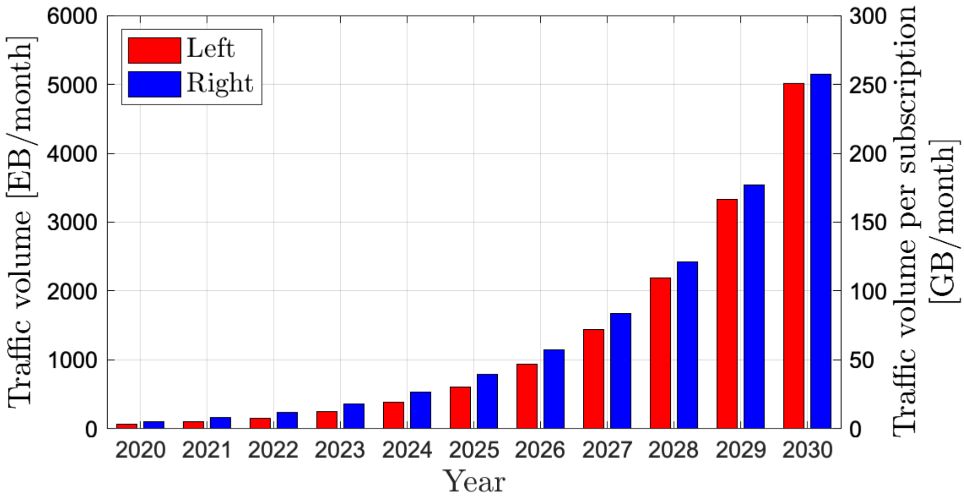

Figure 1.2: Prediction of global mobile traffic connection growth during 2020-2030 [2]

communication system, which utilizes fundamental technologies such as IoT, big data, and artificial intelligence (AI) to realize and accelerate the development of Society 5.0 [4]. Hence, the number of mobile devices, things, and mobile traffic connections is expected to increase dramatically in many categories of the communication system.

1.1.1 Future Wireless Concept

As the latest mobile communication system, 5G is now a commercial reality with the capability of enhanced Mobile Broadband (eMBB), Ultra Reliable Low-Latency Communication (URLLC), and massive Machine Type Communication (mMTC) [5]. Following that, as described in Figure 1.3, the progress of technology in the mobile communication system is heading to highly reliable data-driven wireless networks and human-centric mobile communication systems such as 6G. Maier also mentioned that 6G would play an important role in changing Information Society 4.0 to Super-smart Society 5.0 [6]. More specifically, the future 6G is predicted to be an extremely massive-scale communication system. As a result, more metaverse applications, i.e., augmented reality, telemedicine, smart cities, smart manufacturing, and connected vehicles such as auto-driving cars and drones, etc, with impressive experiences will be evolved in the near future [7–9]. However, such kind of a system and application requires massive spectrum resources, ultra-reliability and extremely low latency, and extremely high capacity than the current communication system. Therefore, the researchers have begun to focus on 6G in different aspects [10–12].

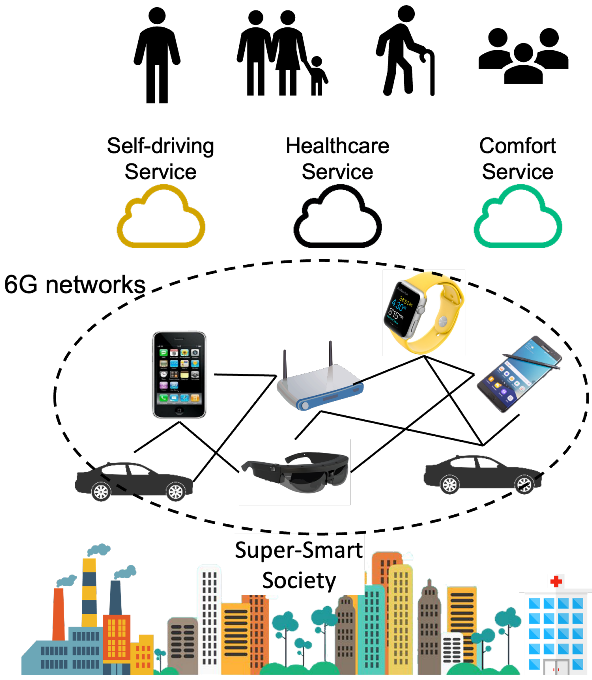

Figure 1.3: 6G networks and super-smart society

It is also noted that 6G is expected to outperform the 5G system and to be featured with the following key capabilities [13, 14]

- Extreme high data rate/capacity: The smart device in real-time and synchronized applications such as smart cities, smart manufacturing, and connected vehicles need to connect with each other, transmit the data and receive the instruction to/from the cloud and AI as the brain and so on. As a result, further improvement in communication speed requires an extremely high data rate/capacity.

- Extreme coverage: The network system in 6G is expected to become the Internet-of-Everything. This means 6G will cover everything, i.e., sky, space, land, and sea. Therefore, the extension of future applications for humans, machines, and industries is expected.

- Extreme high reliability: Metaverse applications, for example, augmented reality, require high data reliability with stable transmission over a high bandwidth network system to provide reliable service to the user.

- Extreme massive connectivity: 6G will require extremely high-quality connections

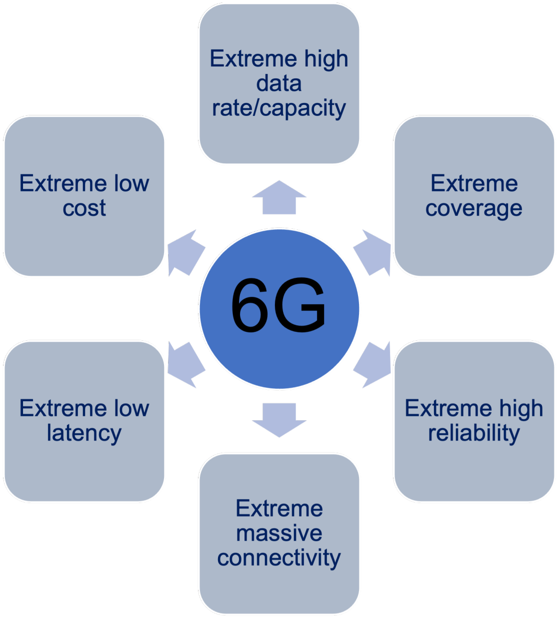

Figure 1.4: Requirement for 6G mobile communication system

to support hundreds of billions of devices and thousands of exabytes of traffic connection and volume for the metaverse applications.

- Extreme low latency: The critical real-time application and highly interactive systems, for example, telemedicine, auto-driving cars and unmanned aerial vehicles (UAVs or drones), require extremely low latency to ensure the quality of user experience and avoid latency dizziness

- Extreme low cost: In recent years, low cost and low power consumption have become important requirements for the communication system. Therefore, the smart device in the 6G system is expected to develop with power distribution technology using wireless signals. So that they do not need to be charged and will benefit both the business and the environment.

1.1.2 Future Challenges for Wireless MAC

The development of the technology put forward ever-increasing demands for wireless communication because of the limited spectrum resource. Hence, it is crucial to utilize the spectrum resource efficiently, and improving the spectrum utilization can always be a hot topic in the wireless communication environment [15]. Otherwise, the shortage of spectrum resources could be a severe problem for future wireless networks. Therefore, it is necessary to consider the possible challenges such as spectrum utilization, capacity demand, high interference, etc.

Without efficient spectrum resource utilization, heavy access to the spectrum creates an unreliable connection over wireless networks. As a result, the problem of low spectrum utilization in the radio device and spectrum scarcity or unused spectrum leads to spectrum holes in the transmission medium. Therefore, the researchers are working on designing and developing the wireless medium access control (MAC) protocol through various approaches to utilize the spectrum with the concept of sharing radio channels.

In addition to spectrum utilization, another challenge of wireless networks is to optimize throughput or to have high user capacity. A wireless network should allow multiple users to use the system simultaneously for capacity optimization. For the high user capacity with the flexible spectrum, 3GPP Release 18 studies the simultaneous uplink and downlink transmission possibility in the existing TDD band [16]. For that reason, multiple users (stations, computers, or devices) often need to share the wireless channel assigned and used by the wireless system. Many research works propose the multiple access protocol with the technique, algorithm, and scheme that enable the sharing mechanism between multiple users and control access to the wireless channel or transmission medium.

There are lots of challenges in designing a MAC protocol in wireless networks. Recently, the FD system has gained attention for spectral efficiency and capacity optimization through simultaneous transmission compared to the half-duplex (HD) system. Group of companies around the world integrates and tests the FD technology on the fourth-generation (4G) and 5G mobile communication systems and showed that FD technology is one of the ways to enable the efficient utilization of the spectrum [17]. For example, Lextrum tests the FD with LTE-Advanced technology and showed that the interference can be mitigated and the throughput improvement can be achieved. However, in the FD system, latency and synchronization issues are considerable factors for transmitting and receiving simultaneously. Likewise, when the wireless channel or transmission medium is shared in either HD or FD systems, the interference can affect the condition for successful transmission at the receiving node. Furthermore, the high error rate for signaling the packet, such as the collision, affects the transmission's performance.

The main focus of this dissertation is capacity optimization in wireless networks. In the super-smart society, the applications are expected to be human-centric mobile communication systems and the network is expected to be a highly reliable data-driven wireless network with interconnected and intercommunicated devices. And, the mission-critical and time-critical applications require high capacity with ultra low-latency communication for real-time interaction through device-to-device communications in wireless networks such as auto-driving cars and drones system [18]. Therefore, following these requirements, this dissertation investigates the potential research works for capacity optimization in wireless networks as the contribution to the new revolution of the Internet society.

1.2 Research Problems and Motivation

Through the development of technology and applications, the way of using the communication system brings the exponential growth of traffic connections that might be a big challenge for capacity optimization for future wireless networks. Therefore, wireless networks require a cooperative MAC, which enables efficient and effective communication through full spectrum utilization for the purpose of capacity optimization. As one of the potential technology in 6G, although FD has the benefits of spectral efficiency and possibly double the wireless transmission capacity, the drawback of high interference still requires working on compared to the HD system for true potential achievement. Besides, FD is not always the best selection compared to HD system without carefully planning [19, 20]. Therefore, this dissertation focuses on the extremely high data rate/capacity requirement for mobile communication systems with the three research problems, i.e., inefficient network capacity, ineffective transmit power control, and inefficacious resource allocation scheme, to provide efficient and effective communication for future wireless networks.

1.2.1 Network Capacity

The current research works mainly focused on the one-size-fits-all approach that only studies the transmission capacity of the HD and/or FD systems. In the HD system, sequential transmission (ST) can reduce interference, but the transmission capacity is limited compared to the FD system, in which concurrent transmission (CT) is employed for transmission capacity gain with the temporal reuse mechanism. However, the CT brings higher interference power and limits potential capacity gain as the network becomes dense. It means that the network capacity is still inefficient, and a comprehensive investigation of transmission schemes is necessary for network capacity management. Therefore, even if the wireless node has the capability of the FD system, ever-increasing capacity demand issues still exist in wireless networks.

1.2.2 Transmit Power Control

When the transmission medium is shared in the network, any unwanted transmission from the nearby wireless node as an interfering signal can affect the successful ongoing transmission if it is not well managed. Therefore, those transmissions are managed through admission control, traffic scheduling, transmit power control (TPC), and the minimum interference management scheme. Here, TPC is a technique that controls the transmit power to suppress unwanted interference between wireless nodes in the network. Through the various algorithms in the TPC technique, the transmit power is controlled and reduced for the purpose of interference mitigation as well as energy-efficient communications. However, the transmit power reduction impacts transmission capacity. Besides, future wireless communications enable many wireless nodes to participate in the transmission and cause a high total interference level in the network. In other words, dense wireless networks could lead to high total network interference. Hence, the effective TPC is required to consider the tradeoff between capacity gain and interference mitigation for transmission capacity optimization. Otherwise, the interference problem still influences the capacity gain of the transmission in the network.

1.2.3 Channel Allocation

In the current wireless networks, the spectrum allocation policy is generally the fixed spectrum allocation policy that makes wireless communications face spectrum scarcity as the number of users increases. Besides, when the transmission medium is shared among several transmissions, a large number of wireless nodes and traffic connections result in high total interference in the network. If the resource allocation scheme is inefficacious, it is difficult to get the desired effect of optimum transmission capacity with low network interference and high resource utilization. Hence, the spectrum utilization problem is considered one of the vital factors for transmission capacity optimization in the network.

Therefore, an efficient MAC framework is crucial to meet future wireless networks' traffic and capacity demands. In this dissertation, a MAC framework is proposed with three schemes to solve the above research problems for efficient and effective communication in wireless networks.

1.3 Research Vision, Purpose and Objectives

This dissertation focuses on capacity optimization by exploring the potential benefit of the FD system for efficient and effective communication for future wireless networks such as auto-driving cars and drones system. The vision is to contribute an efficient and effective communication framework through cooperative communication strategies, i.e., transmission strategy, relaying strategy, and allocation strategy.

The purpose of this dissertation is to explore the concept of cooperative communication strategies for the possibility of a novel MAC framework in FD wireless networks by focusing on the optimum transmission capacity of source-destination pair with high throughput and low network interference and high resource utilization. In particular, the three main objectives of this dissertation are

- to design and present a transmission scheme for efficient network capacity management incorporated with the relaying strategy (the disseminated publications on this objective are [1], [3], [6], [9], [11], and [15])
- to propose a transmit power control scheme for effective communication to achieve high network capacity while minimizing the total interference power and total network energy consumption (the disseminated publications on this objective are [2], [7], [8], and [16])
- to introduce a channel allocation scheme for efficacious spectrum utilization communication with minimum total interference power (the disseminated publication on this objective is [4])

1.4 Research Significance

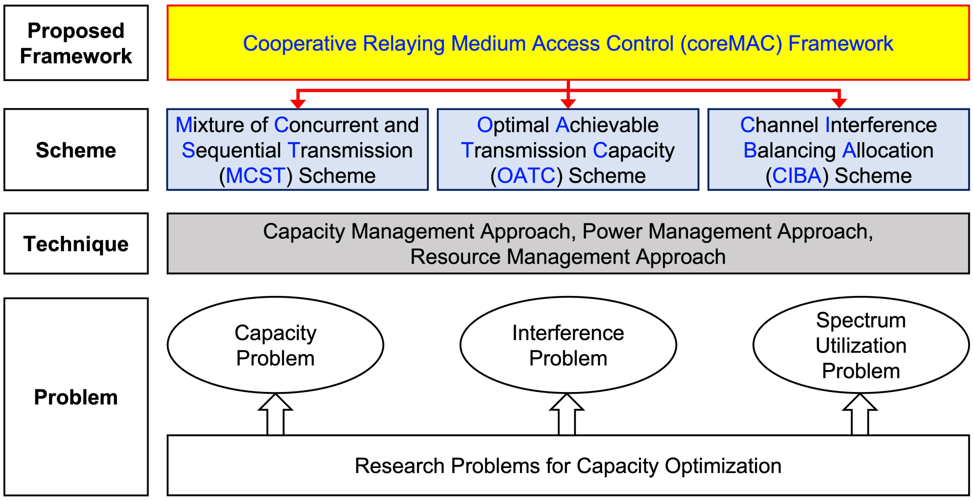

Figure 1.5: Proposed conceptual MAC framework for transmission capacity optimization

The existing research with the one-size-fits-all approach focuses on ST with the benefits of interference-free transmission and CT for capacity achievement in wireless networks. Unlikely, this research integrates both the advantages of ST and CT, TPC, and dynamic channel allocation for the purpose of transmission capacity optimization as well as interference mitigation in the FD wireless networks.

Figure 1.5 describes the conceptual framework for transmission capacity optimization as the main content of this dissertation. The cooperative relaying MAC framework, namely coreMAC, is designed for multihop wireless networks with the three approaches to address the three specific research problems mentioned in the previous section. The three approaches in the framework include designing the transmission scheme with capacity management, proposing a power control scheme with power management, and designing an allocation scheme with resource management. In this way, the proposed coreMAC framework improves the achievable transmission capacity, achievable network capacity, and achievable throughput with the lower achievable transmission latency and lower transmission energy consumption for the multihop wireless networks. As the research impact, this dissertation brings the breakthrough of capacity optimization through FD systems and cooperative communication strategies and presents the solution to support an efficient communication framework for applications with high capacity demand such as auto-driving cars and drones system.

1.5 Dissertation Organization

The rest of this dissertation is structured as follows:

- Chapter 2: Cooperative Relaying Medium Access Control Framework

  This chapter reviews the literature to provide a conceptual discussion for the framework. Besides, the proposed coreMAC framework is discussed as the core of this dissertation. This chapter discusses the related key technologies to the proposed framework, cooperative communication strategies, and the three schemes as the framework components.

- Chapter 3: Mixture of Concurrent and Sequential Transmission (MCST) Scheme

  This chapter discusses capacity optimization through the transmission capacity scheme of the coreMAC framework. The MCST scheme is proposed as an efficient transmission scheme via the capacity management module.

- Chapter 4: Optimal Achievable Transmission Capacity (OATC) Scheme

  This chapter describes the necessity of interference mitigation to optimize the transmission capacity in multihop wireless networks and explains the TPC scheme of the coreMAC framework. OATC scheme is proposed as the effective transmit power control through the power management module.

- Chapter 5: Channel Interference Balancing Allocation (CIBA) Scheme

  Chapter 5 introduces the possible solution for interference mitigation and discusses the dynamic allocation management scheme of the coreMAC framework. CIBA is explained to reduce the interference and to extend the capacity study of the FD system in the multi-channel wireless networks for efficacious resource allocation.

- Chapter 6: Conclusion

  Finally, chapter 6 summarises the findings of the proposed coreMAC framework, concludes the dissertation, and points out possible future research works.

Chapter 2

Cooperative Relaying Medium Access Control Framework

This chapter describes the general overview of the proposed cooperative relaying medium access control (coreMAC) framework as a key role in shaping the future MAC framework for FD wireless networks. First, the related key technologies to the proposed coreMAC framework are discussed. Second, the cooperative communication strategies of the proposed coreMAC framework are presented. Following that, the overview of the proposed framework is explained with the three schemes.

2.1 Related Key Technologies to the Framework

This dissertation only focuses on the FD system, which is trending as one of the potential technologies for 6G over the multihop wireless network environment.

2.1.1 Full-duplex System

In the communication system, the duplex means the communication ability, i.e., transmission and reception, provided by two or more nodes. Based on the data flow capability, the transmission and reception can be performed asynchronously or simultaneously as an HD or FD system, respectively. As the HD system, the communication can perform either transmission or reception in non-overlapping timeslots over a single frequency channel of time-division duplexing (TDD) or the same timeslot over different frequency channels of frequency-division duplexing (FDD). Otherwise, if the wireless system has FD capability, the simultaneous transmission and reception can be done over a single frequency channel. They are also known as FD systems [8, 21–23]. Figure 2.1 illustrates an example of a communication system as the HD and FD systems with two wireless nodes.

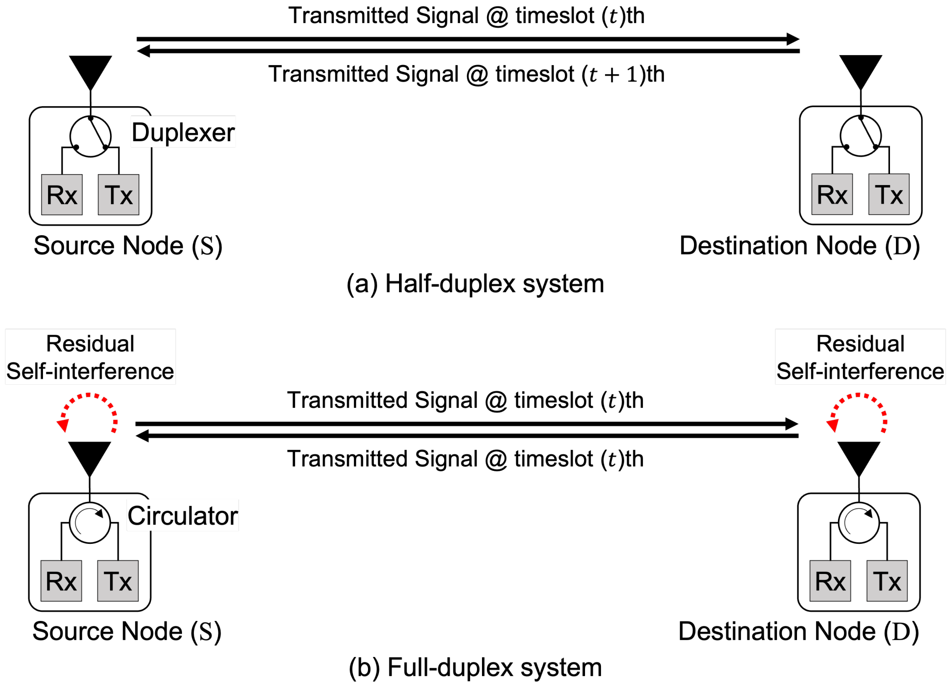

Figure 2.1: Two types of communication system

The FD systems are attractive as a potential technology for future wireless networks with spectral utilization capabilities. Current studies show that the FD systems can theoretically achieve twice the performance of the HD systems. As shown in Figure 2.2, the transmission mode of FD systems can be generally divided into bidirectional FD transmission and unidirectional FD transmission. Specifically, through the bidirectional transmission mode, when a pair of wireless nodes are equipped with the FD system capabilities, they can do the transmission and reception between each other simultaneously over a single frequency channel. In the literature, they are sometimes called symmetric FD transmission. Otherwise, the transmission can be done through unidirectional FD transmission modes via the help of an FD system capability-enabled relay node. The unidirectional FD transmission is also known as relay FD transmission or asymmetric FD transmission and is widely used in infrastructure-based wireless networks [24, 25]. In this dissertation, the relay FD transmission is defined as the basic relaying flow (BRF)

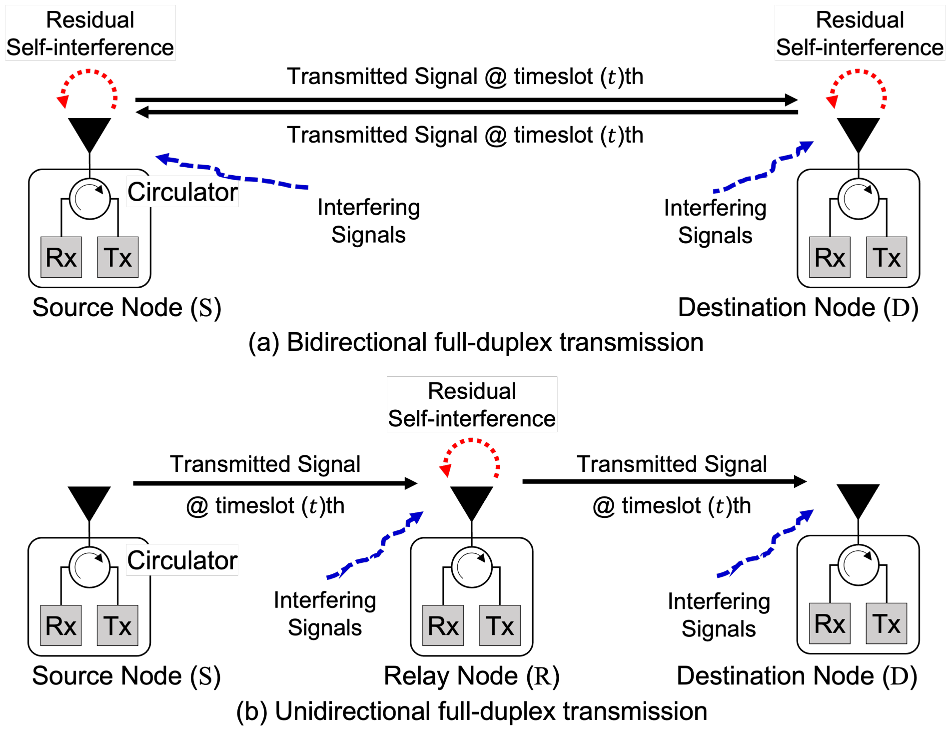

Figure 2.2: Two transmission modes of full-duplex system

transmission that is formed by combining transmission from a source node to a relay node and transmission from the relay node to the destination.

Although the FD system can achieve higher capacity, issues such as interference and noise from simultaneous transmission become more serious as the traffic connection increases. The main challenge to performing simultaneous transmission is the residual self-interference (SI) of the transmitting antenna at the receiving antenna of an FD system [21, 26]. Hence, SI elimination is crucial to enable the simultaneous transmission of the FD system to bring potential capacity improvement to the HD system.

Several research works have been conducted to significantly suppress the SI until the receiver noise power level. There are two main types of SI cancellation techniques: active cancellation and passive suppression in the analog and digital domains [27–32]. The active cancellation technique suppresses SI in the frequency, and analog domain before and after passing the analog-to-digital (ADC) converter through different signal processing techniques [33]. The passive suppression technique increases the physical separation of the antenna and sometimes uses the directional antennas to suppress the SI. Passive suppression is also referred to as the antenna SI-cancellation technique. However, this approach is limited to the device as modern mobile devices are small in size and lack space for antenna separation. In recent years, significant progress in SI cancellation techniques using various methods and hardware design has enabled the implementation of the FD system in wireless networks.

Besides SI, another issue is dealing with co-channel interference (CCI), a.k.a. inter-user interference (IUI) from other nodes that are transmitting concurrently over the same frequency channel in the network [34,35]. Regardless of the HD and/or FD system, CCI from other transmissions still degrades the throughput performance if the transmission medium is shared, especially in the highly-dense wireless network environment [36–38]. Goyal et al. claimed that the SI does not affect the capacity gains of the FD wireless networks, but the CCI does [39]. The main reason is that the strong CCI from other wireless nodes dominates the SI, significantly reducing overall network capacity. Therefore, although SI can be reduced with various cancellation techniques, the FD capacity gains over the HD system can not be guaranteed because of CCI. Several research works have proposed CCI cancellation and MAC protocols to allow several transmissions to perform concurrently in the FD wireless network and improve spectral efficiency. In general, the research on CCI cancellation is divided into three types: MAC protocol, resource allocation, and physical layer technique [40]. In the MAC protocol, protocols have been proposed for a centralized or distributed approach, such as a protocol for selecting the transmitter and/or receiver for routing and user pairing according to the IUI and network traffic connection. Then, the resource allocation technique can reduce the CCI through a scheduling scheme, the TPC technique, interference alignment, and frequency resource allocation. On the other hand, the physical layer technique, such as active cancellation passive suppression and the use of directional antennas, have also been proposed for mitigating the CCI in wireless networks.

Different communication approaches have been investigated to realize the potential benefits of FD systems. Recently, FD systems have made significant progress for simultaneous transmission, mainly focusing on the SI cancellation and power control approach for low-power wireless network scenarios with resource allocation management, MAC protocol, and so on [41]. The MAC protocol for the FD system has been discussed through different approaches. For example, an FD MAC protocol named Janus is proposed for infrastructure-based networks that control transmission based on interference level in [42]. Likewise, Goyal et al. designed a distributed FD MAC based on the IEEE 802.11 Distributed Coordination Function (DCF) that adapts to the traffic conditions by considering the IUI and contention during the transmission in both ad hoc network and infrastructure-based network topologies [43]. Febrianto et al. proposed an FD MAC protocol for a decentralized FD wireless network with cooperative transmission based on carrier-sense multiple access with collision avoidance (CSMA/CA) concept in which several FD transceivers, FD wireless node that can proceed transmission and reception simultaneously, compete for transmission [44]. Meanwhile, Tamaki et al. proposed FD MAC with additional 1-bit information in the successive transmission frame for indicating the primary transmission and selecting the secondary transmission in FD wireless networks [45]. Recently, Maloo et al. proposed a cross-layer MAC protocol with a different framing structure and the dynamic buffer for the asymmetric traffic condition in the IoT networks [46].

2.1.2 Multihop Wireless Network

In wireless communication, there are generally two types of networks: the infrastructure-based wireless network and the wireless mesh network, a.k.a. the multihop wireless network. The infrastructure-based wireless network has base stations or access points deployed throughout the given area. In a network, the mobile terminal transmits data directly to and from the base station for communication. This type of network has demanded to serve an increasing number of devices and traffic connections due to the long distance.

The multihop wireless network is a collection of wireless nodes to form a network without any infrastructure. Unlike infrastructure-based wireless networks, all the wireless nodes work cooperatively to send packets to their destination. The communication is done by peer-to-peer transmission over the network. This means the wireless node can communicate directly with neighbors or forward the packets to their final destination. In multihop wireless networks, the transmissions can be done in the multihop fashion, which has the advantage of increasing the transmission capacity through short distances and high energy efficiency. In addition, the multihop fashion can improve bandwidth

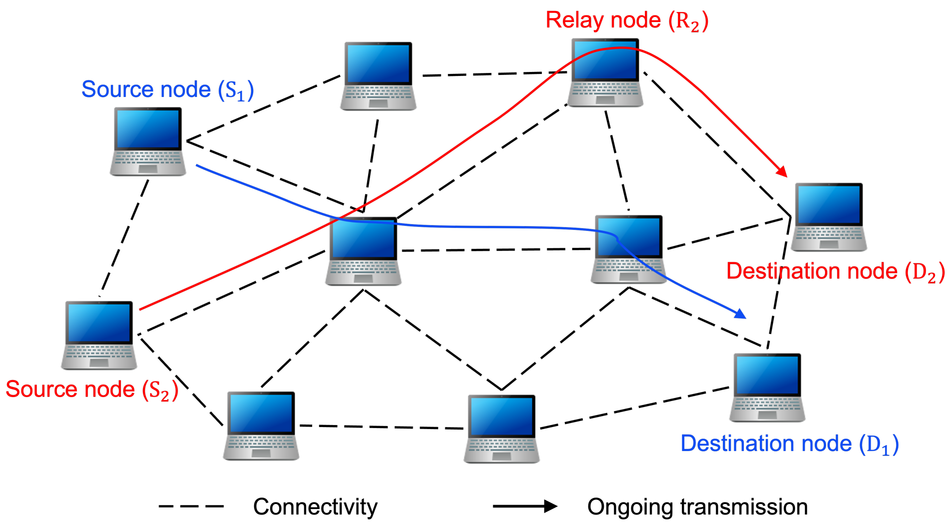

Figure 2.3: An example of a multihop wireless network with two transmission flows

efficiency even under lower end-to-end signal-to-noise ratio (SNR) conditions. Therefore, multihop wireless network is presented as a promising approach for the next-generation mobile communication system due to the cooperative and self-organizing communication without infrastructure. Application scenarios for the multihop wireless network include mobile ad hoc networks, vehicular ad hoc networks, and device-to-device communications.

FD system works well in low-power scenarios as the effect of SI is reduced over shorter distances [47]. Alternatively, the communication in the FD system benefits from shorter distances as interference increases with higher transmit power. Therefore, it is interesting to study the FD system in a multihop wireless network environment since one of the characteristics of the multihop wireless network is communicating with multiple hops over a short distance.

2.2 Cooperative Communication Strategies

In multihop wireless network environment, the wireless relay system with the cooperative transmission, a.k.a. cooperative relay network, is the most active research area in the wireless communication era for capacity optimization. Cooperative communication uses a mobile terminal or node as a relay node to improve the transmission quality. Therefore, the cooperative communication system can be a network with single or multiple relay nodes [48]. In the network with a single relay, the source node has only one option to forward its transmission through relaying strategy to the destination node. On the other hand, the source node has more than one relay node as an option to forward its transmission to a destination node in the network with multiple relay nodes. Then, the cooperative communication system can be operated as a centralized or decentralized network. The centralized network has the root node that selects the relay node to provide the most efficient transmission in the network while the decentralized network allows the nodes can choose a relay node independently to forward the transmission to the destination node. Furthermore, the cooperative communication system can be different in terms of the number of channels in the network.

The cooperation can be performed in many approaches and can be used at different levels of the processing hierarchy [49]. The cooperative algorithms reorganize modulation, coding, and signal processing design at the physical layer. Besides, the algorithms make wireless transmission energy efficient with certain reliability and spectral efficiency. This way, cooperation between the nodes in the wireless multihop network improves communication reliability, reduces energy consumption, and minimizes latency. In addition, the knowledge of the network can be broadened by exchanging the observed information among the devices through cooperation. As such, the cooperative relay network becomes one of the key enabling technologies in the 6G system through research on channel modelling, optimal relay selection, energy efficiency, and cooperative schemes. There are some MAC protocols proposed in the multihop wireless network with the cooperative strategy. For example, Adam et al. propose a MAC protocol for selecting relay nodes in the multihop wireless network [50]. In this protocol, the relay node cooperatively assesses the link quality between the source node and destination node, and reactive relay selection is activated when direct transmission is impossible. Similarly, Kader et al. propose a cooperative relay-sharing protocol to improve the transmission spectral efficiency in the FD networks [51].

In this dissertation, by simply considering that the concept of cooperative communication is applied in multihop wireless networks, the three cooperative communication strategies, i.e., transmission strategy, relaying strategy and allocation strategy, are utilized to propose the novel coreMAC framework for efficient and effective communication in multihop wireless networks.

2.2.1 Transmission Strategy

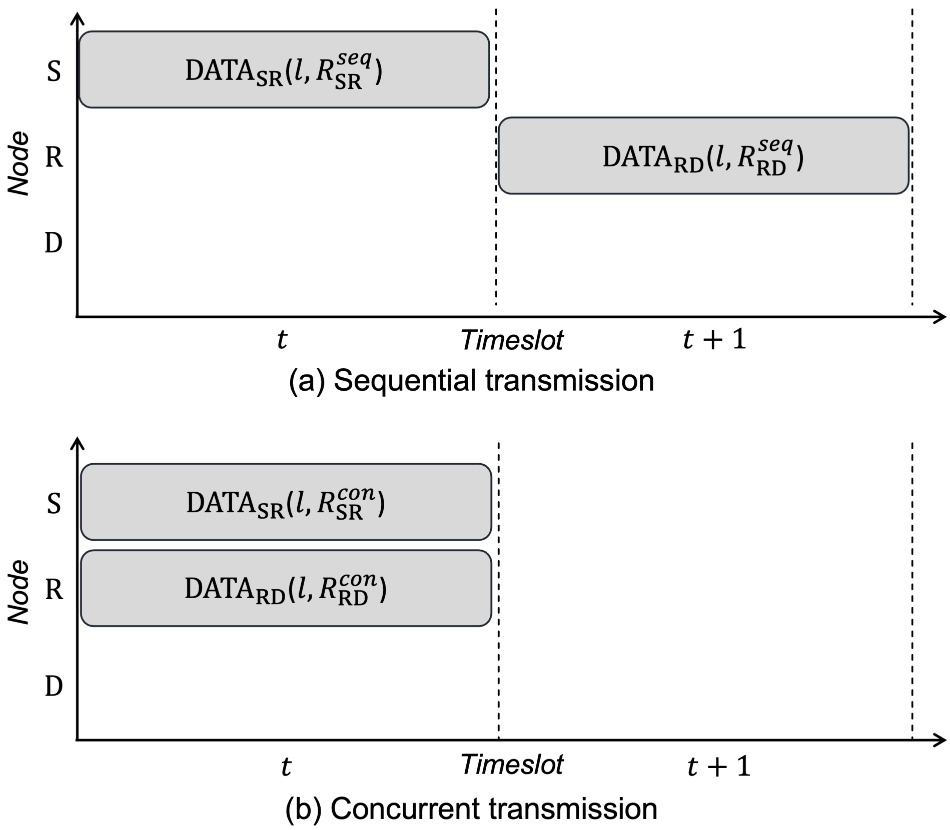

Figure 2.4: Two transmission strategies in the wireless networks

Through cooperative communication, the transmission in the network can be performed via different transmission strategies. The goal of the transmission strategy is to optimize the transmission capacity at the given timeslot with the help of a specific algorithm. The challenge is choosing the appropriate duration of the transmission and the transmission scheme, i.e., the strategy to instruct the transmission. As illustrated in Figure 2.4, the two main transmission strategies in the current wireless networks are as follows:

- Sequential Transmission (ST): A form of transmission in which several transmissions are performed sequentially in non-overlapping timeslots. This transmission strategy allows several nodes to use the same frequency band by separating the communication channel into many timeslots in the shared networks. This concept is the same as time-division multiple access (TDMA) and has the advantage of interference-free transmission.

- Concurrent Transmission (CT): A type of transmission scheduling in which multiple transmissions occur concurrently rather than sequentially during the overlapping period. Multiple transmissions can be performed concurrently by applying the techniques like multiple-input and multiple-output (MIMO) and FD system. Therefore, CT can provide better capacity than ST with the temporal reuse mechanism.

2.2.2 Relaying Strategy

In the wireless relay system, the wireless network with relaying strategy, one transmission flow includes at least three nodes: a source node, a relay node, and a destination node. The relay node uses various relaying strategies to forward the transmission received from the source node to the destination node. The wireless relay system has recently received significant attention due to the benefits of improved coverage, throughput, system capacity, battery life, etc. Therefore, the relaying strategy becomes the fundamental technique in the cellular wireless communication system because it can be efficiently used to expand coverage and enhance network capacity at a low cost. Figure 2.5 shows an example of a wireless relay system for a UAV system that extends coverage to control the drone via the base station as a relay node. With a relaying strategy, a relay node can forward all or part of a message. In addition, according to the transmission protocol, the two-hop channel estimation of the wireless relay system can be performed using the signals received at the relay node and destination node. This way, the relay node can send the signal and/or interference to the destination node and subtract the unwanted interference for interference cancellation purposes. Among the existing research works [52–55], the followings are the

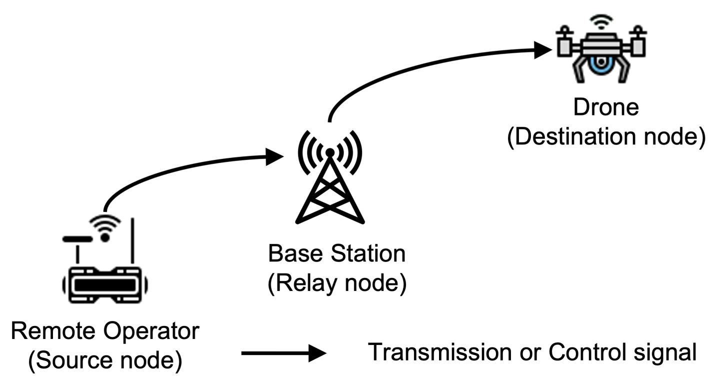

Figure 2.5: An example of unmanned aerial vehicle system as wireless relay system

two main relaying strategies in the wireless network.

- Amplify-and-forward: The relay node simply amplifies the received signal from the source node and forwards it without decoding it to the destination node.
- Decode-and-forward: The relay node decodes the received signal, re-modulates it, and forwards it to the destination node.

2.2.3 Allocation Strategy

The cooperative communication system can be implemented with a single channel or multi-channels for data transmission. When the network is implemented with only one channel, both the transmission from the source node to the relay node and the relay node to the destination node uses the same channel for transmission. Otherwise, the transmission from the source node to the relay node uses one channel, while the relay can perform transmission to the destination with different channels via the channel allocation strategy. Channel allocation is a process in which the transmission medium is divided and allocated to multiple users to perform the transmission. The three types of channel allocation strategies are as follows:

- Fixed Channel Allocation: The fixed channel allocation strategy is a strategy in which a fixed number of communication channels are allocated to the transmission by subjecting to maximize the frequency reuse. And once they are allocated, they cannot be changed.
- Dynamic Channel Allocation: Dynamic channel allocation is a strategy in which the channels are not permanently assigned to the cells. In this type of channel allocation, more channels are used and assigned as the traffic increases and vice-versa.
- Hybrid Channel Allocation: A combination of fixed and dynamic channel allocation is called the hybrid channel allocation strategy. The hybrid channel allocation divides the total number of channels into fixed and dynamic sets. When a user or node proceeds with the transmission, the fixed set of channels will be first utilized. Otherwise, if the fixed sets are busy or crowded, dynamic sets are used. The hybrid channel allocation strategy aims to keep the efficiency under the heavy traffic connection and maintain minimum interference.

2.3 Related Works

Communication frameworks are designed for data transmission between wireless nodes in the network. Nowadays, there are several communication frameworks in various aspects to create a perfect wireless system. Some of the proposed communication frameworks are discussed in the following.

A network resource management framework has been proposed to improve network resource utilization in the wireless mesh networks in [56]. The proposed framework consists of three components: an optimization-based association control algorithm for network resource allocation, an access network channel assignment algorithm to improve network capacity with interference mitigation, and a utility-fair bandwidth allocation algorithm to consider the trade-off between network capacity and user fairness. By taking inter-cell interference into consideration, the simulation results reveal that all three schemes in the proposed framework achieve higher performance, even in the higher-density networks.

In the wireless sensor networks, Moridi et al. proposed a fault management framework based on the Markov Chain (FMMC) to improve the fault tolerance and ensure optimal performance of the network since fault detection and fault management are the required features for an efficient network [57]. FMMC is based on clustering algorithms with two main phases: fault detection and recovery. The simulation results show that FMMC improves energy consumption and accuracy in fault detection and reduces the error alarm rate. Similar research work can be found in [58] in which Ataelmanan and Ali presented an anomaly detection framework to prevent wireless attacks using the machine learning technique.

In the other approach, the spectrum management framework for cognitive radio ad hoc networks has been proposed to overcome the drawback caused by the limited knowledge of the network in [59]. The proposed framework has four spectrum management functions: spectrum sensing, spectrum decision, spectrum sharing, and spectrum mobility. In the framework, the functions are based on cooperative operations, and the information exchanged among the nodes allows the users to determine their actions.

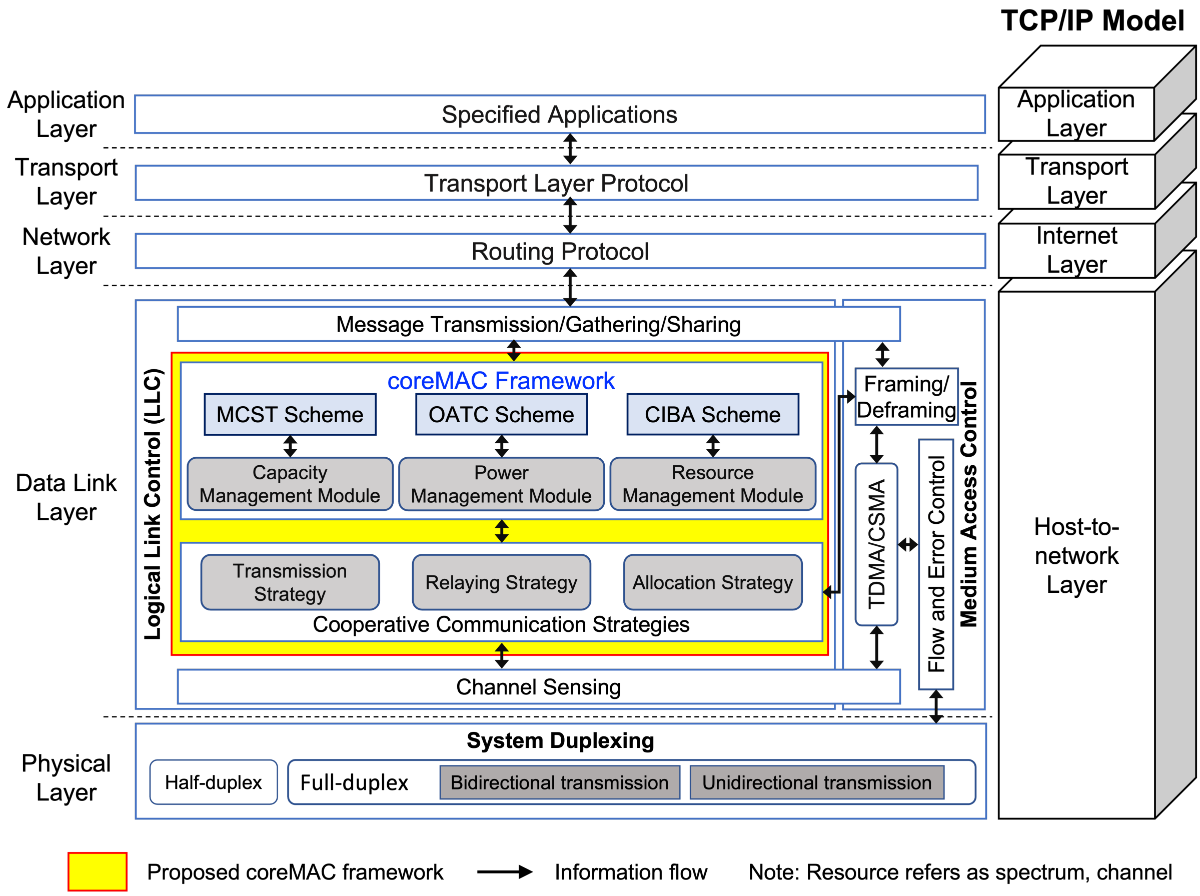

Figure 2.6: Cooperative relaying medium access control (coreMAC) framework

2.4 Proposed coreMAC Framework

In this dissertation, a framework called the coreMAC framework, which refers to the cooperative relaying medium access control framework, is designed for efficient communication for future wireless networks. The block diagram of the coreMAC framework is depicted in Figure 2.6. Multihop wireless networks are expected to become the dominant communication paradigm in the future wireless environment. Similarly, the FD system is as attractive as a potential technology for spectral efficiency. The existing proposed frameworks mainly focus on capacity optimization, fault management, and spectrum management in HD wireless networks. However, this framework is designed mainly based on the FD wireless networks. Using the concept of three cooperative communication strategies: transmission strategy, relaying strategy, and allocation strategy, the framework is conceptualized over the logical link control (LLC) of the host-to-network layer in the TCP/IP model. Through the three schemes, the proposed coreMAC framework addresses the problems of high latency and low throughput in mission-critical and time-critical applications like auto-driving cars and UAVs. The high latency and low throughput in the data link layer influence the transport layer protocol performance, which will affect the quality of service for the specified applications. On the other way, the proposed framework provides efficient and effective communication in the FD wireless networks through three approaches: capacity management module, power management module, and resource management module.

2.4.1 Mixture of Concurrent and Sequential Transmission Scheme

The mixture of concurrent and sequential transmission (MCST) scheme is proposed for transmission capacity optimization to address inefficient capacity management problems through the capacity management module. MCST utilizes the transmission and relaying strategies and operates by formulating a BRF transmission in the multihop wireless networks. As a cooperative transmission scheme considering optimum transmission capacity based on spectral efficiency, MCST combines the concepts of ST and CT in the same timeslot with the time fraction of the concurrent transmissions. Therefore, MCST can be defined as a cooperative transmission scheme operated over BRF transmissions through cooperative communication strategies and optimizes the transmission capacity according to the time fraction.

2.4.2 Optimal Achievable Transmission Capacity Scheme

The optimal achievable transmission capacity (OATC) scheme is proposed to overcome the research problem of ineffective TPC and aims to optimize the transmission capacity as a power management module. OATC is a cooperative transmit power control scheme for efficient transmission with high network capacity, low interference power, and low power consumption through temporal and spatial reuse mechanisms. OATC is designed by integrating the power control scheme into the MCST scheme. Specifically, OATC combines the temporal reuse and spatial reuse mechanisms in the FD wireless networks and intends to minimize transmission interference from other ongoing transmissions in the network. Unlike existing TPC schemes, OATC controls the concurrent transmissions via the MCST scheme and adjusts the transmission coverage area through TPC. OATC operates as a hybrid transmission scheme that considers both interference and capacity at the same time and uses a tradeoff threshold to optimally chooses the CT or MCST as the operational transmission scheme.

2.4.3 Channel Interference Balancing Allocation Scheme

To extend the transmission capacity optimization in the multihop wireless networks, a channel interference balancing allocation (CIBA) is proposed to consider the inefficacious resource management through allocation strategy. CIBA is a cooperative channel allocation management scheme worked as the resource management module that switches the channel allocation to balance the total interference power of the sub-channel among the concurrent transmissions. By considering the wireless node is equipped with multiple radios or multiple transmission channels in multi-channel multihop wireless networks, CIBA optimizes the transmission capacity by minimizing total interference power in the network. Unlike existing research on interference suppression, TPC, and user scheduling, CIBA reduces the interference by spreading the adjacent transmission into a different transmission channel.

2.5 Preliminary Study using Capacity Region

The investigation of achievable capacity is well known in multihop wireless networks. The capacity region represents the achievable transmission rate combination set of the source-destination transmission pairs under a specific transmission strategy in wireless networks. The research work of Gupta and Kumar describe that the achievable throughput under optimum condition for a random network is given by $\Theta(W/\sqrt{n})$ where n is the number of nodes and W is bandwidth [60]. Toumpis and Goldsmith also defined and studied the capacity region as the set of maximum achievable rates under specific transmission protocols [61]. In this research, the capacity region is the union of transmission capacity between all transmission pairs in the network. And, the transmission capacity here means the maximum amount of data that can be transferred from the source node to the destination node under a specific transmission scheme.

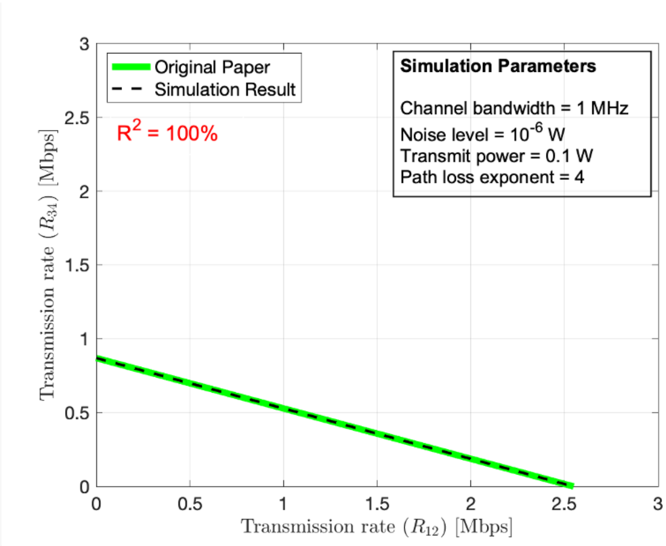

Figure 2.7: Simulation verification

2.5.1 Simulations Verification

Firstly, the correctness of the simulation program is validated through the capacity region study of [61]. By assuming similar simulation parameters in the same network scenario with the same system model, SINR model, and link capacity model mentioned in [61], the transmission rate of the single-hop routing with no spatial reuse is computed. Then, Figure 2.7 verifies the correctness of the simulation program.

2.5.2 Simulation Results and Discussion

This section describes the performance evaluation of the cooperative communication strategies applied in the proposed coreMAC framework. A simple numerical simulation is conducted to evaluate the performance in transmission capacity and network capacity for the network, which has two transmissions from the source node and the destination node. The network capacity refers to the sum of the transmission capacity of every transmission in the network. With the simulation program verified in the previous section, the numerical simulation for performance evaluation is conducted according to the parameters listed in Table 2.1.

The nodes are uniformly distributed and randomly selected to form the transmission in the network. Considering the log-distance pathloss model as the channel model, the transmission rate is computed through Signal-to-Interference-plus-noise-ratio (SINR)

Table 2.1: Simulation parameters for evaluation of cooperative communication strategies

Parameter	Value	Parameter	Value
Network coverage size	100 m × 100 m	Wall attenuation	0 dB
Number of transmissions	2	Shadowing parameter	8 dB [62]
Transmit power	20 dBm	Noise level	-174 dBm
Channel model	Log-distance pathloss	Channel bandwidth	20 MHz
Attenuation constant	3.5	Number of simulations	10,000 times

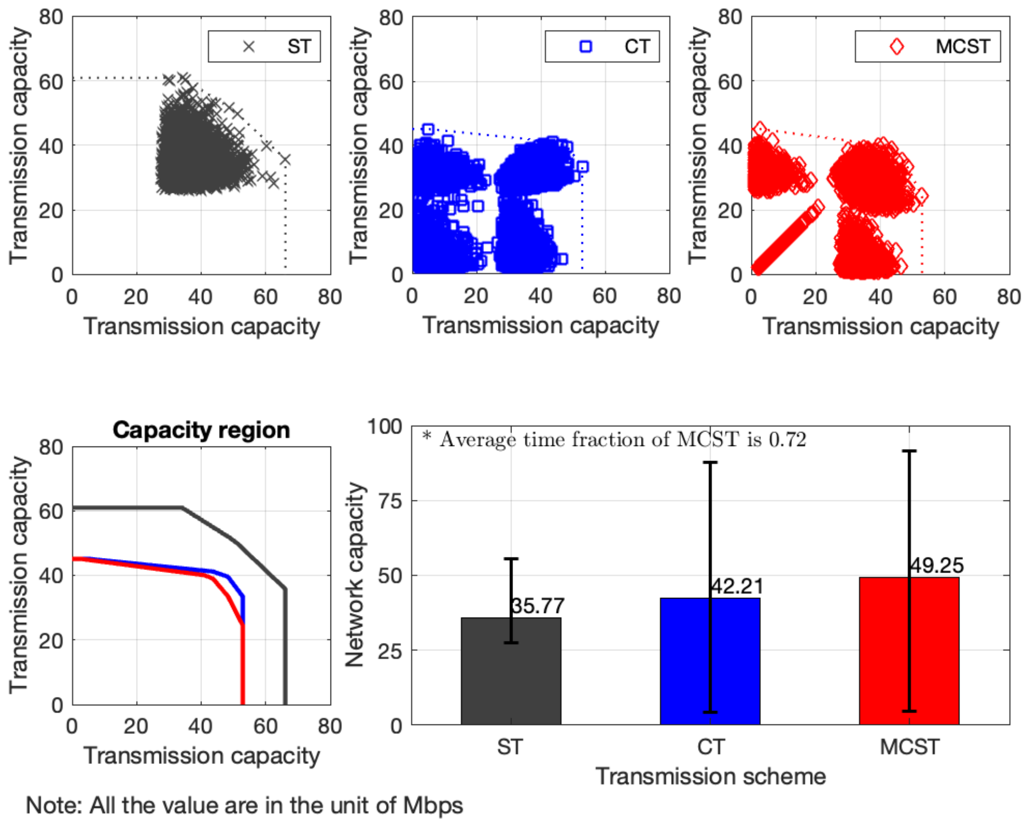

Figure 2.8: Capacity study of transmission strategy in random topology scenario with two transmissions

model and the link capacity model according to Shannon's capacity [63]. Figure 2.8 presents the performance of three transmission strategies of ST, CT, and MCST schemes. A detailed discussion of the MCST scheme is conducted in the following chapter. Through the ST, there is no interference between the two transmissions. Therefore, the transmission capacity is higher than the other two transmission strategies of CT and MCST. This is because the concurrent transmissions cause interference with the other receiving nodes. However, the simulation results show that the network capacity given by CT and MCST schemes is higher than ST because of the temporal reuse mechanism.

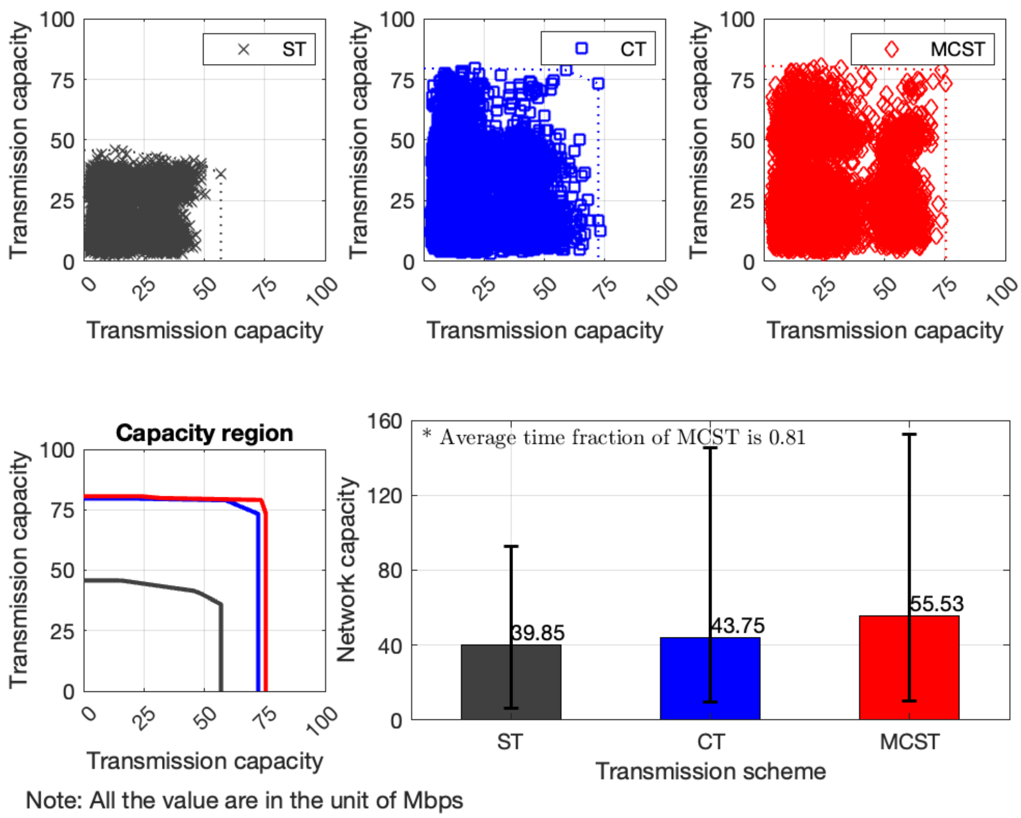

Figure 2.9: Capacity study of relaying strategy in random topology scenario with two transmissions

The simulation of the previous capacity study is extended by considering the transmission as the BRF transmission to study capacity improvement due to the relaying strategy. Therefore, the network has six wireless nodes and two BRF transmissions. Figure 2.9 describes the transmission capacity and network capacity study through the relaying strategy. As illustrated in the figure, the transmission capacity increases due to the probability of the closer distance between the transmitter and receiver. Therefore, by integrating the relaying strategy with the transmission strategy, the transmission capacity can be optimized, leading to a higher network capacity.

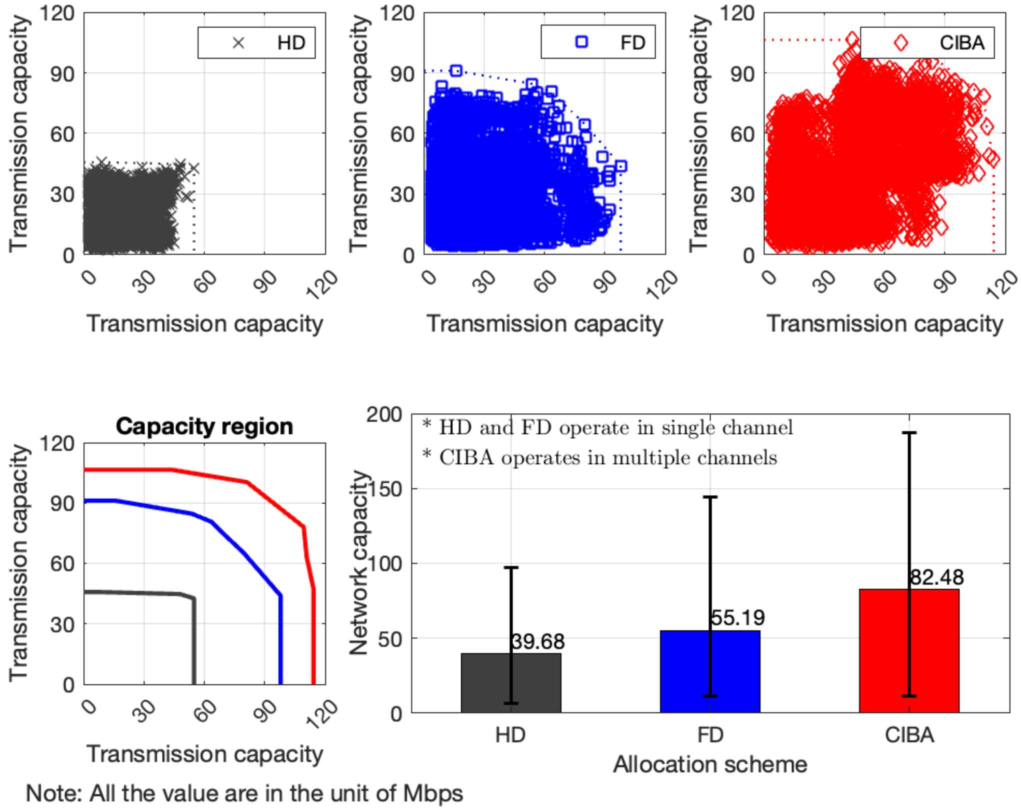

Figure 2.10: Transmission capacity and network capacity study with allocation strategy in random topology scenario with two transmissions

To conduct the capacity study of the channel allocation strategy, the previous simulation is assumed to be the cooperative communication system operated with two sub-channels instead of a single channel. Figure 2.10 shows the transmission and network capacity study of the channel allocation schemes for the network with two BRF transmissions. In the single-channel allocation, the HD system represents the ST, and the FD system represents CT in the networks. On the other hand, for the multi-channel allocation, the dynamic channel allocation of the CIBA scheme is considered with the two sub-channels in the networks. A detailed discussion of the CIBA scheme is conducted in the following chapter. The figure shows that if there is only one channel in the network, CT benefits ST in terms of network capacity. However, the multi-channel allocation strategy via CIBA benefits transmission capacity and brings a higher network capacity than the single-channel allocation regardless of HD or FD systems. In conclusion, the simulation results reveal that communication strategies of transmission strategy, relaying strategy and allocation strategy can provide impressive benefits for optimum transmission capacity in multihop wireless networks.

2.6 Assumptions and Constraints

The coreMAC framework is proposed for wireless networks with cooperative communication strategies. In this dissertation, the network is assumed to be the distributed cooperative communication system with a single relay node. Only BRF transmission with two-hop data transfer operation is considered in multihop wireless networks. Generally, cooperative communication can be implemented through amplify-and-forward, decode-and-forward and coded cooperation methods [48]. However, the discussion of relaying strategy for implementing cooperative communication, for example, amplify-and-forward, decode-and-forward, and the overhead required to perform the cooperative communication are ignored in this dissertation. And, the transmission is assumed or treated as a cooperative communication for exchanging information with each other under perfect channel state information. Furthermore, in the FD system, the SI can be successfully suppressed until the noise level through the SI cancellation techniques is an assumption in this dissertation. Therefore, only the IUI from the concurrent ongoing transmissions is taken into account in this research. In the network, the nodes are randomly distributed, and the node mobility model is not considered. The node selection to form the BRF transmission is random, and the relay node selection is ignored in the research. Besides, all the transmitting nodes are in saturated traffic conditions and have the same sized DATA frame for transmission. In addition, the time synchronization issue on simultaneous transmission is neglected for simplicity.

As the constraint, all the nodes have to be enabled with FD capability since the proposed framework performs the mixture of concurrent and sequential transmission in multihop wireless networks. The nodes are equipped with SI cancellation techniques for simultaneous transmission and reception. Besides, the devices with static transmit power, and static channel allocation cannot be used for the proposed framework.

2.7 Summary

This chapter has discussed the key technologies associated with the proposed framework. Additionally, the three cooperative communication strategies of the framework are presented. Following that, this chapter also describes the whole framework for efficient communication of future wireless networks.

Chapter 3

Mixture of Concurrent and Sequential Transmission Scheme

In this chapter, the MCST scheme is designed as a capacity management module of the coreMAC framework. Compared with the existing transmission schemes, the proposed MCST scheme optimizes the BRF transmission capacity with transmission and relaying strategies. As a result, the superiority in achievable network capacity and achievable throughput can be acquired even in a dense network.

The chapter is structured with six main sections. First, a broad overview of the research and literature on capacity management is enclosed. Second, the system model and assumption are described. Third, the proposed MCST scheme is presented in detail. The fourth section presents the numerical simulation to show the capacity improvement of the MCST scheme. Besides, the fifth section describes the performance of the MCST scheme over LoRa networks. Then, the sixth section draws the summary of the chapter.

3.1 Research Background

The FD system is well known for increasing the achievable spectral efficiency of wireless transmission. Although the simultaneous transmission of the FD system results in the residual SI, its potential transmission capacity gain of communicating pair improves the overall network capacity. Many research works have been done for capacity optimization of the FD systems through concurrent transmissions, with or without the relaying strategy, in wireless LAN and mobile wireless (cellular) networks.

This chapter proposes a new MAC with an efficient transmission scheme in the FD wireless networks. There are three objectives in this chapter as follows:

- design an algorithm for the transmission capacity optimization through the MCST scheme
- propose an FD MAC protocol with MCST scheme as FD-MCST for the BRF transmission
- conduct the performance investigation of the proposed MAC using the Markov Chain approach and evaluate the performance by comparing the current FD MAC

3.1.1 Literature Review

There is a list of literature reviews conducted on FD systems for improving transmission performance in wireless networks.

Related Works in Wireless LAN

In wireless LAN, Cheng et al. proposed an RTS/FCTS FD MAC protocol by utilizing the idea of request-to-send (RTS) and clear-to-send (CTS) handshaking mechanism for the FD wireless networks [64]. A simple FD MAC protocol with CSMA/CA mechanism is proposed in [65]. The simulation results show that detecting and monitoring channel usage can reduce the average collision length. Similarly, an analytical framework with a Markov Chain approach is proposed for FD MAC protocol with CSMA/CA mechanism by modifying the network settings [66]. The simulation results reveal that the FD system gain compared to the HD system decreases as the network grows due to collisions. Similarly, with CSMA/CA mechanism, Song et al. designed their FD protocol for the single-hop network which lets the node detect collisions while transmitting and abort transmission when there is a collision [67]. The results show the system throughput improved at least two times more than the HD system. Zuo et al. also proposed FD-distributed MAC protocol, namely FD-DMAC, and theoretically analyzed with the Markov Chain to show almost 90% throughput improvement over HD MAC protocol [68]. Kim et al. conducted the study of network capacity through the user scheduling with and without the relay node in the FD wireless networks [69]. This research argues that as the number of nodes in the network increases, the probability of FD transmission pair is high, and the throughput gains also increase regardless of the collision probability. Furthermore, Choi et al. proposed an antenna allocation scheme for the capacity improvement of FD systems in the IEEE 802.11ac WLAN [70].

Related Works in Mobile Wireless

Meanwhile, some research work on the network capacity of FD systems can be found in mobile wireless networks. For example, Kim et al. proposed a centralized FD MAC protocol that increases the number of CT pairs with the spatial reuse for the device-to-device (D2D) communications [71]. The simulation results show almost twice of throughput performance of HD. Using theoretical analysis, similar research has been done in [72] that derives the outage probability as well as transmission rate as channel characteristics for selecting parameters of the optimal power allocation and successive interference cancellation (SIC).

Related Works in Interference Cancellation

The other way to guarantee and improve the FD performance is the cancellation techniques of SI, and IUI [73]. A great deal of research has been done to address the interference issues in wireless LAN. For example, Yau et al. designed the SI suppression algorithm to decode the received signal from the specific interference region [38]. In addition, Anttila et al. proposed a digital SI cancellation in [74] and showed the achievement of up to 103 dB of the total interference cancellation that gives the FD system almost 90% throughput improvement to the HD system. Ji et al. also proposed an advanced duplex scheme for SI suppression and optimizing capacity in FD infrastructure-based networks [75]. Additionally, Na and Lee also argued that the downlink spectral efficiency can be enhanced by canceling IUI through the orthogonal matrices selecting the antenna of the base station in the FD wireless networks [76]. Similarly, Shi et al. designed an optimization algorithm for SIC and showed up to 5x throughput improvement in [26]. In addition, Han et al. derived the FD performance with SI and IUI in the network with the relaying strategy and argues that the interference limits the transmission capacity [77]. Recently, Yang et al. [78] proposed an FD MAC with a TPC similar to [79] and the results reveal that nearly 35% of the throughput can be improved than the other FD MAC. Throughout the above research, it can conclude that the concept of interference cancellation, as well as the relaying strategy, can bring higher network capacity to the FD system.

Related Works in Hybrid-duplex Systems

Recently, a hybrid HD/FD system approach, also referred to as a hybrid-duplex system, along with management and control of CT has been discussed in the FD system. Hybrid duplex systems have demonstrated the ability to increase capacity and reduce interference by enabling the node as HD or FD system. In the hybrid FD/HD system approach, [80] analyzes the throughput of adaptive FD and HD communication modes according to the interference power of the wireless nodes. According to the theoretical study in [81], the performance gain of the FD system over the HD system cannot be guaranteed because of the IUI. However, the hybrid-duplex systems can achieve performance comparable to the capacity of the HD and FD systems [82–85]. In particular, Yao et al. proposed an X-Duplex with flexible and switchable transmission modes to optimize the network capacity [82]. The proposed X-Duplex selects ST or CT based on the channel state information (CSI) affected by SI. However, Tand et al. [83] also proposed a hybrid-duplex system that switches the transmission mode depending on the received power and showed around 45% network capacity improvement than the pure FD system. Also, Huang et al. proposed an idea for frame allocation and power allocation according to the transmission traffic in the hybrid-duplex system [85]. Even so, the flexible allocation of the hybrid-duplex system does not consider the tradeoff between optimal energy consumption and capacity gain in the network.

Related Works in Hybrid-duplex Systems with Relaying Strategy

The hybrid-duplex system is integrated with the relaying strategy in [86], and the outage probability is used to switch the transmission between direct transmission or transmission via the relay node. Chen and Zhao also proposed a hybrid system that allows transmission mode switching according to SINR [87]. Unlike [87], the transmission is switched between the primary and secondary transmitters according to SI in [88]. However, this proposed hybrid system gives the optimum throughput only if the two transmitters have equal transmit power. In [89], Li et al. proposed the hybrid-duplex system in which the wireless node has more than one antenna. If the system works as the HD, in the transmitting timeslot, the relay node combines the received signal and forwards it to the destination asynchronously. But, the proposed system is useful when the ratio of the hybrid system works as the HD is higher than the FD system. Khafagy et al. proposed the buffer-aided hybrid system with buffer support that switches transmission mode according to SI [90]. For the fixed-rate transmission, the proposed protocol uses the transmission as either HD or FD system depending on the link outage conditions.

The transmission efficiency of the FD wireless networks depends on the difference in packet size and the uplink and downlink transmission time of CT [91]. Hence, Lee designed a MAC protocol that can adaptively switch between the FD or a multiuser multi-input-multi-output system [92] and improved the throughput by up to 15% to a pure FD system. In addition, Kim et al. introduced the algorithm for transmission mode switching by taking into account the coding and modulation schemes [93]. The algorithm changes to ST for using the uplink and downlink transmission timeslot unused by CT. Recently, Gupta and Venkatesh proposed FD MAC protocol based on IEEE 802.11 with the distributed coordination function (DCF) [94]. Their MAC works as HD MAC when huge SI is detected, and the simulation result reveals double the throughput capacity compared to HD. Although their research does not consider the IUI, at least twice the throughput improvement than HD can be achieved. In addition to the capacity, [95] presented the application of the FD system in the radar communication system for localization and user tracking. Bazzi et al. also presented the CSMA/CA mechanism-based FD system for wireless networks with IEEE 802.11p standard in vehicular environments [96]. In the research, the proposed FD system allows the vehicles to send messages to each other and improves transmission reliability because the sensing capability of FD while transmitting can detect the collision and avoid late retransmission. Currently, there are research studies on FD wireless network capacity investigation through interference cancellation, MAC protocol, TPC, user scheduling, and the hybrid system approach. But, the cooperative transmission scheme is still lacking in the FD systems to guarantee the optimal transmission capacity.

3.1.2 Motivation

The hybrid-duplex system has been investigated with and without the relaying strategy, but ST alone is used in the HD system, and only CT is considered in the FD systems. Indeed, the communications in the FD system are not performing well, especially in a highly dense network environment [20, 73, 97]. This is because the vast caused CCI from CT among the wireless nodes in the FD system strongly degrades the overall network capacity. Additionally, there are some compatibility issues with the hybrid system that pose at the MAC layer and get attention as the possible solution for capacity optimization in the wireless networks [98]. Throughout those related works, a comprehensive study of transmission schemes in the hybrid system is still missing. As mentioned earlier, CT in the FD system provides spectral efficiency and produces a huge total interference power in the network. Therefore, as mentioned in [99], it is worth considering integrating the ST for low interference power in the FD wireless networks instead of combining HD and FD systems as a hybrid system. However, there is no transmission scheme considering both ST and CT in FD wireless networks. Although the hybrid-duplex system is well known for providing benefits to both the HD and FD systems, the MAC protocol for these systems must be investigated with its theoretical capacity studies. Besides, the tradeoff between capacity gain and interference of the CT in the FD wireless networks is not mentioned in the above studies. Therefore, these discussions provide the motivation for proposing a novel MAC protocol with a transmission scheme that cooperatively manages both CT and ST to optimize transmission capacity and reduce interference power while optimizing the overall capacity in the FD wireless networks.

3.2 System Model

This research considers the FD wireless network with no central control node as the distributed multiple wireless networks. All wireless nodes are assumed as the shared-antenna FD system so that they can simultaneously transmit and receive in a single-frequency band through a circulator. As illustrated in Figure 3.1, in the network, the relay FD transmission is considered as a single relaying transmission flow in which a source node (S) transmits to a destination node (D) through a relay node (R). As an

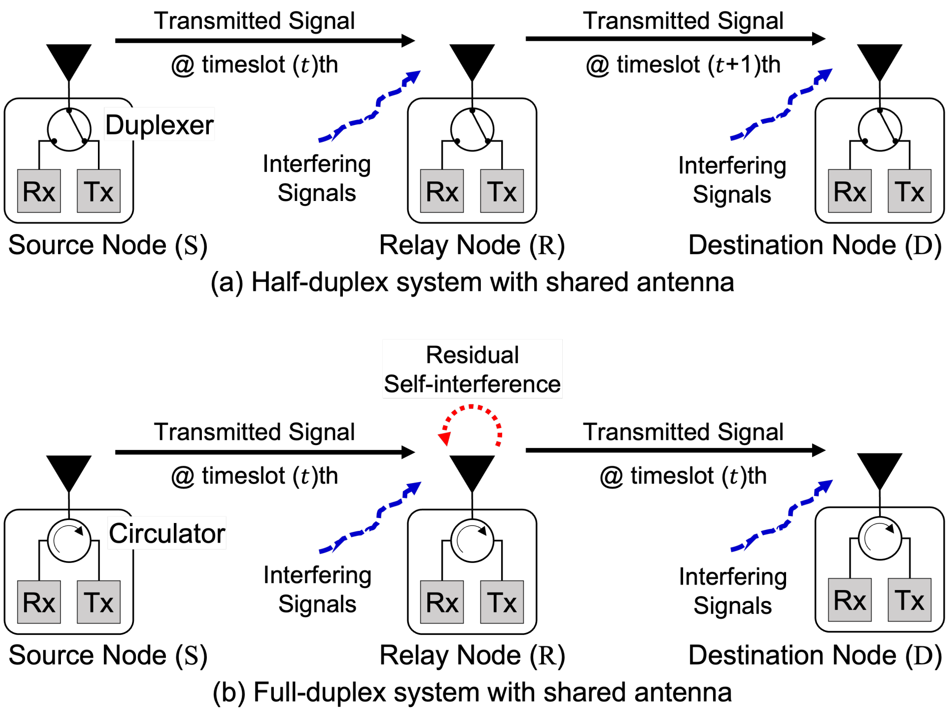

Figure 3.1: An example of a single relaying transmission in two types of communication system

assumption, the FD-enabled wireless node adopts the SI cancellation techniques, and the SI can be suppressed until the noise level [81,100]. Therefore, this research totally neglects the effect of SI. Generally, the wireless relay system can apply the relaying strategies of amplify-and-forward relaying strategy, decode-and-forward relaying strategy, etc, as a cooperative communication strategy. However, to focus on the study of capacity, this research neglects the discussion of applied relaying strategy for the purpose of simplicity. It considers the transmission in the network as the cooperative transmission by assuming the wireless node knows the perfect CSI from the other nodes. Therefore, the single relaying transmission flow is simply defined as the BRF transmission, which is the combination of source-relay (SR) transmission and relay-destination (RD) transmission by neglecting the time synchronization problem in the network. Due to the shadowing effects, this research assumes that there is no direct transmission from S to D.

As the system model, let $\mathbb{N} = \{1, \ldots, n, \ldots, N\}$ denote the set of nodes where N is the total number of nodes. Each BRF transmission can be selected from the set of BRF transmissions $\mathbb{F} = \{1, \ldots, f, \ldots, F\}$ where F is the number of BRF transmissions and $F = N/3$. In this research, the selection of node combinations in a single BRF transmission is random for the theoretical analysis purpose in the single network.

3.2.1 Channel Model

The signal attenuation of the transmission link over a communication channel depends on the propagation model of the log-distance pathloss model without considering the frequency parameter. With the Friis free space model, the channel gain in the unit of decibel [dB] from the transmitting node i to the receiving node j, where $i, j \in \mathbb{N}$, is given as

$$PL_{ij} = PL_0 + 10 \cdot \alpha \cdot \log_{10}(\frac{d_{ij}}{d_0}) - W_{ij} + X_\sigma \tag{3.1}$$

where $PL_0 = 20 \cdot log_{10}(d_0)$, d_0 is the decorrelation distance which is 1 meter, α is the pathloss attenuation constant, d_{ij} is the euclidean distance between node i and node j and W_{ij} is the wall attenuation of the transmission. In the research, the pathloss model considers an instantaneous fading as a Gaussian random variable (X_σ) with zero mean and standard deviation of σ. Therefore, the received power ratio between the transmitting node i and receiving node j is

$$G_{ij} = \frac{1}{10^{\left(\frac{PL_{ij}}{10}\right)}} \tag{3.2}$$

3.2.2 Interference Model

The interference model is used to determine the amount of power level of interfering nodes, i.e., IUI, on an ongoing transmission from node i to node j. With the concept of a well-known power capture model [101], a signal-to-noise ratio (SNR)-based interference model is defined to obtain the set of interfering nodes ($\mathcal{I}$) of ongoing transmission. With the assumption of a similar transmission range and carrier sensing range, Figure 3.2 illustrates an example of an SNR-based interference model that uses the SNR of the ongoing transmission to determine $\mathcal{I}$, which is given as

$$SNR_{ij} = \frac{G_{ij} \cdot P_i}{\eta_j \cdot B} \tag{3.3}$$

where P_i is the transmit power of node i, η_j is the noise level of node j and B is the channel bandwidth of the transmission. If node k is the concurrent transmitting node in the same transmission medium, the SNR of node k to node i and node j of the ongoing transmission is SNR_{ki} and SNR_{kj}, respectively. In the interference mode, the concurrent

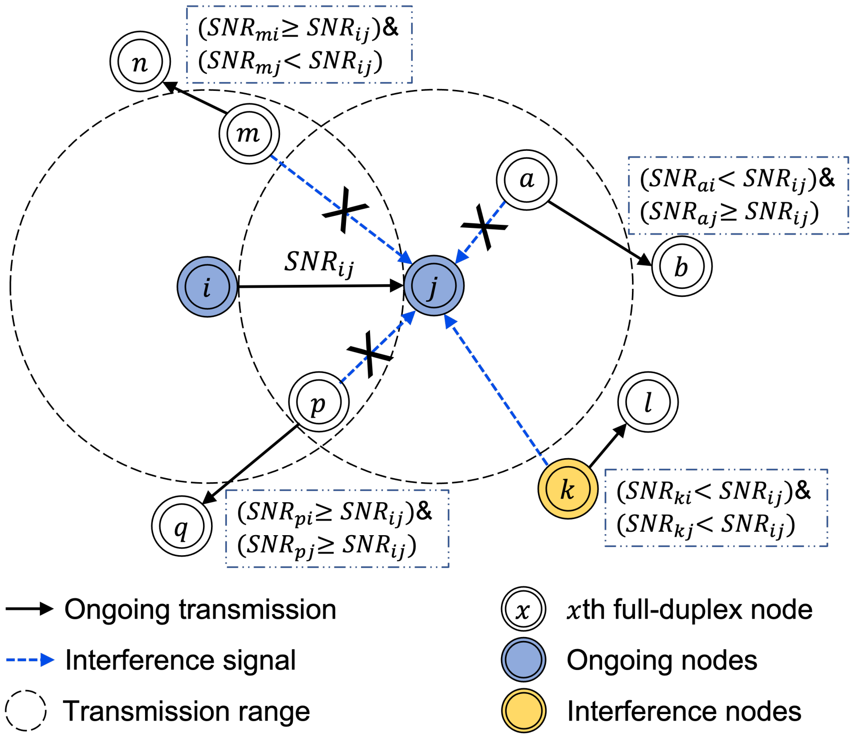

Figure 3.2: An example of SNR-based interference model

transmitting node k is defined as the interfering node; on the other way, $k \in \mathcal{I}$ if and only if $SNR_{ki} < SNR_{ij}$ and/or $SNR_{kj} < SNR_{ij}$.

3.2.3 SINR Model

A successful transmission occurs only if the SINR is above a certain threshold β. The SINR obtained at the node j from the node i is computed as

$$SINR_{ij} = \frac{G_{ij} \cdot P_i}{\eta_j \cdot B + \sum_{k \in \mathcal{I}, k \neq i} G_{kj} \cdot P_k} \tag{3.4}$$

3.2.4 Link Capacity Model

The transmission rate R in the unit of bit/s over a communication channel of the ongoing transmission from node i to node j is defined according to Shannon's capacity [63] and is computed as

$$R_{ij} = B \cdot log_2(1 + SINR_{ij}) \tag{3.5}$$

3.2.5 Transmission Capacity

Through the transmission scheme, the BRF transmission can be completed sequentially or concurrently in the FD system. The transmission capacity C of a single BRF transmission through the ST strategy is computed as

$$C = \frac{(R_{\mathrm{SR}}^{seq})^2 + (R_{\mathrm{RD}}^{seq})^2}{R_{\mathrm{SR}}^{seq} + R_{\mathrm{RD}}^{seq}} \tag{3.6}$$

where R_{SR}^{seq} and R_{RD}^{seq} are the transmission rates R_{SR} and R_{RD} based on the SNR_{SR} of SR transmission and the SNR_{RD} of RD transmission of a BRF, respectively.

With the CT strategy, the transmission capacity of a single BRF transmission is computed as

$$C = R_{\mathrm{SR}}^{con} + R_{\mathrm{RD}}^{con} \tag{3.7}$$

where R_{SR}^{con} and R_{RD}^{con} are the transmission rates R_{SR} and R_{RD} based on the $SINR_{\mathrm{SR}}$ of SR transmission and the $SINR_{\mathrm{RD}}$ of RD transmission of a BRF, respectively.

3.3 MCST Scheme

This section describes the MCST scheme for transmission capacity optimization through the capacity management module, especially in the FD wireless networks.

3.3.1 Algorithm for MCST Scheme

The MCST scheme is a cooperative transmission scheme that operates over the BRF transmission through cooperative communication strategies, i.e., transmission and relaying strategies, in the FD wireless networks. The ST can give less interference power and moderated capacity with sequential transmissions while CT can improve the spectral efficiency of the transmission. However, the interference also increases due to the spatial reuse mechanism of CT and the increased number of transmissions in the network. With the concept of the HD/FD system, the MCST scheme combines ST and CT in the allocated timeslot to obtain the optimum transmission capacity with the low IUI. MCST scheme optimizes the transmission capacity of the BRF transmission with the time fraction of the CT. In this way, MCST gives a higher transmission capacity than ST and CT. The reason is the SR and RD transmission rates are different in ST and CT, and equal

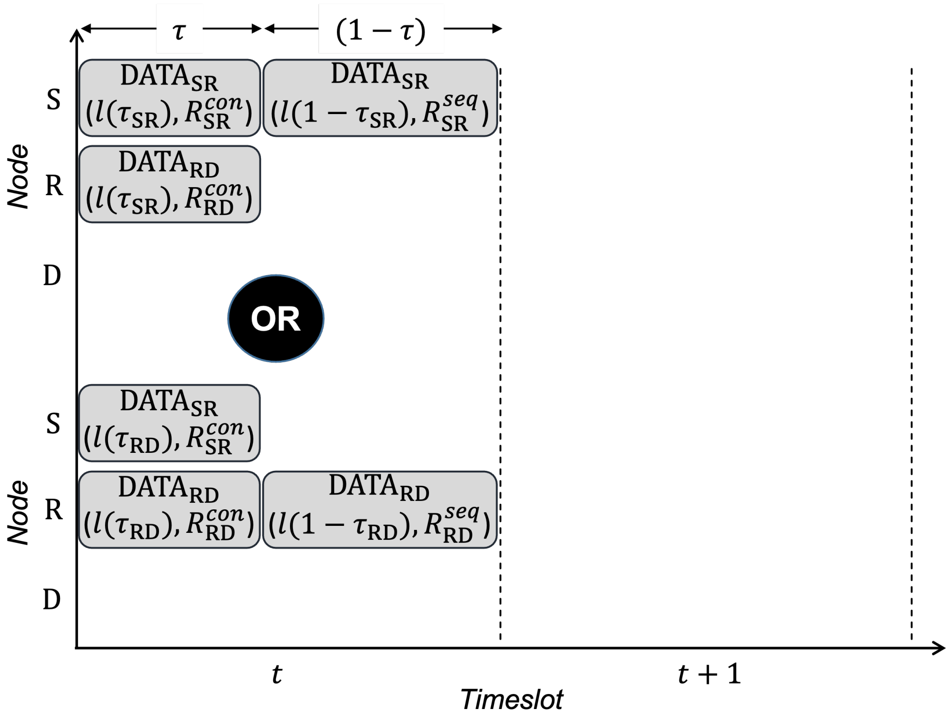

Figure 3.3: An example of MCST scheme for a BRF transmission

in the MCST scheme via the time fraction. The optimal achievable transmission capacity (OATC) algorithm is designed to support the MCST scheme in determining the optimum transmission capacity of the BRF transmission. Figure 3.3 illustrates an example of the MCST scheme with the SR transmission or RD transmission as sequential transmission depending on the source node or the relay node of a BRF transmission, respectively. Since the discussion about synchronization issues is omitted in this dissertation, the order of concurrent transmission or sequential transmission is neglected for theoretical study purposes. In this example, the MCST scheme performs the CT of SR and RD transmissions of the BRF transmission in the time fraction of τ and either SR transmission or RD transmission in $(1-\tau)$. However, allowing the sequential transmission in the first time fraction gives benefits to consider synchronization in the implementation of the real network scenarios. The time fraction is computed at the relay node for both conditions of either SR transmission or RD transmission performing sequential transmission by assuming the transmission rates are equal in the MCST scheme. **Algorithm** 1 describes the OATC algorithm for the MCST scheme through the measured signal quality, i.e., SNR_{SR}, SNR_{RD}, $SINR_{\text{SR}}$ and $SINR_{\text{RD}}$, of a BRF transmission and observes the following steps:

Algorithm 1 Optimum Achievable Transmission Capacity Algorithm

Definition: C_{SR} and C_{RD} are the transmission capacity of a BRF transmission as SR transmission and RD transmission are choices of sequential transmissions, respectively, $MCST(\tau, \mathcal{R})$ is MCST information in which τ is time fraction and $\mathcal{R}$ is the transmission control

Input: SNR_{SR}, SNR_{RD}, $SINR_{\mathrm{SR}}$, $SINR_{\mathrm{RD}}$

Output: τ and $\mathcal{R}$

function OATC
  Calculate R^{seq}_{SR}, R^{seq}_{RD}, R^{con}_{SR}, R^{con}_{RD}
  Compute $\tau_{\mathrm{SR}} = \frac{R^{seq}_{\mathrm{SR}}}{R^{seq}_{\mathrm{SR}} - R^{con}_{\mathrm{SR}} + R^{con}_{\mathrm{RD}}}$
  Compute $\tau_{\mathrm{RD}} = \frac{R^{seq}_{\mathrm{RD}}}{R^{seq}_{\mathrm{RD}} - R^{con}_{\mathrm{RD}} + R^{con}_{\mathrm{SR}}}$
  Compute $C_{\mathrm{SR}} = \tau_{\mathrm{SR}} \cdot (R^{con}_{\mathrm{SR}} + R^{con}_{\mathrm{RD}}) + (1 - \tau_{\mathrm{SR}}) \cdot R^{seq}_{\mathrm{SR}}$
  Compute $C_{\mathrm{RD}} = \tau_{\mathrm{RD}} \cdot (R^{con}_{\mathrm{SR}} + R^{con}_{\mathrm{RD}}) + (1 - \tau_{\mathrm{RD}}) \cdot R^{seq}_{\mathrm{RD}}$
    if $C_{\mathrm{SR}} > C_{\mathrm{RD}}$ **then**
      Set $\tau \leftarrow \tau_{\mathrm{SR}}$
      Set $\mathcal{R} \leftarrow 0$ ▷ $\mathcal{R}$ has '0' bit
    else
      Set $\tau \leftarrow \tau_{\mathrm{RD}}$
      Set $\mathcal{R} \leftarrow 1$ ▷ $\mathcal{R}$ has '1' bit
    end if
  return $MCST(\tau, \mathcal{R})$
end function

1. With the previously mentioned channel model, interference model, SINR model, and link capacity model, the relay node calculates the transmission rates, i.e., R^{seq}_{SR}, R^{seq}_{RD}, R^{con}_{SR} and R^{con}_{RD} through the measured signal quality.

2. The time fraction of τ is computed as τ_{SR} or τ_{RD} for either SR transmission or RD transmission performing sequential transmission in $(1 - \tau)$, respectively, as follows:

$$\tau_{\mathrm{SR}} = \frac{R^{seq}_{\mathrm{SR}}}{R^{seq}_{\mathrm{SR}} - R^{con}_{\mathrm{SR}} + R^{con}_{\mathrm{RD}}} \tag{3.8}$$

and

$$\tau_{\mathrm{RD}} = \frac{R^{seq}_{\mathrm{RD}}}{R^{seq}_{\mathrm{RD}} - R^{con}_{\mathrm{RD}} + R^{con}_{\mathrm{SR}}} \tag{3.9}$$

3. The transmission capacity, C, of a single BRF transmission through MCST, is computed as C_{SR} and C_{RD} for either SR transmission or RD transmission performing sequential transmission in $(1-\tau)$, respectively, as follows:

$$C_{\mathrm{SR}} = \tau_{\mathrm{SR}} \cdot (R_{\mathrm{SR}}^{con} + R_{\mathrm{RD}}^{con}) + (1-\tau_{\mathrm{SR}}) \cdot R_{\mathrm{SR}}^{seq} \tag{3.10}$$

and

$$C_{\mathrm{RD}} = \tau_{\mathrm{RD}} \cdot (R_{\mathrm{SR}}^{con} + R_{\mathrm{RD}}^{con}) + (1-\tau_{\mathrm{RD}}) \cdot R_{\mathrm{RD}}^{seq} \tag{3.11}$$

4. The transmission capacity is optimally selected upon the computed transmission capacity with the condition of either SR or RD transmission performing sequential transmission. The algorithm determines and results in the time fraction, τ, and the transmission control, $\mathcal{R}$, to instruct for the sequential transmission by setting either '0' or '1' to indicate SR transmission or RD transmission as sequential transmission, respectively, for the optimum transmission capacity as follows:

$$(\tau, \mathcal{R}) \Leftarrow \begin{cases} (\tau_{\mathrm{SR}}, 0) \text{ if SR performs sequential transmission} \\ (\tau_{\mathrm{RD}}, 1) \text{ if RD performs sequential transmission} \end{cases} \tag{3.12}$$

3.3.2 FD-MCST Protocol

This section discusses the design of the FD-MCST to optimize the transmission capacity in FD wireless networks. Based on the basic access mechanism of DCF in IEEE 802.11 Wireless LAN, FD-MCST is designed with the minor modification of the four-way handshaking technique. In the network, when a node wants to start transmitting new data, it first senses the state of the channel. If the channel is free for DCF interframe space (DIFS), the data transmission can be done with the four-way handshaking mechanism. Otherwise, the node holds the transmission and continues to sense the channel. Upon the DIFS, the node running the DCF mechanism adopts a binary exponential backoff algorithm. In the algorithm, the backoff time is uniformly selected within the range of $[0, CW)$, where CW is the contention window and the size increases depending on the number of retransmissions. The initial backoff contention window size is the same as the minimum contention window size $CW = CW_{min}$, for the first transmission attempt. After each failed transmission, CW is doubled up to $CW_{max} = 2^m \cdot CW_{min}$ where m is the maximum number of retransmission stages.

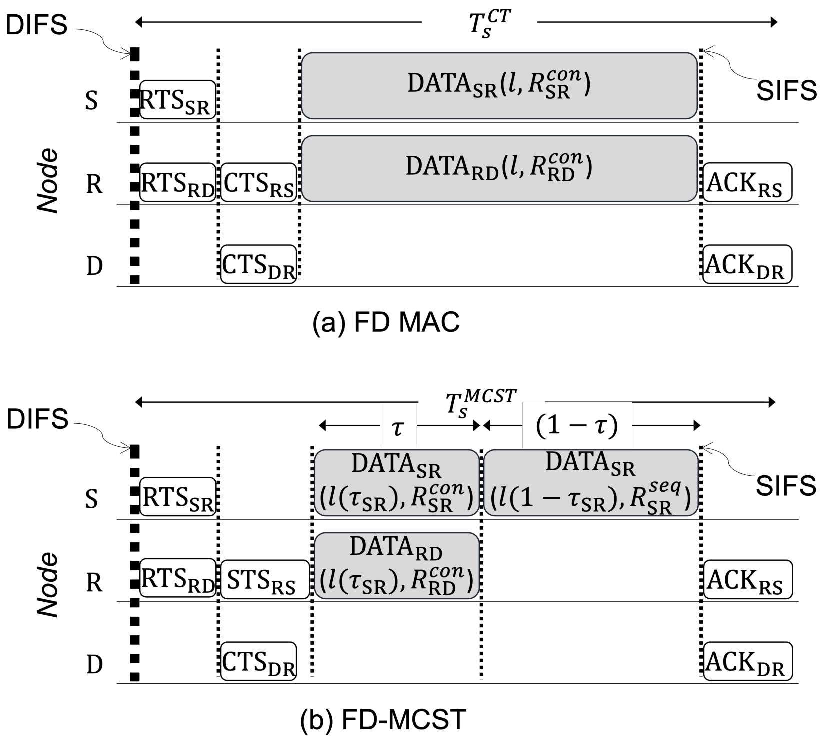

Figure 3.4: The frame exchanging sequence for the successful transmission time of a BRF transmission with (a) FD MAC with concurrent transmission and (b) an FD-MCST when SR transmission performs sequential transmission after time fraction of τ_{SR}

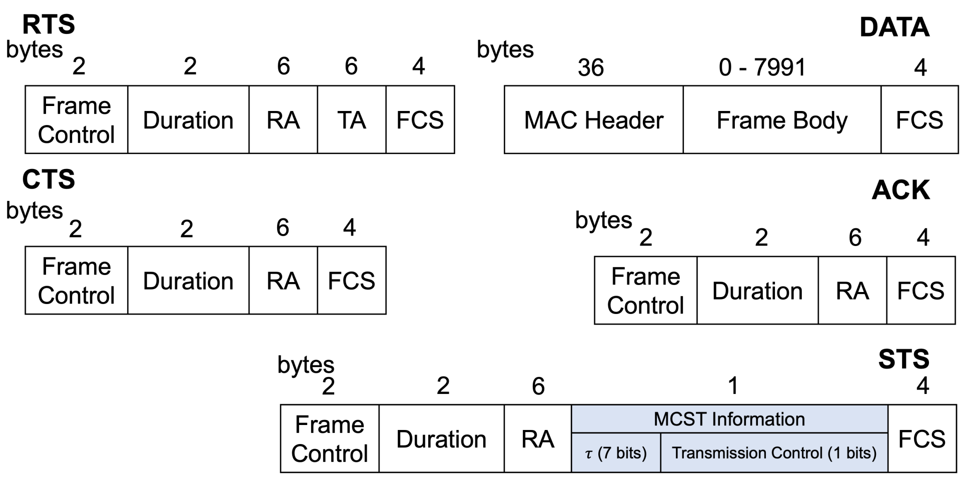

Figure 3.5: The frame formats of the control and DATA for FD-MCST

Figure 3.4(a) represents an example of the frame exchanging sequence for the successful transmission of a BRF transmission through an FD MAC with the CT. Similarly, the frame exchanging sequence of a BRF transmission for an example of SR transmission performs sequential transmission over FD-MCST protocol is illustrated in Figure 3.4(b) with a new set-to-send (STS) control frame. The STS control frame is adopted in the IEEE 802.11 wireless LAN frame format specification. In FD-MCST, the source and relay nodes start the data transmission using the request-to-send (RTS) and clear-to-send (CTS) handshaking mechanism. Specifically, the source and relay nodes transmit the RTS control frames to the relay node and destination node, respectively. Upon receiving the RTS control frame, the destination node replies with the CTS control frame to the relay node for proceeding with the data transmission. Then, the relay node transmits the STS control frame to the source and destination nodes at the basic rate by applying the OATC algorithm described in the previous section. The STS control frame contains the MCST information for time fraction τ and transmission control $\mathcal{R}$ for the sequential transmission instruction. When an STS frame is received, the source or relay node performs the sequential transmission for the remaining time fraction. However, if the relay node discovers that the transmission capacity through the MCST scheme is not higher than CT, CTS control frame will be sent instead of STS control frame to keep CT as FD MAC. When the data transmission is complete, the relay and destination nodes send the acknowledgement (ACK) control frame to acknowledge the transmission completion. Figure 3.5 shows the slightly modified frame format of the control and DATA frames for the transmission with IEEE 802.11 specification for FD-MCST.

Successful Transmission Analysis

According to the schematic analysis of frame exchange in Figure 3.4 for a BRF transmission, the total time required for the successful transmission can be obtained. Suppose that T_{DIFS} is the duration of DIFS, T_{SIFS} is the duration of short interframe space (SIFS), T_{RTS} is the duration for RTS control frame, T_{CTS} is the duration of CTS control frame, T_{STS} is the duration of STS control frame, T_{ACK} is the duration of ACK control frame, T_{PHY} is the time of physical preamble and header, H is the size of the MAC header and trailer, and R_{base} is the basic rate. The propagation delay or overhead for cooperative transmission is neglected in this research with the assumption that the distance between two communications is too small enough. Therefore, upon the successful transmission of the control frame exchange, the transmission overhead time, T_o for FD MAC and FD-MCST defined by T_o^{CT} and T_o^{MCST}, respectively, are

$$\begin{aligned} T_o^{CT} &= T_{DIFS} + T_{RTS} + T_{CTS} + T_{PHY} + \frac{H}{R_{base}} + T_{ACK} + 4T_{SIFS} \\ T_o^{MCST} &= T_{DIFS} + T_{RTS} + T_{STS} + T_{PHY} + \frac{H}{R_{base}} + T_{ACK} + 4T_{SIFS} \end{aligned} \tag{3.13}$$

Then, this research supposes that a node starts transmitting the data at the beginning of the timeslot with the DCF mechanism in which T_{BK} is the time of the initial backoff timer in the unit of slot time. Therefore, to transmit an l-byte DATA length, the successful transmission time, T_s for FD MAC and FD-MCST defined by T_s^{CT} and T_s^{MCST}, respectively, are

$$\begin{aligned} T_s^{CT} &= T_{BK} + T_o^{CT} + \frac{l}{\min\{R_{\text{SR}}^{con}, R_{\text{RD}}^{con}\}} \\ T_s^{MCST} &= T_{BK} + T_o^{MCST} + \frac{l}{R^{MCST}} \end{aligned} \tag{3.14}$$

where R^{MCST} is the transmission rate of SR transmission and RD transmission of the BRF transmission through the MCST scheme, which is computed as

$$R^{MCST} = \begin{cases} \tau_{\text{SR}} \cdot R_{\text{SR}}^{con} + (1 - \tau_{\text{SR}}) \cdot R_{\text{SR}}^{seq} \text{ if } \mathcal{R} \text{ has ‘0’ bit} \\ \tau_{\text{RD}} \cdot R_{\text{RD}}^{con} + (1 - \tau_{\text{RD}}) \cdot R_{\text{RD}}^{seq} \text{ if } \mathcal{R} \text{ has ‘1’ bit} \end{cases} \tag{3.15}$$

When a transmitting node starts the data transmission in a backoff slot, a transmission collision happens if one or more other nodes start transmission in the same backoff slot. As an assumption, a collision occurs upon the failure of the exchange of the RTS/CTS control frame. On the other hand, a collision is detected during the initial stage of data transmission, and the transmission time that faces the collision, T_c, is computed as

$$T_c = T_{BK} + T_{DIFS} + T_{RTS} + T_{timeout} \tag{3.16}$$

where $T_{timeout}$ is the duration for the timeout and T_c is similar for FD MAC with CT and FD-MCST in this dissertation.

3.3.3 Saturation Throughput Analysis

The FD-MCST is analyzed with the Markov Chain approach. Hence, all the nodes are assumed to be in saturated traffic conditions in the network. In other words, the transmis-

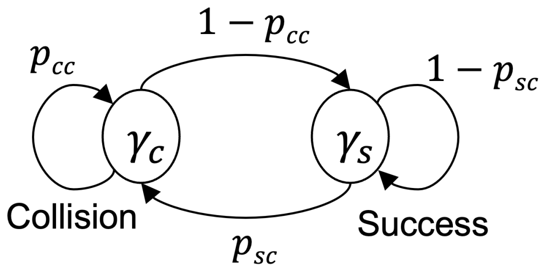

Figure 3.6: Two-state Markov Chain for the state transition of a receiving node

sion queues of the transmitting nodes are assumed to be always non-empty [65]. Based on the FD-MCST, the two-state Markov Chain, i.e., collision (γ_c) and success (γ_s) is applied for the state transition of a receiving node as shown in Figure 3.6. In this research, a collision occurs when a node fails to transmit the RTS frame. On the other hand, a success state occurs when a node has completely sent the last ACK frame. The next transmission state in the discrete-time Markov Chain depends on the previous state as in [102, 103]. Figure 3.6 illustrates the transition probability of the collision state and success state of the transmission. In this research, collision happens according to the conditional collision probability, p, which is computed as

$$p = \frac{2p'}{1 + p'} \tag{3.17}$$

where p' is the probability that the wireless node observes a collision and is computed as

$$p' = \gamma_c = \frac{p_{sc}}{1 - p_{cc} + p_{sc}} \tag{3.18}$$

where p_{cc} and p_{sc} denote the probability of the transmission transitions that a collision state is detected after the collision state and success state, respectively.

Figure 3.7 describes an example of the schematic analysis of the state transition between collision and success of two communicating nodes, i.e., node A and node B, with another transmitting node C, for the probability of p_{cc} and p_{sc} calculation. As an assumption, when node A starts to send an RTS control frame to node B, node C cannot transmit an RTS control frame in more than $c = (T_{RTS} + T_{SIFS})/\theta$ times where θ is the slot time length. Otherwise, as illustrated in Figure 3.7(a), a collision will occur. And, nodes A and C will uniformly select the backoff timer in the range of $[0, CW)$ as X_{A} and X_{C}, respectively. Then, the difference in beginning time for RTS control frame transmission in the state n is assumed as Y_{n}, which is chosen in $[-c, +c]$. In this way, the probability of

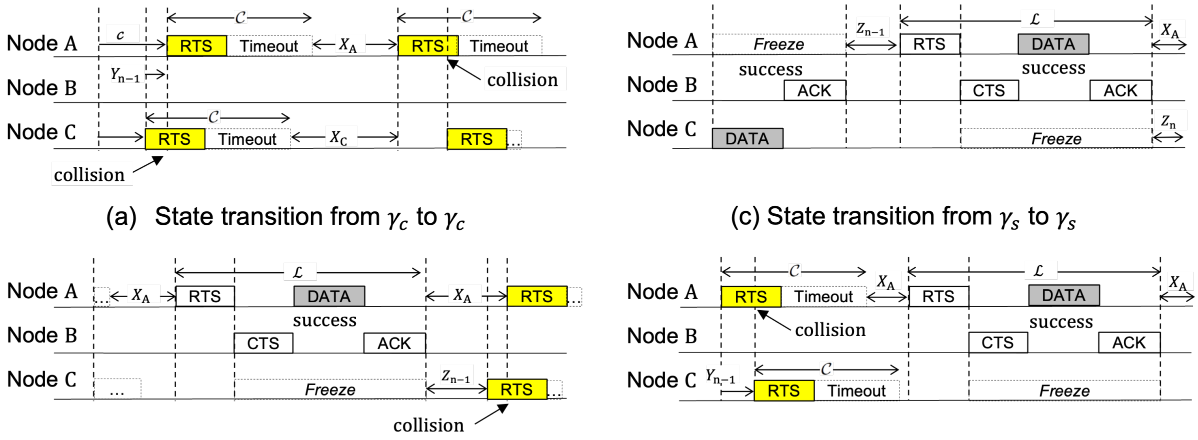

(a) State transition from γ_c to γ_c

(b) State transition from γ_s to γ_c

(c) State transition from γ_s to γ_s

(d) State transition from γ_c to γ_s

Figure 3.7: Schematic analysis of the state transitions for two communicating nodes

the transmission transition that a collision state is detected after a collision state becomes

$$p_{cc} = P\{-c \leq Y_{\mathrm{n}-1} + X_{\mathrm{C}} - X_{\mathrm{A}} \leq c\} \tag{3.19}$$

Besides, as shown in Figure 3.7(b), after the transmission is successful, the remaining backoff timeslot of a freezing node C at the state n is assumed as Z_{n}. And the probability of transition from a success state to a collision state is given as

$$p_{sc} = P\{-c \leq Z_{\mathrm{n}-1} - X_{\mathrm{A}} \leq c\} \tag{3.20}$$

Therefore, in the saturated traffic condition, the saturation throughput (S) of ongoing transmission is defined as the number of data frames transmitted during a specific time divided by the time of that period, and S is computed as

$$S = p_t \cdot \frac{(1-p)\mathcal{L}}{(1-p)\mathcal{L} + p\mathcal{C}} \cdot \frac{1}{\mathcal{L}} \tag{3.21}$$

where p_t is the transmission probability, $\mathcal{L}$ and $\mathcal{C}$ are the successful and collision period of transmission, respectively.

3.4 Numerical Simulations

This section evaluates the performance of the proposed FD-MCST through numerical simulation, which is discussed in the previous section. The performance evaluation is conducted by comparing the existing FD MAC protocols with RTS/FCTS [64] and FD-DMAC [68] in the FD wireless network. The original research work of FD-DMAC applies the TPC techniques to optimize the transmit power by satisfying the SINR threshold. However, only FD-DMAC without TPC is considered in this dissertation for a fair comparison. In addition, both of the existing protocols are one-size-fits-all protocols that consider only CT without any ST. The simulation is written using MATLAB R2021a for performance comparison. The verification of the program is done through section 2.5.1.

3.4.1 Simulation Scenarios and Settings

In this research, there are two simulation scenarios in this research. First, the performance analysis of the proposed FD-MCST is conducted with the influence of the number of BRF transmissions in the network and the influence on the DATA length in the 30-node random network topology. Second, the performance comparison between the proposed FD-MCST and two referenced FD MAC protocols is conducted. To perform the performance evaluation of the proposed FD-MCST, the simulation parameters and settings listed in Table 3.1 with the standard specification of IEEE 802.11ac [104] and the system model described in the previous section are applied. Figure 3.8 describes the block diagram of the numerical analysis for the proposed FD-MCST. In the network model, the wireless nodes are uniformly distributed over the 100 m $\times$ 100 m of the coverage area without considering the node mobility model. Besides, all the wireless nodes are identical, which means they are FD capability-enabled nodes with the same transmit power and the same channel bandwidth. In the traffic model, the transmission in the network is assumed as a single relaying transmission with a relay node or BRF transmission. The node combination in a BRF transmission is randomly selected in the network. And all the transmitters always have a DATA frame of the same size to send to other nodes. Furthermore, this research

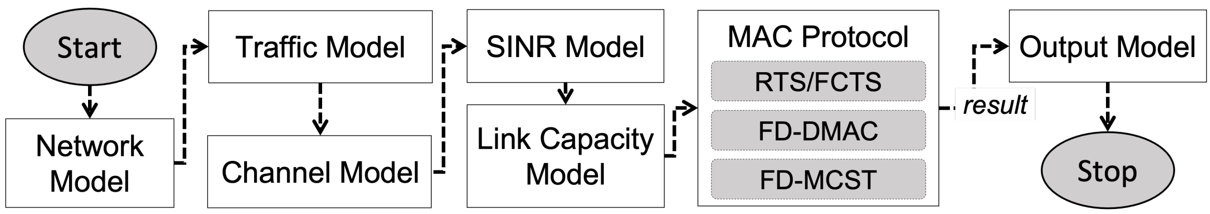

Figure 3.8: Block diagram of numerical analysis for MCST scheme

Table 3.1: Simulation parameters for evaluation of MCST scheme

Parameter	Value
Network coverage size	100 m × 100 m
Number of nodes (N)	3, 6, 9, 12, 15, 30, 60, 90, 120, 150
Transmit power (P)	20 dBm
Channel model	Log-distance pathloss
Attenuation constant (α)	3.5
Wall attenuation (W_{ij})	0 dB
Shadowing parameter (X_σ)	8 dB [62]
Noise level (η)	-174 dBm
Channel bandwidth (B)	20 MHz
Basic rate (R_{base})	24 Mbps
PHY header duration	44 μs
MAC header	320 bits
RTS size	160 bits
CTS size	112 bits
STS size	120 bits
ACK size	112 bits
DIFS length	34 μs
SIFS length	16 μs
Contention window (CW)	16 Slot time
Slot time length (θ)	9 μs
DATA length (l)	1500, 2500, 3500, 4500, 5500, 6500 bytes
Number of simulations	10,000 times

considers only one transmission per DATA for the theoretical study of network capacity purposes. All the MAC protocols are fairly evaluated without retransmission even when the collision happens. Therefore, the backoff timer is set to the initial backoff contention window, and $T_{timeout}$ is assumed as zero. Since the purpose is designing and evaluating the performance of the proposed FD-MCST by comparing it with other FD MAC protocols, the routing protocols are not considered. An example of a 9-node random network with three BRF transmissions is illustrated in Figure 3.9. In addition, the log-distance

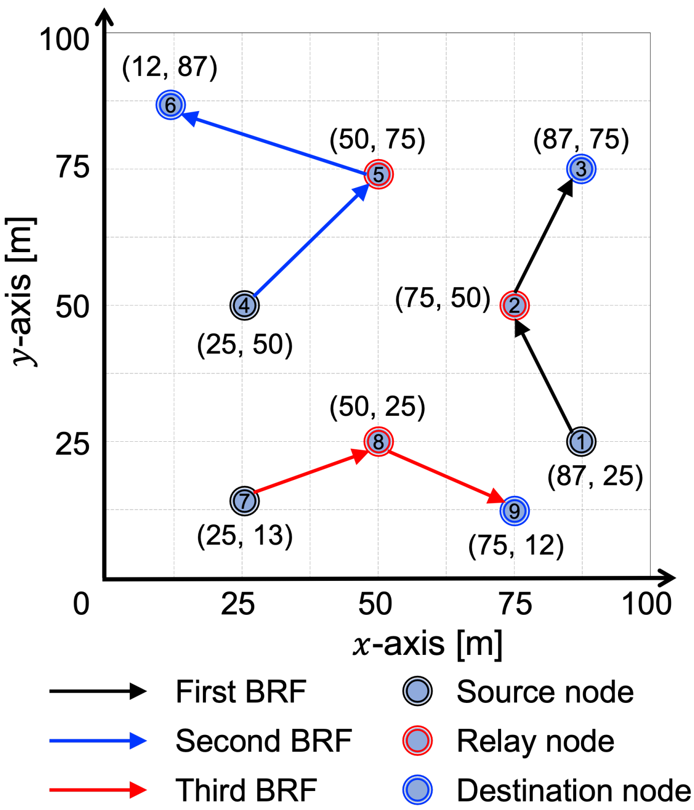

Figure 3.9: An example of a 9-node network with three BRF transmissions

pathloss model without considering the frequency parameter is considered as the channel model and the transmission rate is computed through the SINR model and link capacity model, as discussed in the previous section. From the numerical simulation of the proposed FD-MCST, RTS/FCTS, and FD-DMAC, the simulation results are based on an average of 10,000 different experiments. In the output model, the evaluation matrices of achievable network capacity, average achievable throughput, and average achievable transmission overhead are mainly considered in the research.

3.4.2 Evaluation Metrics

This section explains the evaluation matrices for performance comparison in the numerical simulations.

Achievable Network Capacity

The achievable network capacity (C_a) is defined as the summation of the transmission capacity of every single BRF transmission in the network and is computed as

$$C_a = \sum_{f=1}^{F} C_f \tag{3.22}$$

where C_f is the transmission capacity, C of fth BRF transmission.

Achievable Throughput

The achievable throughput (S_a) is the average value of the total number of successfully transferred data in a second by a transmitting node in the network. With the SNR-based interference model, the achievable throughput is computed based on the SINR constraint condition for successful reception of the BRF transmission. On the other way, the minimum of $SINR_{\mathrm{SR}}$ and $SINR_{\mathrm{RD}}$ of a BRF transmission must be higher than an SINR threshold β, where β is assumed as 6 dB in this research. Then, the formulation of S_a is given as follow:

$$S_a = \frac{p_s}{F} \sum_{f=1}^{F} S_f \tag{3.23}$$

where p_s is the probability of successful transmission based on the SINR constraint condition of the transmission and S_f is the saturation throughput (S) of fth BRF transmission.

Achievable Transmission Overhead

The achievable transmission overhead (O_a) is the average value of the overhead that is required to successfully carry out a transmission without considering the retransmission for any collision scenario in the network, and O_a is computed as

$$O_a = \frac{1}{F} \sum_{f=1}^{F} O_f \times 100\% \tag{3.24}$$

where O_f is the transmission overhead ratio (O) of fth BRF transmission, which is given as

$$O = \frac{T_o}{T_s} \tag{3.25}$$

where T_o and T_s are the transmission overhead time and successful transmission time in (3.13) and (3.14), respectively.

Total Interference Power

Total interference power is the total amount of the interference power caused to the successful transmission from the other concurrent ongoing transmissions in the whole network according to the interference model.

Average Transmitter-to-receiver Distance

Average transmitter-to-receiver distance (d_{tr}) is the average distance between the transmitting node and receiving node and is computed by averaging the distance from the transmitting node and receiving node of every ongoing transmission, i.e., the distance of SR transmission and RD transmission of a BRF transmission, as follows:

$$d_{tr} = \frac{1}{2F} \sum_{f=1}^{F} (d_{SR,f} + d_{RD,f}) \tag{3.26}$$

where $d_{SR,f}$ and $d_{RD,f}$ are the distance between S to R and R and D of the fth BRF transmission.

3.4.3 Simulation Results and Discussion

The simulation discussion consists of two parts for two simulation scenarios, i.e., performance analysis of FD-MCST and comparison analysis of FD-MCST.

Performance Analysis of FD-MCST

This section discusses the performance analysis of the proposed FD-MCST according to the number of BRF transmissions in the network and DATA length in the 30-node random network topology.

Figure 3.10 shows the influence of the time fraction on the achievable network capacity. The simulation results show an increase in the achievable network capacity with the optimal time fraction as the number of BRF transmissions increases. Specifically, when the number of BRF transmissions is one and 50 in the network, FD-MCST uses 0.74 and 0.94 of time fraction to give 67.72 Mbps and 596.81 Mbps of achievable network capacity, respectively. In other words, a larger value of the time fraction benefits FD-MCST when the network is dense. Furthermore, the simulation results reveal that the constant time fraction, i.e., 0.8 in this simulation scenario, never gives a better achievable network

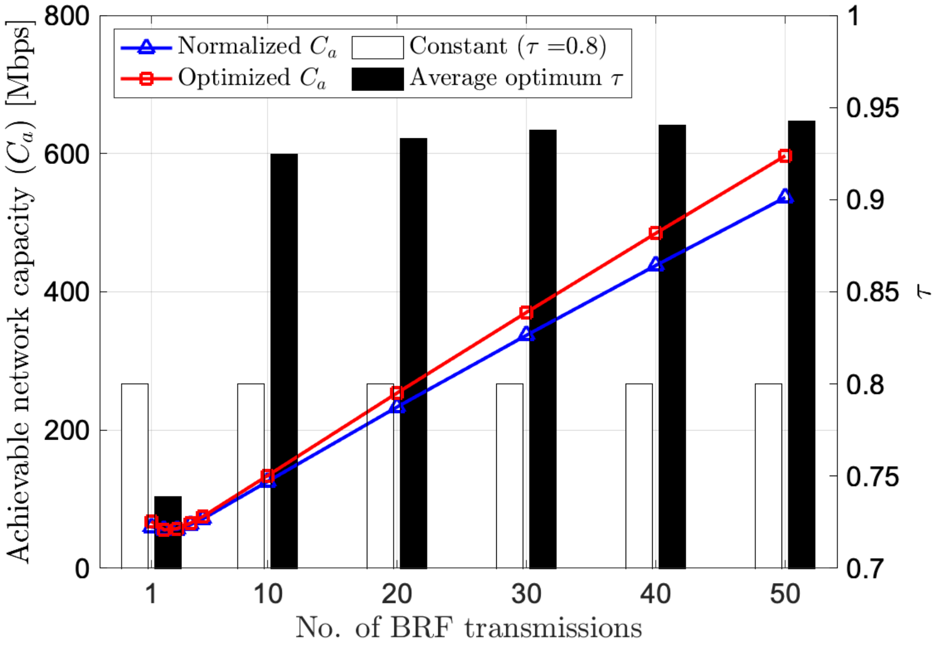

Figure 3.10: Performance analysis of FD-MCST in achievable network capacity and time fraction

capacity than the optimal time fraction resulting from the OATC algorithm. Conversely, the optimal time fraction can give around 11% achievable network capacity improvement compared to the constant time fraction when the number of BRF transmissions is 50 in the network.

However, Figure 3.11 shows that the total interference power increases as the number of BRF transmissions increases in the network. This increase is because FD-MCST uses more concurrent transmissions than sequential transmissions to increase the achievable network capacity. Therefore, as the number of BRF transmissions increases, a larger portion of the concurrent transmission leads to an exponential saturation of the total interference power.

Figure 3.12 and 3.13 illustrate the effect of the SINR threshold on the protocol performance regarding achievable throughput and achievable transmission overhead, respectively. As illustrated in Figure 3.12, increasing the number of BRF transmissions with a fixed DATA length of 1500 bytes will reduce the achievable throughput. The reason is that as the network becomes more congested, the probability of successful transmission decreases. Furthermore, the achievable throughput drops severely as the SINR threshold

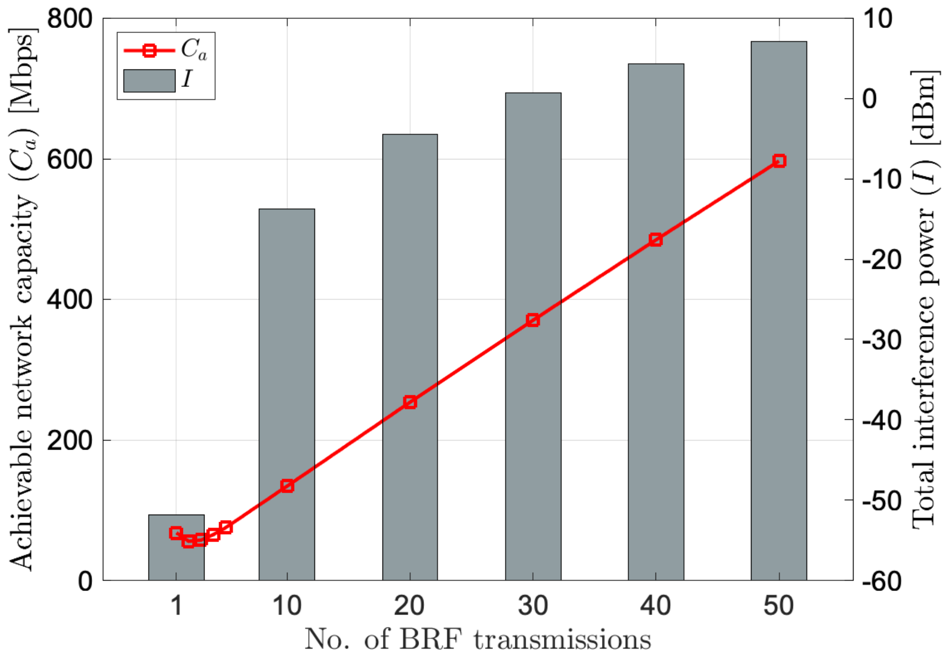

Figure 3.11: Performance analysis of FD-MCST in achievable network capacity and total interference power

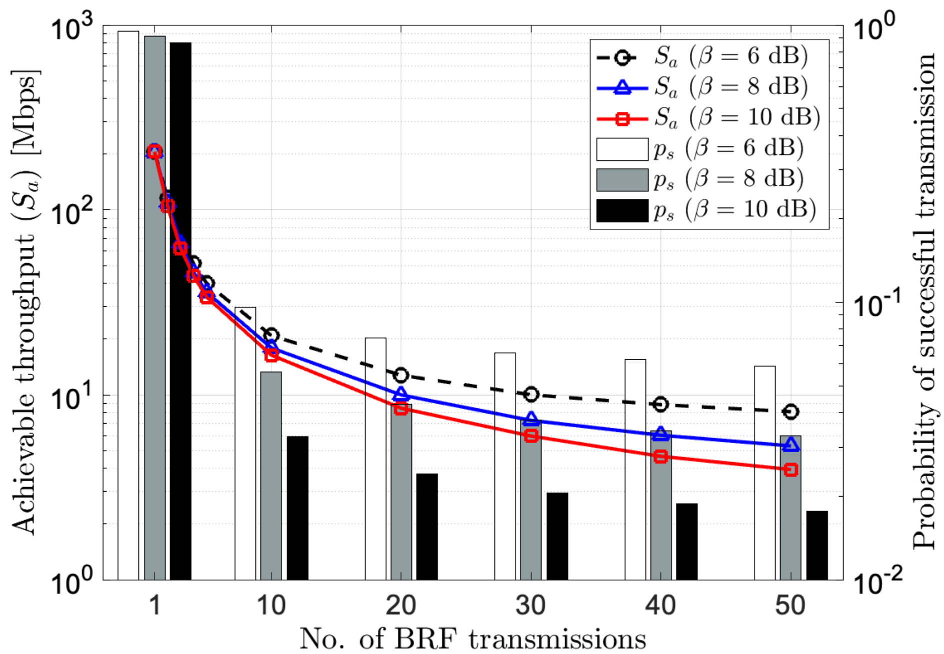

Figure 3.12: Performance analysis of FD-MCST in average achievable throughput and probability of successful transmission

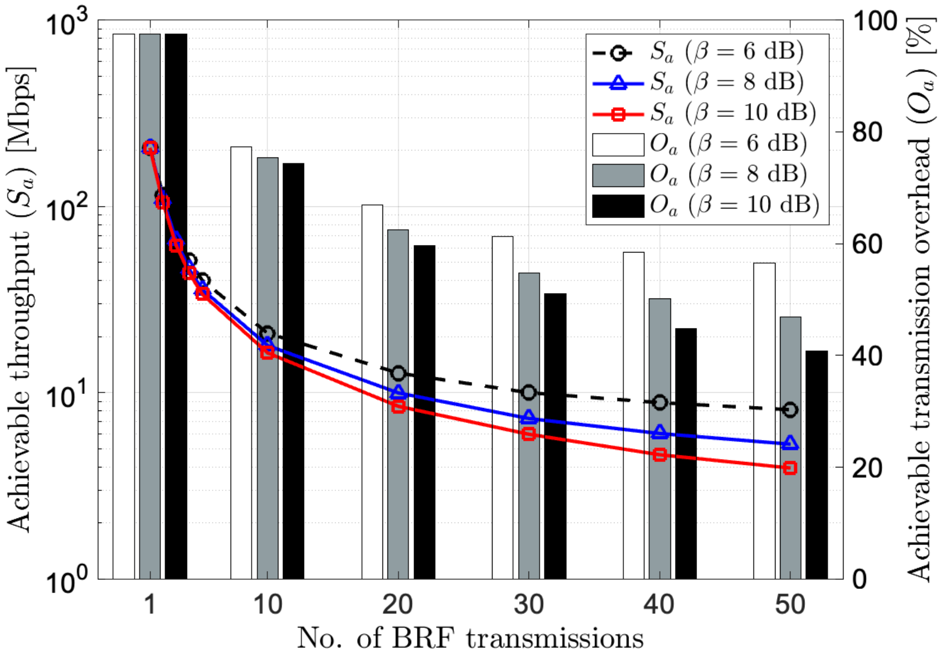

Figure 3.13: Performance analysis of FD-MCST in average achievable throughput and average achievable transmission overhead

increases. Quantitatively, simulation results show that FD-MCST achieves 8.10 Mbps and 3.94 Mbps when the SINR threshold is 6 dB and 10 dB, respectively, for the number of BRF transmissions is 50. On the other hand, Figure 3.13 shows that the achievable transmission overhead also decreases when the number of BRF transmissions increases. The reason is that the FD-MCST can provide a higher transmission rate for each successful transmission which benefits the low achievable transmission overhead. In other words, the higher the SINR threshold, the lower the probability of successful transmission. The results quantitatively show that the FD-MCST yields an achievable transmission overhead of 0.57 and 0.41 for 50 BRF transmissions when β is 6 dB and 10 dB, respectively.

Figure 3.14 describes the performance of the achievable throughput and achievable transmission overhead when the DATA length varies from 1500 bytes to 6500 bytes with an interval of 1000 bytes with different SINR thresholds in the 30-node random topology. The simulation results show that as the DATA length increases, the achievable throughput increases and the achievable transmission overhead decreases. Furthermore, the achievable transmission overhead is higher for lower SINR thresholds that give the higher achievable throughput of FD-MCST. Therefore, from the first simulation scenario, the simulation

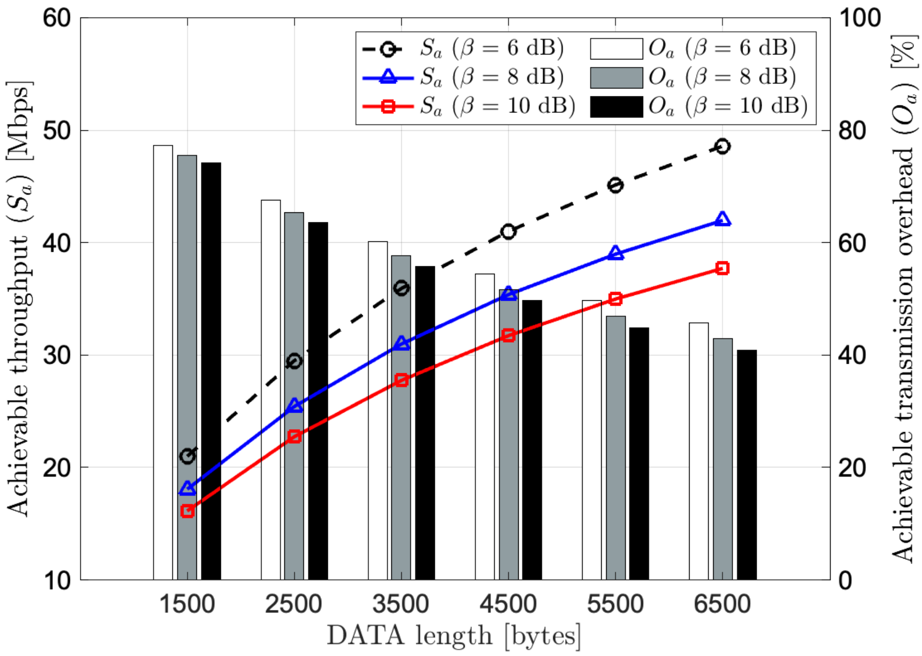

Figure 3.14: Performance analysis of FD-MCST in average achievable throughput and average achievable transmission overhead for different DATA length in 30-node random network

results show that FD-MCST can benefit high-density wireless networks with lower SINR thresholds and longer DATA transmission lengths.

Comparison Analysis of FD-MCST

In this section, the performance of the proposed FD-MCST is compared with two FD MAC protocols, i.e., RTS/FCTS and FD-DMAC, in the FD wireless networks.

Figure 3.15 shows the achievable network capacity and total interference power for the different numbers of BRF transmissions in the network. The simulation results show that the achievable network capacity and total interference power of all MAC increase when the network becomes dense. However, as the number of BRF transmissions increases, FD-MCST has advantages over both RTS/FCTS and FD-DMAC in achievable network capacity. The reason is that RTS/FCTS and FD-DMAC only apply the concurrent transmissions, while FD-MCST optimizes the transmission capacity of all BRF transmissions through an optimal time fraction of the MCST scheme. Specifically, with 50 BRF trans-

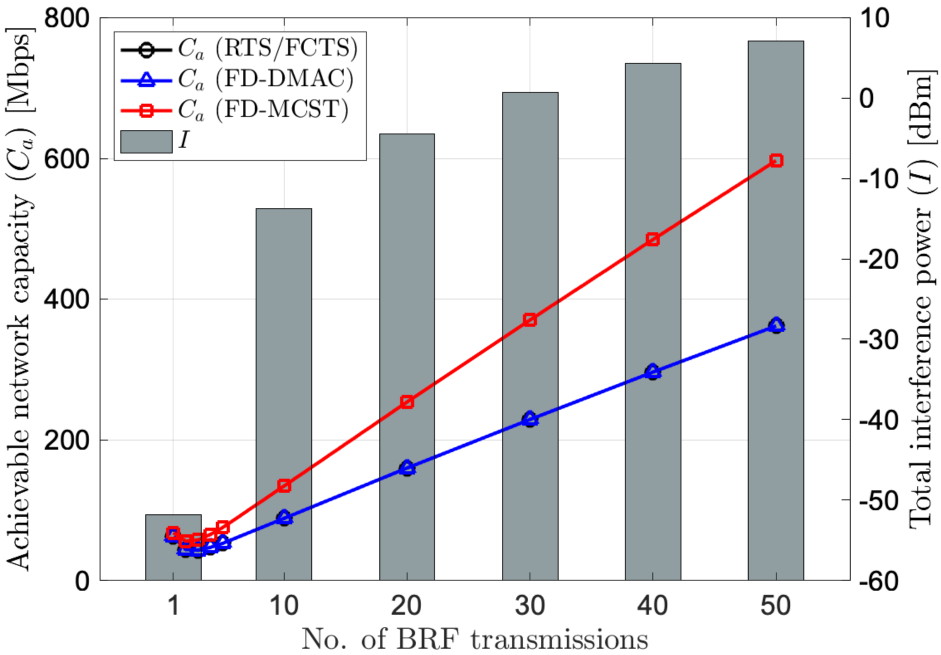

Figure 3.15: Performance comparison in achievable network capacity and total interference power

missions, FD-MCST can achieve 596.81 Mbps, while RTS/FCTS and FD-DMAC can give the same 361.77 Mbps. It means that for 50 BRF transmissions in the network, FD-MCST achieves around 1.7 times the achievable network capacity improvement than RTS/FCTS and FD-DMAC.

Figure 3.16 and 3.17 discuss the performance comparison regarding achievable throughput with average transmitter-to-receiver distance and achievable transmission overhead for three MAC protocols when the number of BRF transmissions increases with the fixed DATA length of 1500 bytes. As illustrated in Figure 3.16, the simulation results show that FD-MCST achieves higher achievable throughput than RTS/FCTS and FD-DMAC, regardless of the number of BRF transmissions. The reason is that FD-MCST optimizes the transmission capacity of each BRF transmission to achieve a higher achievable throughput than the other MAC. Although the achievable throughput decreases with the number of BRF transmissions, FD-MCST still outperforms RTS/FCTS and FD-DMAC. The reason is that for a fixed network coverage size, the transmitter-to-receiver distance decreases for each BRF transmission. The simulation results show that, compared to RTS/FCTS and FD-DMAC, FD-MCST can improve the achievable throughput by up to 69% ad 65%,

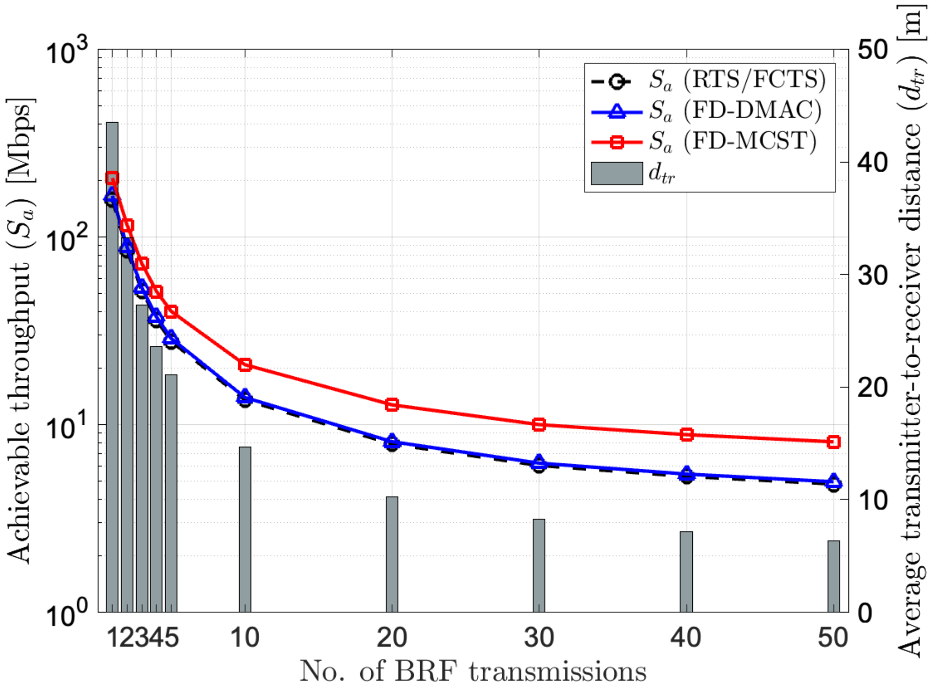

Figure 3.16: Performance comparison in average achievable throughput and average transmitter-to-receiver distance with DATA length of 1500 bytes

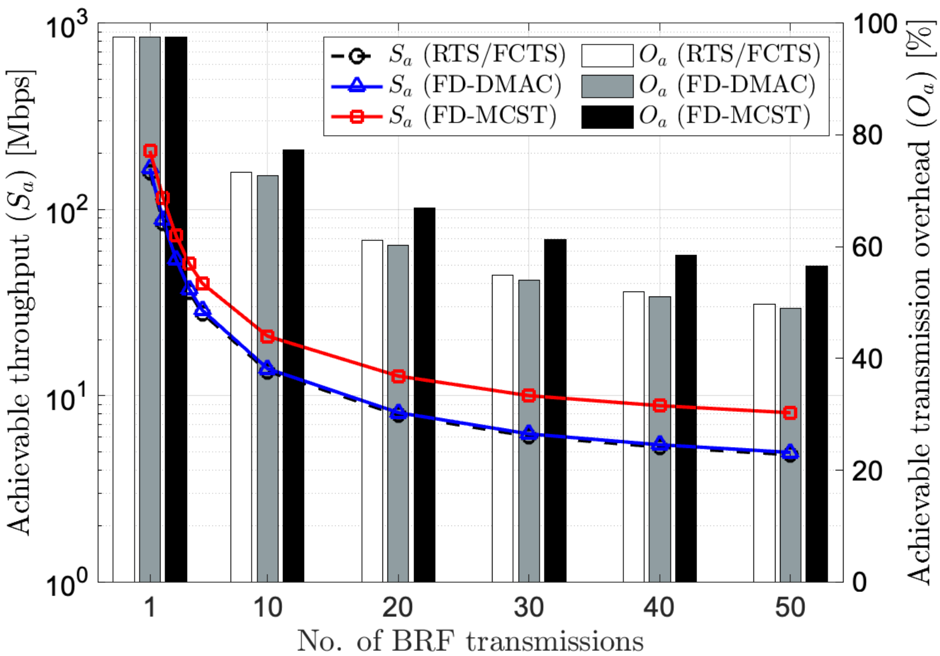

Figure 3.17: Performance comparison of average achievable throughput and average achievable transmission overhead versus the number of BRF transmissions

respectively, when the number of BRF transmissions is 50 in the network.

Also, as shown in Figure 3.17, FD-MCST has higher achievable transmission overhead regardless of the number of BRF transmissions. Especially for FD-MCST, the more BRF transmissions, the higher the achievable transmission overhead. Simulation results show that in the network with 50 BRF transmissions, RTS/FCTS and FD-DMAC give 49.8% and 48.9% achievable transmission overlead, respectively, while FD-MCST gives 56.6%. The reason is that the relay node in the FD-MCST has to broadcast the new STS frame to share the MCST information of time fraction and transmission control for sequential transmission indication.

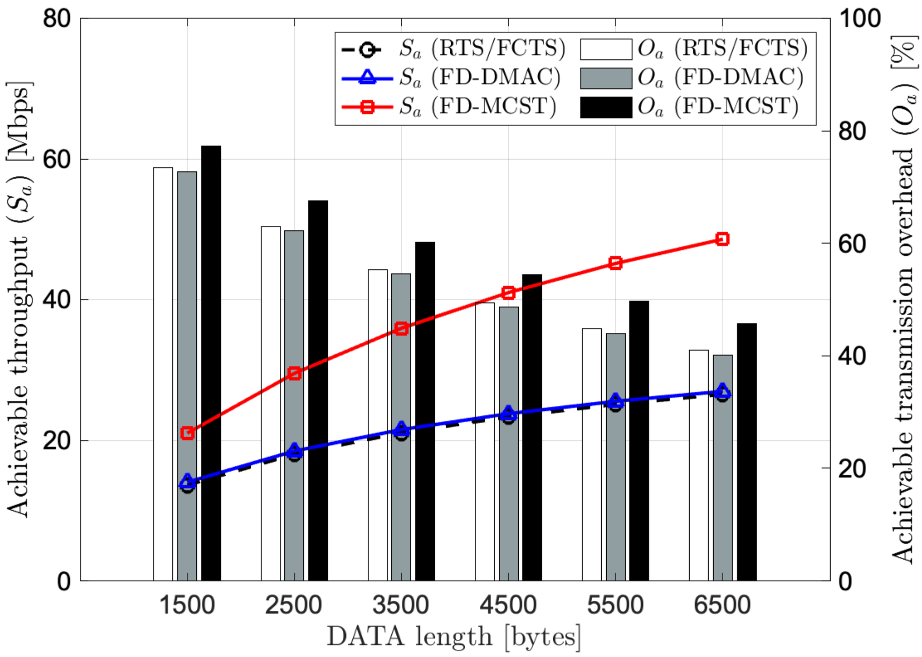

Figure 3.18: Performance comparison in average achievable throughput and average achievable transmission overhead for different DATA length in 30-node for random network

In Figure 3.18, the performance comparison is done for the FD-MCST, RTS/FCTS, and FD-DMAC regarding achievable throughput and achievable transmission overhead when the DATA length varies in the 30-node random network topology. FD-MCST shows advantages when the DATA length is large. Quantitatively, compared to RTS/FCTS, for a DATA length is 1500 bytes, FD-MCST achieves 5.3% and 54.3% improvements in achievable transmission overhead and achievable throughput, respectively. Likewise, the performance change to 11.7% and 83.2% as the DATA length is 6500 bytes. In other words, FD-MCST results in better achievable throughput with high achievable transmission overhead when the DATA length is larger. Therefore, from the second numerical simulation scenario, the simulation results show that the proposed FD-MCST is better than FD MAC protocols of RTS/FCTS and FD-DMAC in terms of achievable network capacity and average achievable throughput with high achievable transmission overhead regardless of the number of BRF transmissions and DATA length in the FD wireless networks.

3.5 Implementation of MCST in LoRaWAN

Long-range low-power wireless communication in the IoT system, a.k.a. LoRa, is attractive in academia and industrial communities. Plenty of research work has investigated the application of LoRa in different low-power wireless systems such as sensor networks, UAV networks, and so on [105–107]. In this section, the network capacity improvement is investigated when the MCST scheme is used for remote identification and tracking of the UAV system that provides low-cost broadcast-based location information sharing between drones over the LoRa network.

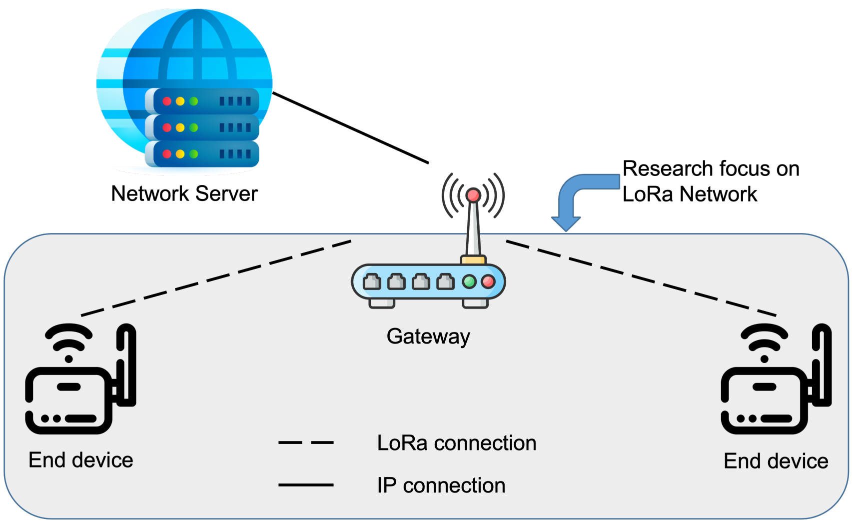

Figure 3.19: An example of LoRaWAN network architecture and research focus on LoRa network

LoRa generally follows the standard of IEEE 802.15.4 for low-rate wireless personal

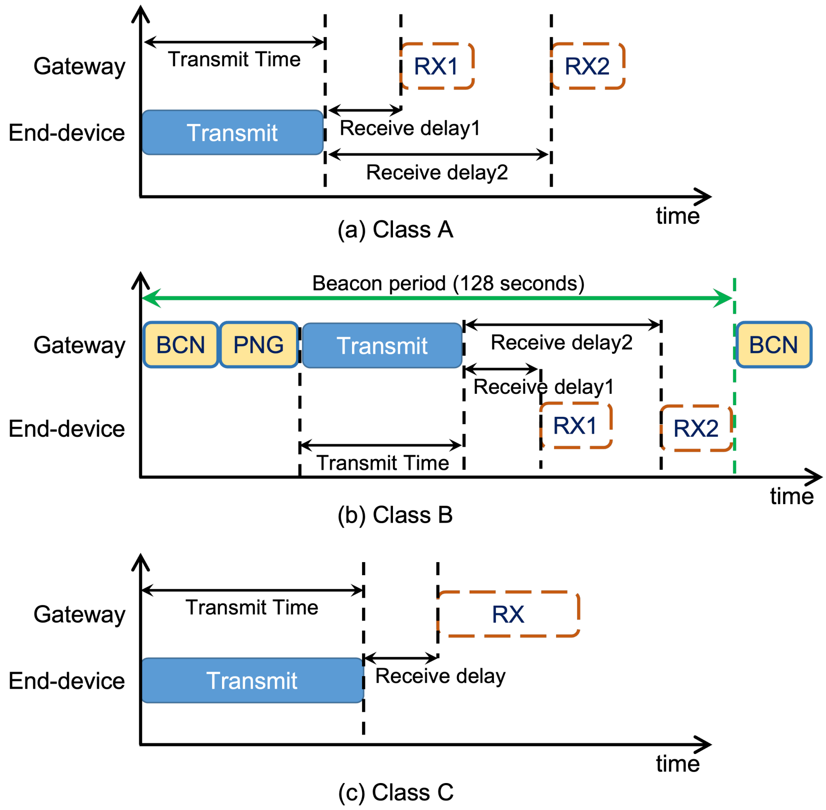

Figure 3.20: Three classes of LoRaWAN MAC

area networks and is mainly used to increase device lifetime and reduce device cost. LoRa wide area network (LoRaWAN) is a star network topology in which the end devices connect to the network server through the gateway as illustrated in Figure 3.19. There are three classes of LoRaWAN MAC protocol, i.e., class A, class B, and class C, to define how the end device process the communication in the LoRaWAN as shown in Figure 3.20. Class A is the baseline MAC in which the end device allows the bi-directional communication, a set of uplink transmissions from the end device to the gateway and two short receive windows, i.e., RX1 and RX2, for downlink transmission from the gateway to the end device. The end device initiates the transmission based on their need according to the random time basic ALOHA-type protocol. In class B, the gateway initiates the transmission by sending the PNG packet as a ping message to the end device. Besides, the gateway sends a beacon every 128 seconds for synchronization purposes. Unlike class A, the end device opens the scheduled receive windows for downlink transmission with the synchronized beacon. The end device in class C continuously opens the receive window (RX) until there is an unlink transmission. Hence, the end device consumes more energy than class A and class B.

LoRaWAN generally operates as the standard of pure-ALOHA protocol, which has the drawback of a high packet loss rate due to collisions. To address these issues, Polonelli et al. used the concept of slotted ALOHA and acknowledgement for successful transmission on their new design of LoRaWAN protocol in [108]. Generally, LoRaWAN cannot be implemented with the handshaking mechanism because the end device in the network does not always listen to the incoming transmission. They only take action if they have data for uplink transmission. In [109], Ahsan et al. proposed the modified listen-before-talk mechanism to overcome the high packet loss and showed the improvement of channel utilization with energy consumption even in the dense network. Likewise, the design of LoRaWAN protocol with CSMA mechanism is proposed for reducing the collision and optimizing the channel capacity in [107, 110]. However, the ever-increasing number of devices in the network and the growth of traffic still lead to capacity demand and energy consumption for better transmission performance. The existing research in the area of LoRa mainly considered proposing the approaches of MAC for minimizing energy consumption and optimizing the throughput in the network. Throughout those related works, there is still a lack of investigation into the transmission scheme.

This research will focus on studying network capacity improvement for the MCST scheme. In the LoRa network, only the connection between the end device and gateway is considered for network capacity via the transmission scheme, which differs from the existing research approach. As the research scope, the consideration of the underlying physical layer of the LoRa network is omitted.

3.5.1 Channel Model

The signal attenuation of the transmission link over a communication channel depends on the log-distance pathloss model with ITU recommendation [111]. The channel gain in terms of dB from node i and node j is given as

$$PL_{ij} = 10 \cdot \alpha \cdot \log_{10}(d_{ij}) + \delta + 10 \cdot \gamma \cdot \log_{10} \mathrm{F} + X_\sigma \qquad (3.27)$$

where δ is the coefficient associated with the offset value of pathloss and $\delta = 29.2$, γ is the coefficient associated with the increase of pathloss according to frequency, and $\gamma = 2.11$, F is the operating frequency of the transmission.

3.5.2 MCST Scheme over LoRa Network

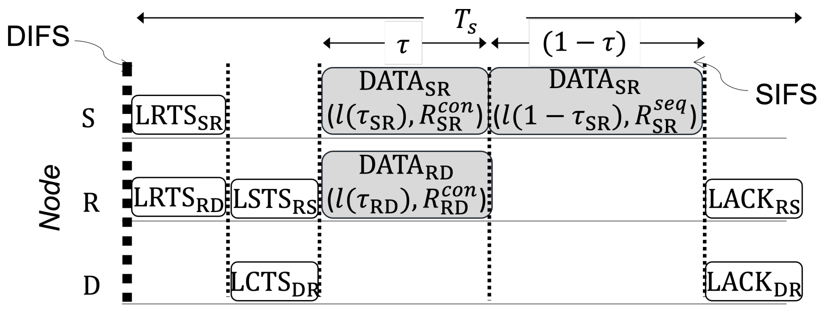

Figure 3.21: The sequence of frame exchanging for successful transmission with an example of SR transmission performs sequential transmission through MCST over LoRa network (MCST/LoRa scheme)

This section describes the design of the MCST scheme for optimizing the transmission performance in the LoRa network. The MCST over the LoRa network is designed as MCST/LoRa scheme by integrating and modifying the three classes of LoRaWAN MAC, especially class A and class B, to enable the DCF mechanism. Figure 3.21 presents an example frame exchange sequence of the MCST/LoRa scheme in which SR transmission performs the sequential transmission in the time fraction of $(1 - \tau)$ for the optimum transmission capacity.

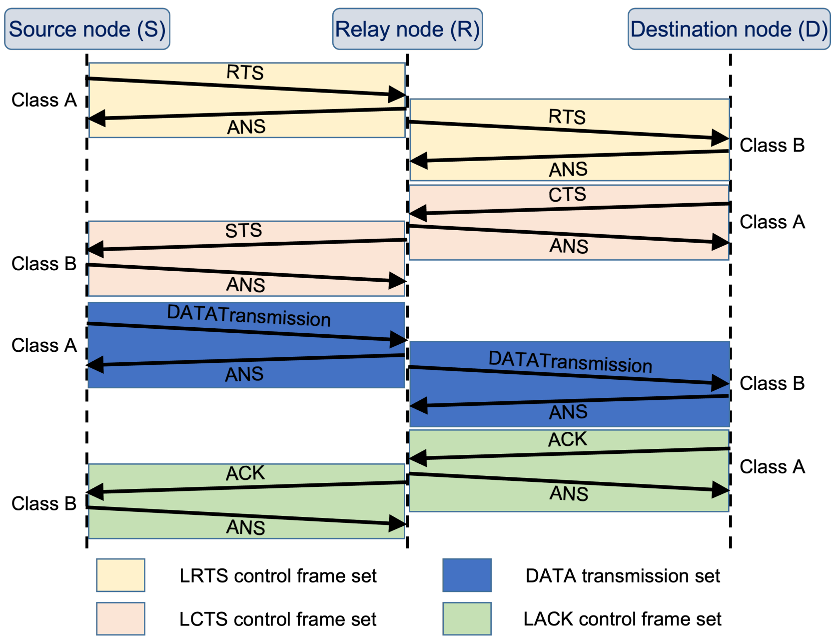

Figure 3.22: The message handshaking of MCST/LoRa scheme

Figure 3.22 describes the message handshaking of the MCST/LoRa scheme. As presented in the figure, if the node wants to transmit the data, it will first send the LoRaWAN request-to-send (LRTS) control frame set, which is a combination of the RTS control frame uplink transmission and LoRa answer (ANS) frame from the gateway. The LoRaWAN-enabled end device in the network is assumed in the acknowledged configuration unlikely from [108]. Therefore, the gateway sends the ANS frame in the receive window to indicate the reception of the uplink/downlink transmission to form a bi-directional transmission as in [112]. The ANS frame transmission is assumed as a function of transmit power, transmission channel, and transmission rate of the uplink/downlink transmission and has a similar transmission time to the uplink/downlink transmission. If the receiving end device is ready to accept the transmission, it will send the LoRaWAN clear-to-send (LCTS) control frame set, a combination of the CTS and ANS frames. However, before DATA transmission, the relay node sends the LoRaWAN set-to-send (LSTS) control frame set to pass the MCST information of time fraction and transmission control for instructing the sequential transmission of the MCST scheme. After the DATA transmission is completed, the destination node and relay node will inform the transmission completion with the LoRaWAN acknowledgement (LACK) control frame set. The receive delay is also neglected and only considers the first receive window with a simple ANS frame downlink/uplink transmission following each uplink/downlink transmission for both class A and class B LoRaWAN MAC.

However, Bouguera et al. described that the acknowledgement control frame transmission consumes the end device's energy [112]. To address this issue, a modified MCST

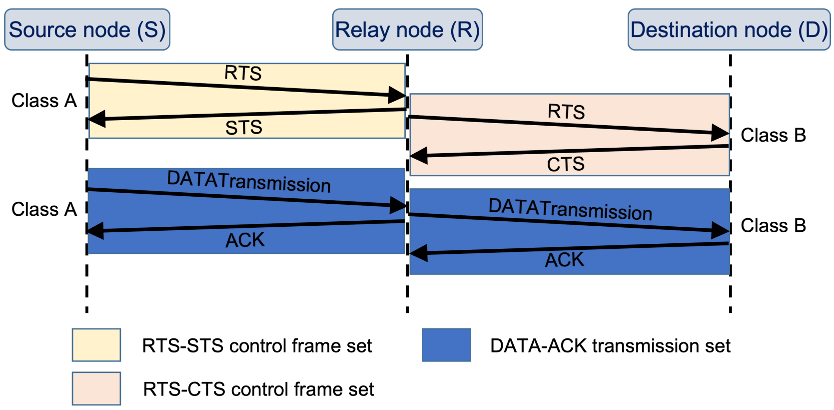

Figure 3.23: The proposed mMCST/LoRa scheme

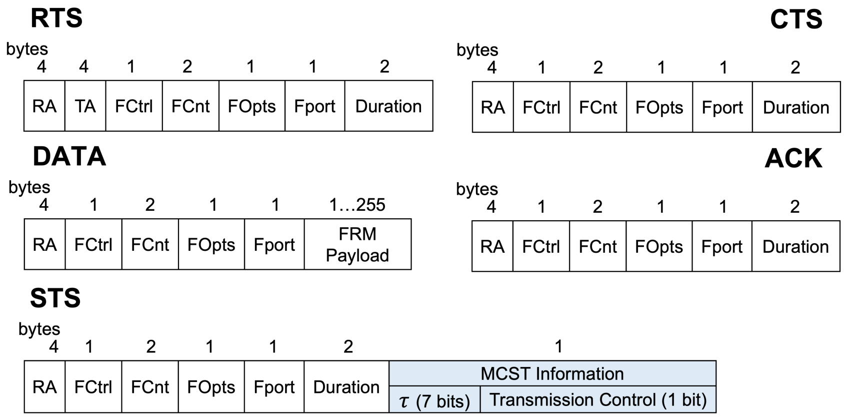

Figure 3.24: The frame formats of the control and DATA messages for MCST/LoRa

over the LoRa network is proposed as mMCST/LoRa scheme by keeping the LoRaWAN standard of bi-directional transmission as shown in Figure 3.23. In the proposed mMCST/LoRa scheme, the control frames of the handshaking mechanism are reduced by considering the downlink transmissions as the transmission in the receive window. In this way, the transmission time and latency can be reduced, and the throughput, as well as energy consumption, can be optimized. With the minor modification of the LoRaWAN format in [113], Figure 3.24 shows the frame formats of the control, i.e., RTS, CTS, STS, ACK, and DATA messages as the MAC payload frame of MCST/LoRa scheme used in the LoRa network with minor modification of LoRaWAN [113].

3.5.3 Numerical Simulations

The simulation is conducted by MATLAB R2022b, and the performance of the proposed MCST/LoRa scheme and mMCST/LoRa scheme is evaluated by comparing them with the existing LoRAWAN MAC based on the CSMA mechanism (CSMA/LoRa) proposed in [107].

Simulation Scenarios and Settings

The two simulation scenarios are the network capacity study according to the frame (FRM) payload size in a 30-node random network topology and the performance study according to the number of nodes in the network with an FRM payload size of 250 bytes. The simulation parameters and settings are listed in Table 3.2 with the standard specifi-

Table 3.2: Simulation parameters for evaluation of MCST/LoRa and mMCST/LoRa schemes

Parameter	**Value**
Network coverage size	1 km × 1 km × 150 m
Number of nodes (N)	30, 60, 90, 120, 150, 180, 210, 240
Transmit power (P)	13 dBm
Channel model	Log-distance pathloss model with ITU recommendation
Attenuation constant (α)	2.34 [106]
Hardware specification	IEEE 802.15.8/LoRa
Shadowing parameter (X_σ)	5.06 dB [111]
Frequency (F)	920 MHz
Channel bandwidth (B)	400 kHz [106]
RSSI, Basic rate (R_{base})	-98 dBm, 200 kbps -117 dBm, 20 kbps [106]
RTS size	120 bits
CTS size	88 bits
STS size	96 bits
ACK size	88 bits
Frame payload	50, 100, 150, 200, 250 bytes
Number of simulations	10,000 times

cation of the LoRa network [113]. In the network, the wireless end devices are uniformly distributed in the coverage area with no node mobility model. The node combination of the end devices and gateway is randomly selected to form a BRF transmission. Under the specific frequency channel, the log-distance pathloss model with ITU recommendation is treated as the channel model. Assuming the network is operating as similarly as [106], the attenuation constant is estimated from the network model of [106] using the particle filters algorithm. Besides, all the end devices are always assumed to have an FRM payload of the same size for DATA transmission and consider only one transmission per DATA transmission for theoretical capacity study purposes. In the random topology scenario, 10,000 simulations are performed and averaged to obtain the performance metrics of achievable throughput, achievable transmission latency, and transmission energy consumption.

Achievable transmission latency (L_a) is the average summation of the transmission delay and propagation delay of a BRF transmission, in which the transmission delay (D_{tran}) means the time required to transmit the DATA frame from the source node to the destination node and the propagation delay (D_{prop}) means the time required to propagate the DATA frame across the channel. In this way, L_a is computed as

$$L_a = \frac{1}{F} \sum_{f=1}^{F} L_f \tag{3.28}$$

where L_f is the latency (L) of fth BRF transmission, which is given as

$$L = D_{tran} + D_{prop} \tag{3.29}$$

where $D_{tran} = T_{preamble} + T_{DIFS} + T_{LRTS} + T_{LSTS} + \frac{H}{R_{base}} + \frac{l}{R^{MCST}} + T_{LACK} + 4T_{SIFS}$ where $T_{preamble}$ is the preamble time for synchronization, T_{LRTS} is the duration for LRTS control frame set, T_{LSTS} is duration for LSTS control frame set, T_{LACK} is the duration for LACK control frame set and $D_{prop} = \frac{l}{\mathsf{c}}$ where c is speed of light equal to 3×10^8 [m/s].

Transmission energy consumption (E_a) is the average summation of the total energy consumed for transmitting both the control and DATA frame from the source node to the destination node and is computed as

$$E_a = \frac{1}{F} \sum_{f=1}^{F} P \times L_f \tag{3.30}$$

Simulation Results and Discussions

Figure 3.25 shows the performance comparison by varying FRM payload size in the 30-node random topology. The simulation results reveal that MCST gives higher achievable throughput than the CSMA mechanism. Quantitatively, when MCST/LoRa and mMCST/LoRa give 24.22 Mbps and 24.32 Mbps achievable throughput, respectively, CSMA/LoRa gives 23.63 Mbps when the size of FRM payload is 250 bytes in a 30-node random topology scenario. It means that MCST can achieve around 2.5% of network capacity improvement. This is because MCST optimizes the transmission capacity and results in better throughput. In addition, the figure presents that MCST/LoRa and mMCST/LoRa reduce the latency with the optimized transmission capacity through the

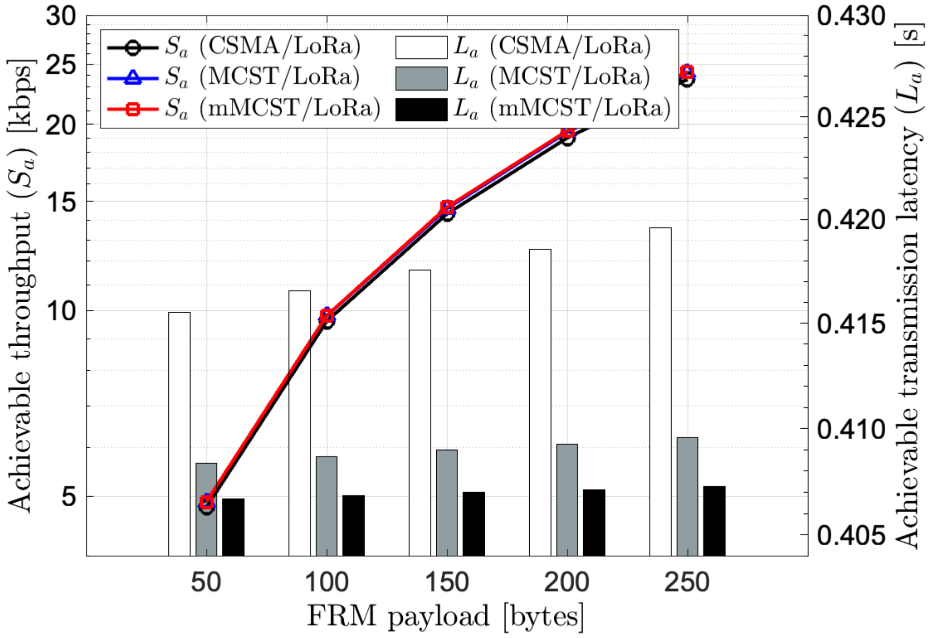

Figure 3.25: Performance comparison in average achievable throughput and latency for 30-node random network

MCST scheme. When the FRM payload size is 250 bytes, MCST/LoRa scheme and mMCST/LoRa can reduce up to 2.4% and 2.9%, respectively, compared to CSMA/LoRa.

Table 3.3 shows the performance comparison regarding energy consumption for the 30-node random topology scenario. The result shows that the MCST scheme is a better energy-efficient MAC than the CSMA mechanism. This is because MCST/LoRa and mMCST/LoRa reduce the latency with the optimized transmission capacity through the

Table 3.3: Performance comparison between CSMA/LoRa, MCST/LoRa and mMCST/LoRa in energy consumption versus FRM payload for 30-node random topology

	FRM payload [bytes]				
	50	100	150	200	250
CSMA/LoRa	8.31	8.33	8.35	8.37	8.40
MCST/LoRa	8.17	8.17	8.18	8.19	8.20
mMCST/LoRa	8.13	8.14	8.14	8.14	8.15

Notes: All the values is in the unit of mJ.

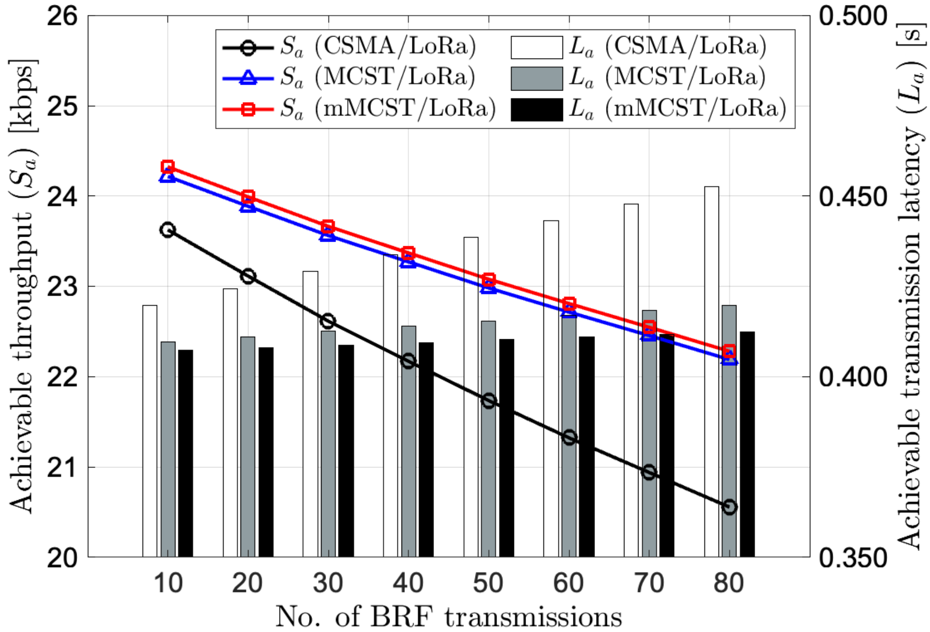

Figure 3.26: Performance comparison in average achievable throughput and latency for different numbers of BRF transmissions

MCST scheme, resulting in less energy consumption.

Figure 3.26 illustrates the performance comparison of the proposed MCST/LoRa scheme and mMCST/LoRa scheme with CSMA/LoRa in terms of achievable throughput and achievable transmission latency. The results show that the MCST scheme can accomplish a higher achievable throughput than CSMA/LoRa regardless of the number of BRF transmissions in the network. The achievable transmission latency increases and the achievable throughput decreases as the number of nodes increases because of the interference in the dense network and the resulting low transmission rate. However, MCST still shows superiority over the CSMA mechanism in the LoRa network. When the number of BRF transmissions is 80 in the network, the network capacity improvement can be achieved up to 7.9% compared to the CSMA mechanism. Besides, the simulation results reveal that a higher achievable throughput can be obtained through the proposed mMCST/LoRa scheme by reducing the control frame transmission time.

Table 3.4 depicts the performance comparison in energy consumption when the number of BRF transmissions increases in the network with the fixed FRM payload size of 250 bytes. The results show that MCST/LoRa and mMCST/LoRa can save energy up to

Table 3.4: Performance comparison between CSMA/LoRa, MCST/LoRa and mMCST/LoRa in energy consumption versus the number of BRF transmissions

	No. of BRF transmissions							
	10	20	30	40	50	60	70	80
CSMA/LoRa	8.40	8.50	8.59	8.68	8.77	8.86	8.95	9.05
MCST/LoRa	8.20	8.20	8.25	8.30	8.30	8.33	8.38	8.40
mMCST/LoRa	8.15	8.20	8.20	8.20	8.20	8.20	8.20	8.24

Notes: All the values is in the unit of mJ.

7.2% 9.0%, respectively, than CSMA/LoRa when the number of BRF transmissions is 80 in the network. The reason is MCST enables DATA transmission at a higher rate and results in a shorter time for successful transmission, leading to less energy consumption than the CSMA mechanism. In conclusion, applying the MCST scheme is beneficial as a contribution to the advantage of the transmission scheme in the LoRa network, and the optimum achievable throughput with minimum latency and energy consumption can be accomplished.

3.6 Summary

In this chapter, the MCST scheme is proposed for capacity optimization in the FD wireless networks. FD-MCST is designed for the MCST scheme, and the performance analysis is conducted using the Markov Chain approach. Through the numerical simulations, the performance evolution of the proposed FD-MCST is performed by comparing it with the existing FD MAC protocols. The simulation results reveal that the proposed FD-MCST gives superiority over existing FD MAC protocols regardless of the number of BRF transmissions in the network and DATA length. Specifically, the proposed FD-MCST can give about 1.7 times and nearly two times in terms of achievable network capacity and achievable throughput, respectively, compared to the existing FD MAC protocols.

In the basic TCP/IP model, the maximum size of an IP packet, packet loss rate and round-trip time is the important network performance metrics to influence the throughput of TCP connections [114]. The TCP connections have to ensure the transporting data is successfully completed at the destination. If the latency is very high, it will influence the round trip time, which leads to the degradation of TCP transmission throughput performance. As a result, this low throughput at the transport layer could not support mission-critical and time-critical applications.

In other words, the MCST scheme that is proposed to mainly focus on MAC designing in both IEEE 802.11ac and LoRa network standard specifications at the data link layer contributes to the latency reduction at the transport layer. Specifically, through the network capacity improvement study in the LoRa network, the proposed MCST shows high performance in minimizing latency and energy consumption as well as maximizing achievable throughput for low-power wireless systems such as UAV networks. It is expected also to contribute much to the application of the auto-driving car. However, the other parameters, i.e., the maximum size of an IP packet and packet loss rate, are not studied in this chapter, which they can be further extended as additional research and future work.

Chapter 4

Optimal Achievable Transmission Capacity Scheme

In this chapter, the optimal achievable transmission capacity (OATC) scheme is designed as a power management module for efficient communication in future wireless networks. Extending to the proposed MCST scheme, the OATC scheme is proposed to optimize the achievable transmission capacity with minimum interference through the temporal and spatial reuse mechanisms in FD wireless networks.

The chapter is structured with four sections. First, an overview of the research in resource management is enclosed with the related works. Second, the proposed OATC scheme is discussed in detail. Third, the performance analysis is conducted through numerical simulation scenarios. Finally, the summary of the chapter is drawn in the fourth section.

4.1 Research Background

Interference is the distracted signal that degrades the transmission performance in the wireless network. It poses the most critical problem in wireless systems, especially in the FD systems, for energy scarcity since it affects the quality of wireless communication. The FD system has to encounter its residual SI and interference from other uplink transmissions in the network. Therefore, optimum resource allocation with user pairing, power allocation, and interference management is necessary for potential achievement. Various research approaches have been conducted in wireless networks to suppress interference. Under the transmission conditions chosen in the network, TPC is one of the well-known techniques which employs the power control approach to adjust the operating transmit power of the device and access point. At a fixed/maximum power, the transmission consumes energy and also increases the possibility of network interference. Hence, not only the interference can be reduced, but also energy consumption can be mitigated with TPC.

In this dissertation, the OATC scheme is proposed to focus on minimizing the IUI interference in the FD wireless networks. Unlike existing interference cancellation techniques and TPC techniques, OATC manages the concurrent transmissions and control transmit power by combining transmission schemes and adjusting the transmission coverage. Therefore, the objective of this chapter is to propose a new OATC scheme to optimize the transmission capacity with low interference in the FD wireless networks.

4.1.1 Related Works

Many research works have designed MAC protocols for simultaneous transmission in FD wireless networks to optimize capacity from various perspectives [115]. As the different approaches for interference mitigation, the TPC scheme is also utilized to mitigate IUI [116]. For example, Tang et al. proposed capacity optimization by IUI cancellation of other transmissions in mobile wireless networks [117]. The simulation result shows that the perfect cancellation generates more than 60% capacity gain, even in dense networks. In similar research on mobile wireless, Wu et al. proposed the IUI suppression scheme by transmitting an additional reversed signal at the base station [40]. This research shows that the suppression scheme offers advantages for FD systems over HD systems. However, sending the additional signals consumes more power. Qu et al. also proposed a multiuser FD MAC protocol with TPC to control the uplink transmission for interference mitigation [118]. In their research, the simulation result shows that the lower transmit power that meets the SINR threshold yields a better network capacity. Another related work can be found in [119] that uses TPC to propose the restricted area-based interference control scheme in mobile wireless.

One way to reduce the interference problem and improve the performance of the entire network capacity is the TPC technique [120]. To optimize transmission capacity, the distributed transmit power control (DTPC) algorithm is proposed in the distributed manner in [121]. The algorithm averages the occupied link rate of the transmitting nodes and controls the transmit power to increase the end-to-end throughput. Following that, in the wireless multihop networks, Yu et al. proposed a consensus transmit power control (CTPC) algorithm that uses the consensus coefficient to maximize the average end-to-end throughput [62]. The research in [53] also proposed a TPC scheme in FD networks, arguing that the high transmit power of the relay node is always suboptimal for increasing network capacity. Aslani and Rasti studied the problem of minimizing the transmit power and maximizing throughput in the in-band FD energy harvesting wireless networks and designed a distributed TPC scheme for the FD wireless networks [122]. In [123], Han et al. investigated a TPC scheme that maximizes the total achievable rate of the communication links in the FD wireless networks while meeting the minimum rate requirement for the device-to-device (D2D) communications in the cellular network. Furthermore, Samy et al. presented a transmit power optimization problem to maximize the sum rate and received SINR in the wireless relay networks [124]. Similarly, Kai et al. presented the joint user scheduling and TPC scheme to optimize transmission capacity in the WLAN networks [125]. In their simulation results, the proposed scheme provides up to 80% capacity improvement than the HD system. Likewise, Goyal et al. proposed a distributed joint user scheduling and TPC scheme, which shows nearly 2-fold capacity improvement performance in an indoor multicell network [39].

Among transmission resource management approaches, Amin and Hossain recently designed a distributed MAC protocol with TPC based on the RTS/CTS mechanism for the FD wireless networks [126]. The authors view TPC as an efficient technique for adjusting the carrier sensing range and reducing inter-station interference. In their study, the proposed protocol can improve the throughput by up to 41% than the existing FD MAC. Therefore, TPC has gained a significant research interest in FD systems for low transmit power scenarios.

4.1.2 Motivation

Current FD MAC protocols only consider CT with temporal reuse for capacity optimization in wireless networks. Even in the hybrid approach with FD/HD system, MAC protocol only considers the CT in FD mode and ST in HD mode. Therefore, an MCST scheme is proposed to optimize the capacity with both CT and ST in the previous chapter. However, the tradeoff between the interference power and capacity gain of the transmission has not yet been considered. Besides, it can be found that, through the TPC, the network capacity can be optimized with minimum transmit power in the network. Specifically, TPC gives benefits to the FD systems. Hence, it motivates us to study network capacity optimization by combining the transmission and TPC schemes in the FD wireless networks.

4.2 OATC Scheme

This section describes the OATC scheme for optimizing the transmission capacity of the BRF transmission in the FD wireless networks. OATC uses a temporal reuse mechanism to enable the relay node to cooperatively select either the CT or MCST scheme to realize the optimum transmission capacity of the BRF transmission. By applying the concept of hybrid scheduling policy [39], OATC adopts the MCST scheme that provides the advantage of capacity gain. Otherwise, the default CT is applied for BRF transmission on the network. OATC also integrates with the TPC technique to minimize the IUI and satisfies the objective function of transmission capacity while meeting the SINR threshold constraint. Current transmission schemes tend to achieve the optimum transmission capacity without considering the tradeoff between interference power and capacity gain of the transmission. Additionally, as discussed in the previous section, although the MCST scheme can achieve high achievable network capacity, it still has the probability of high interference and limited transmission capacity as the network becomes dense. OATC seeks to overcome interference problems and optimize transmission capacity by incorporating temporal and spatial reuse mechanisms in wireless networks. In this way, the OATC scheme optimizes the transmission performance of CT and MCST schemes by utilizing TPC techniques with the transmission schemes and selecting either the CT scheme with TPC or the MCST scheme with TPC according to the tradeoff threshold.

4.2.1 Transmit Power Control Scheme

The transmission rate and achievable transmission capacity can be computed through the mentioned channel model, SINR model, and link capacity model. Hereafter, the TPC is adopted to improve the transmission capacity while minimizing the interference with the minimum transmit power of the nodes. For this purpose, the CTPC algorithm is used in this research among the existing TPC schemes. The reason is that the distributed TPC schemes converge to the minimum transmission rate value of each transmission flow, which may not be optimal for the average end-to-end throughput of the wireless networks. However, CTPC adjusts the transmit power of each node to an average transmission rate according to the consensus coefficient [62]. In CTPC, the algorithm controls the transmit power with a consensus coefficient to maximize the minimum transmission rate of the ongoing transmission. As a result, all transmission rates converge on the average transmission rate of all existing BRF transmissions, which optimizes the achievable network capacity. As such, this research aims to attempt the capacity optimization of the transmission with the concept of CTPC by keeping the SINR constraint condition. Then, the optimization problem for TPC is formulated as

$$\begin{aligned} \mathcal{F} = \max_{P_i} \quad & \text{mean}\{\forall R_{ij}\} \\ \mathcal{A} = \max_{P_i} \quad & \text{mean}\{\forall \mathcal{F}\} \times \mathscr{C} \\ \text{subject to} \quad & 0 \leq P_i \leq P_{max} \quad , \quad i \in \mathbb{N} \\ & SINR_{ij} \geq \beta \quad , \quad i, j \in \mathbb{N} \end{aligned} \tag{4.1}$$

where R_{ij} is the transmission rate from node i to node j of a BRF transmission, $\mathcal{F}$ is the minimum link rate of each BRF transmission, $\mathscr{C}$ is the consensus coefficient that depends on the node-to-node distance of the network topology, $\mathcal{A}$ is the average link rate of all BRF transmissions, P_i is the transmit power of node i, P_{max} is the transmit power budget, and β is the SINR threshold.

4.2.2 Algorithm for OATC Scheme

The proposed OATC scheme achieves the optimum transmission capacity with limited transmit power through three main steps. First, OATC calculates the transmission rate of each transmission through the CT scheme and MCST scheme. Second, the CTPC algorithm is applied to the CT and MCST scheme to obtain the appropriate transmit power for optimizing the transmission capacity while minimizing the total interference power in the network. Third, the transmission scheme of either the CT or MCST scheme with TPC is determined by a defined tradeoff threshold. The tradeoff threshold $\mathcal{T}$ is the ratio of the interference power to the received power of the receiving nodes in the BRF

Algorithm 2 CT with CTPC Algorithm

Definition: $TC_{CT}(P_{CT}, \mathscr{R}_{CT}, \mathcal{T}_{CT})$ is transmission control set, P is the transmit power and $\mathscr{R}$ is the choice transmission rate, $\mathcal{T}_{\mathcal{CT}}$ is the threshold of CT, t is timeslot, i is the transmitting node, j is the receiving node

Input: SNR_{SR}, SNR_{RD}, $SINR_{\text{SR}}$, $SINR_{\text{RD}}$

Output: $TC_{CT}(P_{CT}, \mathscr{R}_{CT}, \mathcal{T}_{CT})$

1: **function** CT/CTPC
2: Calculate $R^{con}_{\text{SR}}(t)$, $R^{con}_{\text{RD}}(t)$
3: Calculate target rate of each flow $F(t)$ where
$\mathcal{F}(t) \Leftarrow mean\{R^{con}_{\text{SR}}(t), R^{con}_{\text{RD}}(t)\}$
4: Calculate the next target rate of all flows $A(t+1)$ where
$\mathcal{A}(t) \Leftarrow mean\{\forall \mathcal{F}(t)\}$
5: $\mathcal{A}(t+1) = \mathcal{A}(t) \times \mathscr{C}$
6: **if** $\mathcal{A}(t+1) = \mathcal{F}(t)$ **then**
7: $P_i(t+1) = P_i(t)$
8: Set $t \leftarrow t+1$. Go to step 13
9: **else**
10: Calculate $P_i(t+1)$ from $A(t+1)$
11: Set $t \leftarrow t+1$. Go to step 2
12: **end if**
13: Set $P_{CT} = P_i(t)$
14: Set $\mathscr{R}_{CT} = R^{con}_{ij}(t)$
15: Calculate $\mathcal{T}_{CT}$
16: **return** $P_{CT}, \mathscr{R}_{CT}, \mathcal{T}_{CT}$
17: **end function**

Algorithm 3 MCST with CTPC Algorithm

Definition: $TC_{mcst}(P_{mcst}, \mathscr{R}_{mcst}, \mathcal{T}_{mcst})$ is transmission control set, P is the transmit power and $\mathscr{R}$ is choice transmission rate, $\mathcal{T}_{\mathcal{MCST}}$ is the threshold of MCST, t is timeslot

Input: SNR_{SR}, SNR_{RD}, $SINR_{\mathrm{SR}}$, $SINR_{\mathrm{RD}}$

Output: $TC_{mcst}(P_{mcst}, \mathscr{R}_{mcst}, \mathcal{T}_{mcst})$

1: **function** MCST/CTPC
2: Calculate $R^{seq}_{\mathrm{SR}}(t)$, $R^{seq}_{\mathrm{RD}}(t)$, $R^{con}_{\mathrm{SR}}(t)$, $R^{con}_{\mathrm{RD}}(t)$
3: Compute $\tau_{\mathrm{SR}}(t) = \frac{R^{seq}_{\mathrm{SR}}(t)}{R^{seq}_{\mathrm{SR}}(t) - R^{con}_{\mathrm{SR}}(t) + R^{con}_{\mathrm{RD}}(t)}$
4: Compute $\tau_{\mathrm{RD}}(t) = \frac{R^{seq}_{\mathrm{RD}}(t)}{R^{seq}_{\mathrm{RD}}(t) - R^{con}_{\mathrm{RD}}(t) + R^{con}_{\mathrm{SR}}(t)}$
5: Compute $C_{\mathrm{SR}}(t) = \tau_{\mathrm{SR}}(t) \cdot (R^{con}_{\mathrm{SR}}(t) + R^{con}_{\mathrm{RD}}(t)) + (1 - \tau_{\mathrm{SR}}(t)) \cdot R^{seq}_{\mathrm{SR}}(t)$
6: Compute $C_{\mathrm{RD}}(t) = \tau_{\mathrm{RD}}(t) \cdot (R^{con}_{\mathrm{SR}}(t) + R^{con}_{\mathrm{RD}}(t)) + (1 - \tau_{\mathrm{RD}}(t)) \cdot R^{seq}_{\mathrm{RD}}(t)$
7: **if** $C_{\mathrm{SR}}(t) > C_{\mathrm{RD}}(t)$ **then**
8: Set $R(t) \leftarrow \tau_{\mathrm{SR}} \cdot (R^{con}_{\mathrm{SR}}) + (1 - \tau_{\mathrm{SR}}) \cdot R^{seq}_{\mathrm{SR}}$
9: **else**
10: Set $R(t) \leftarrow \tau_{\mathrm{RD}} \cdot (R^{con}_{\mathrm{RD}}) + (1 - \tau_{\mathrm{RD}}) \cdot R^{seq}_{\mathrm{RD}}$
11: **end if**
12: Calculate target rate of each flow $\mathcal{F}(t)$ where
$\mathcal{F}(t) \Leftarrow mean\{R(t)\}$
13: Calculate the next target rate of all flows $\mathcal{A}(t+1)$ where
$\mathcal{A}(t) \Leftarrow mean\{\forall \mathcal{F}(t)\}$
14: $\mathcal{A}(t+1) = \mathcal{A}(t) \times \mathscr{C}$
15: **if** $\mathcal{A}(t+1) = \mathcal{F}(t)$ **then**
16: $P_i(t+1) = P_i(t)$
17: Set $t \leftarrow t+1$. Go to step 22
18: **else**
19: Calculate $P_i(t+1)$ from $A(t+1)$
20: Set $t \leftarrow t+1$. Go to step 2
21: **end if**
22: Set $P_{mcst} = P_i(t)$
23: Set $\mathscr{R}_{mcst} = R(t)$
24: Calculate $\mathcal{T}_{mcst}$
25: **return** $P_{mcst}, \mathscr{R}_{mcst}, \mathcal{T}_{mcst}$
26: **end function**

Algorithm 4 OATC with CTPC Algorithm

Input: $TC_{ct}(P_{ct}, \mathscr{R}_{ct}, \mathcal{T}_{ct})$,

$TC_{mcst}(P_{mcst}, \mathscr{R}_{mcst}, \mathcal{T}_{mcst})$

Output: P and $\mathscr{R}$

function OATC
    if $\mathcal{T}_{mcst} \leq \mathcal{T}_{ct}$ **then**
        Apply MCST/CTPC
        Set $P = P_{mcst}$, $\mathscr{R} = \mathscr{R}_{mcst}$
    else
        Apply CT/CTPC
        Set $P = P_{ct}$, $\mathscr{R} = \mathscr{R}_{ct}$
    end if
  return $P, \mathscr{R}$
end function

transmission and is computed as

$$\mathcal{T} = \frac{\mathscr{I}^*}{\mathscr{G}^*} \tag{4.2}$$

where $\mathscr{I}^* = \sum_{k \in \mathcal{I}, k \neq i} G_{kj} \cdot P_k$ is the interference power and $\mathscr{G}^* = G_{ij} \cdot P_i$ is the received power of the ongoing transmission. OATC selects the operational transmission scheme with the lower $\mathcal{T}$ for higher achievable transmission capacity. The lower tradeoff threshold, the lower interference power, and the higher achievable transmission capacity optimize the achievable network capacity of the entire network.

With the simple compute-and-compare mechanism as in [127], the OATC scheme works cooperatively through the three algorithms executed in the relay node. Algorithm 2 denotes the CT with CTPC, computes the required transmit power, the transmission rate of each transmitting node as the choice of transmission rate $\mathscr{R}$, and the threshold for BRF transmission through the CT. The algorithm is simply designed with two steps. First, the transmission rate of each ongoing transmission is computed according to the channel model, SINR model, and link capacity model. Second, the transmit power is optimized by applying the CTPC algorithm for transmission capacity optimization. As a result, the algorithm returns the transmit power, the transmission rate of each transmitting node, and the tradeoff threshold. Similarly, Algorithm 3 describes the operation of MCST with CTPC. The algorithm computes the transmission rate through the MCST scheme from step 2 to step 11. CTPC has then applied to average the transmission capacity and minimize the interference power by meeting the threshold condition required for successful transmission. Then, the algorithm returns the transmit power, transmission rate, and tradeoff threshold as the results. Finally, Algorithm 4 is the main algorithm for the OATC scheme that selects either the CT scheme or MCST scheme with TPC as the operational transmission scheme based on the returned $\mathcal{T}$ from Algorithm 2 and Algorithm 3 and returns the transmit power and transmission rate for the transmission.

4.3 Numerical Simulations

This section evaluates the performance of the proposed OATC scheme through numerical simulation. The performance evaluation compares the existing FD MAC protocol of RTS/FCTS [64], which considers only the CT without any ST, and the FD-MCST that considers both transmissions, which is discussed in the previous chapter, in the FD wireless networks.

4.3.1 Simulation Scenarios and Settings

The simulation program is written using MATLAB R2021a and is verified according to section 2.5.1. In this research, there are two scenarios to compare the proposed OATC scheme, RTS/FCTS, and FD-MCST in the FD networks. The first scenario is the influence on the DATA length in the 30-node random network topology. And the second scenario is the influence on the network density with a fixed DATA length. Table 4.1 lists the simulation parameter and settings with the standard specification of IEEE 802.11ac [104].

Figure 4.1 shows the block diagram of the analysis for the OATC scheme. The network model randomly generates different network topologies in which the node are uniformly distributed. Assuming that the wireless nodes are considered FD-capable nodes with the same initial transmit power and same channel bandwidth without taking into account the mobility model of the node. Then, the traffic model randomly selects a combination of nodes that form a BRF transmission. The transmission rate is computed through the

Table 4.1: Simulation parameters for evaluation of OATC scheme

Parameter	Value
Network coverage size	100 m × 100 m
Number of nodes (N)	30, 60, 90, 120, 150
Transmit power (P)	20 dBm
Channel model	Log-distance pathloss
Attenuation constant (α)	3.5
Wall attenuation (W_{ij})	0 dB
Shadowing parameter (X_{σ})	8 dB
Noise level (η)	-174 dBm
Channel bandwidth (B)	20 MHz
Basic rate (R_{base})	24 Mbps
PHY header duration	44 μs
MAC header	320 bits
RTS size	160 bits
CTS size	112 bits
STS size	120 bits
ACK size	112 bits
DIFS length	34 μs
SIFS length	16 μs
Contention window (CW)	16 Slot time
Slot time length (θ)	9 μs
DATA length (l)	1500, 2500, 3500, 4500, 5500, 6500 bytes
Consensus coefficient ($\mathscr{C}$)	0.5 $\sim$ 3
Number of simulations	1,000 times

log-distance pathloss without considering the frequency parameter as the channel model, SINR model, and link capacity model, which are discussed in the previous section. For theoretical study purposes, the simulation only considers one transmission per DATA frame without transmission scenarios. Thus, the proposed OATC scheme, RTS/FCTS, and FD-MCST are fairly evaluated by setting the backoff timer as the initial backoff contention window. Simulation results are based on performance metrics of achievable

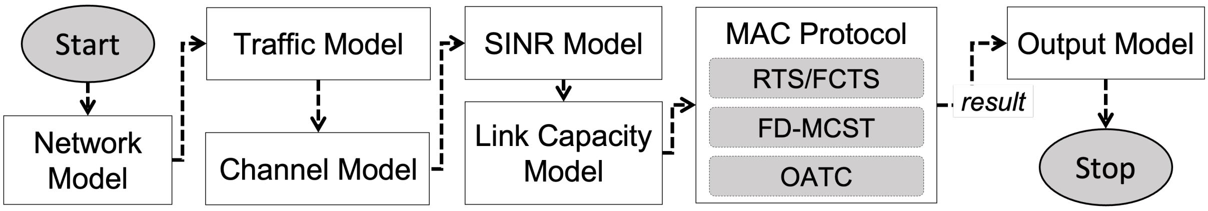

Figure 4.1: Block diagram of numerical analysis for OATC scheme

network capacity, achievable throughput, and achievable transmission overhead with a 6 dB SINR threshold considered over 1,000 different simulations.

4.3.2 Simulation Results and Discussion

The simulation discussion mainly consists of two parts for two simulation scenarios: the influence of DATA length in the 30-node random topology scenario and the influence of network density.

Influence on DATA Length

In this section, the performance of the proposed OATC scheme with RTS/FCTS and FD-MCST is described when the DATA length is varied in the 30-node random network topology.

Firstly, Table 4.2 shows the performance of the proposed OATC scheme with the two reference MAC protocol, i.e., RTS/FCTS and FD-MCST in achievable network capacity and achievable throughput for the network with a single BRF transmission and fixed DATA length of 1500 bytes. The simulation results indicate that a single BRF transmission is free from interference in the network. Then, the selection of the MCST scheme in

Table 4.2: Performance comparison between RTS/FCTS, FD-MCST, and OATC scheme for the network with single BRF transmission and a fixed DATA length of 1500 bytes

	Achievable network capacity [Mbps]	**Achievable throughput [Mbps]**
RTS/FCTS	77.07	150.04
FD-MCST	78.47	195.92
OATC	78.47	195.92

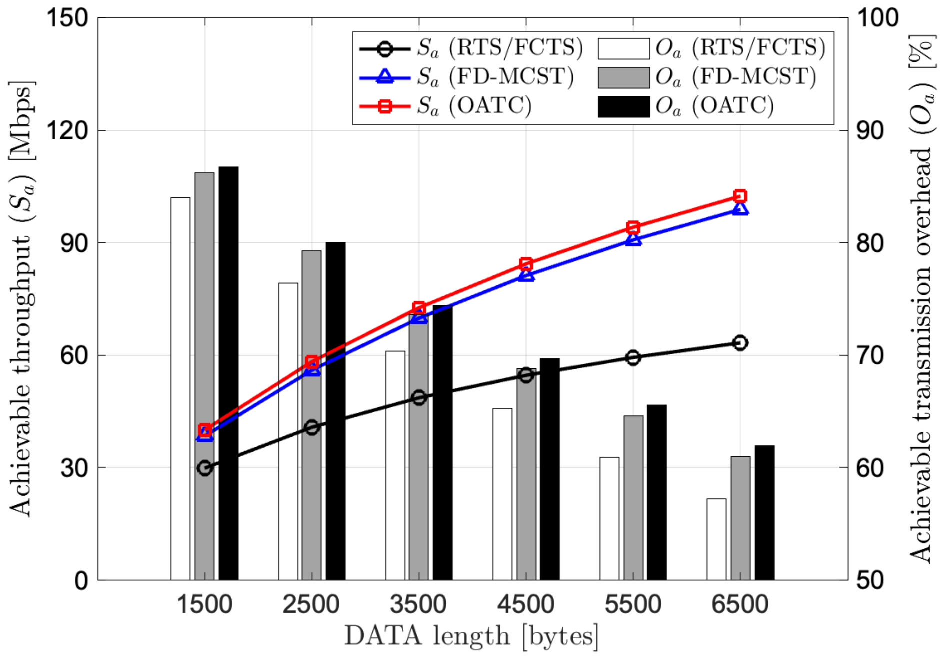

Figure 4.2: Performance comparison in achievable throughput and achievable transmission overhead with the influence of DATA length

the OATC gives high transmission capacity to improve the achievable throughput of the BRF transmission.

Figure 4.2 shows the performance in the achievable throughout and overhead ratio for the 30-node random network topology. The simulation results show that OATC has an advantage in achievable throughput compared to RTS/FCTS and FD-MCST without TPC techniques, regardless of the DATA length. In specific, when the DATA length is 1500 bytes, OATC achieves 40.02 Mbps, while RTS/FCTS and FD-MCST bring 29.84 Mbps and 38.42 Mbps, respectively. When the DATA length is 6500 bytes, OATC gives 102.41 Mbps, while RTS/FCTS and FD-MCST give 63.28 Mbps and 98.84 Mbps, respectively. That is, when the DATA length is 1500 bytes, OATC provides 34% and 4% of achievable throughput improvement compared to RTS/FCTS and FD-MCST, respectively. When the data length is 6500 bytes, the improvement increases up to 62% and 4% than RTS/FCTS and FD-MCST, respectively. The reason is that OATC optimizes the transmission capacity by considering the tradeoff threshold through the algorithm. In other words, the optimum transmission capacity provided by OATC shortens the successful transmission time and increases the achievable transmission overhead. Therefore, compared to the other two protocols, the throughput improvement of OATC increases with high achievable transmission overhead as the DATA length increases.

Influence on Network Density

Table 4.3 presents the RTS/FCTS and FD-MCST performance with and without the TPC by comparing with OATC when the number of BRF transmissions is varied in the network. When the DATA length is set to 1500 bytes, the simulation results show that the CTPC algorithm can give a higher achievable throughput than both the RTS/FCTS and FD-MCST. However, OATC can achieve a higher achievable throughput by exploiting the temporal and spatial reuse and considering the tradeoff threshold between the interference power and capacity gain.

Table 4.3: Performance analysis of OATC scheme in achievable throughput when the DATA length is 1500 bytes

	Achievable throughput [Mbps]				
No. of BRF transmissions	**RTS/FCTS**		**FD-MCST**		**OATC**
	no TPC	**TPC**	**no TPC**	**TPC**	
10	29.84	31.78	38.42	39.68	40.02
20	20.79	23.52	27.75	29.99	30.23
30	18.48	21.34	24.99	27.28	27.51
40	17.27	20.45	23.54	26.17	26.40
50	16.22	19.49	22.30	25.13	25.36

Figure 4.3 shows the performance comparison of OATC to RTS/FCTS and FD-MCST without TPC techniques regarding achievable network capacity and total interference power when the number of BRF transmissions is varied in the FD networks. As shown in the figure, OATC is capable of achieving better network capacity compared to RTS/FCTS. Quantitatively, with 50 BRF transmissions, OATC reaches up to 781.63 Mbps, and RTS/FCTS gives 529.45 Mbps. In other words, when the number of BRF transmissions in the network varies from 10 to 50, OATC can increase the achievable network capacity by 36% to 48%, respectively, compared to RTS/FCTS. However, when the network is congested, the achievable network capacity of OATC is less than that of FD-MCST.

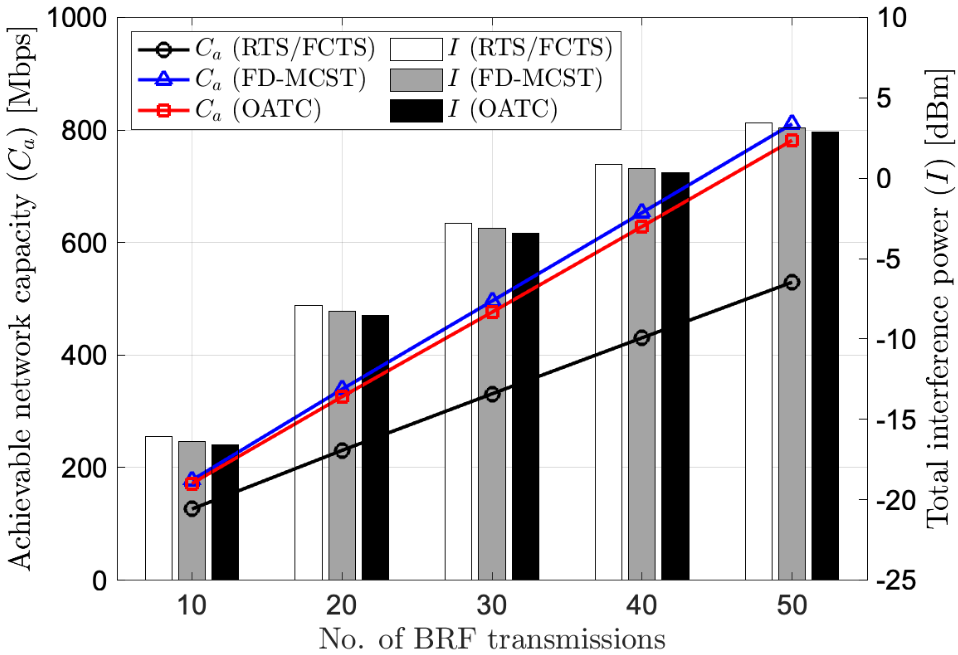

Figure 4.3: Performance comparison in achievable network capacity and total interference power with the influence of network density

When there are 50 BRF transmissions in the network, the achievable network capacity of OATC is about 4% lower than that of FD-MCST, which is neglectfully compared to the achievement over RTS/FCTS. The reason is that OATC applies the CTPC algorithm and control transmit power with consensus coefficient to average the transmission capacity and reduce the interference power. In addition, the OATC algorithm selects the active transmission scheme that minimizes the total interference power. As shown in Figure 4.3, a higher network density will increase the total interference power. However, the comparison shows that OATC is superior to RTS/FCTS and FD-MCST in total interference power. Therefore, the simulation results show that OATC can achieve a high network capacity and low interference power, regardless of the number of BRF transmissions in the network.

Figure 4.4 compares the performance of the number of BRF transmissions in the network regarding the achievable throughput and achievable transmission overhead. OATC describes the higher achievable throughput than RTS/FCTS and FD-MCST with a fixed DATA length of 1500 bytes. The reason is that OATC uses the CTPC scheme to control the transmit power. This allows the interference power to be reduced while meeting the

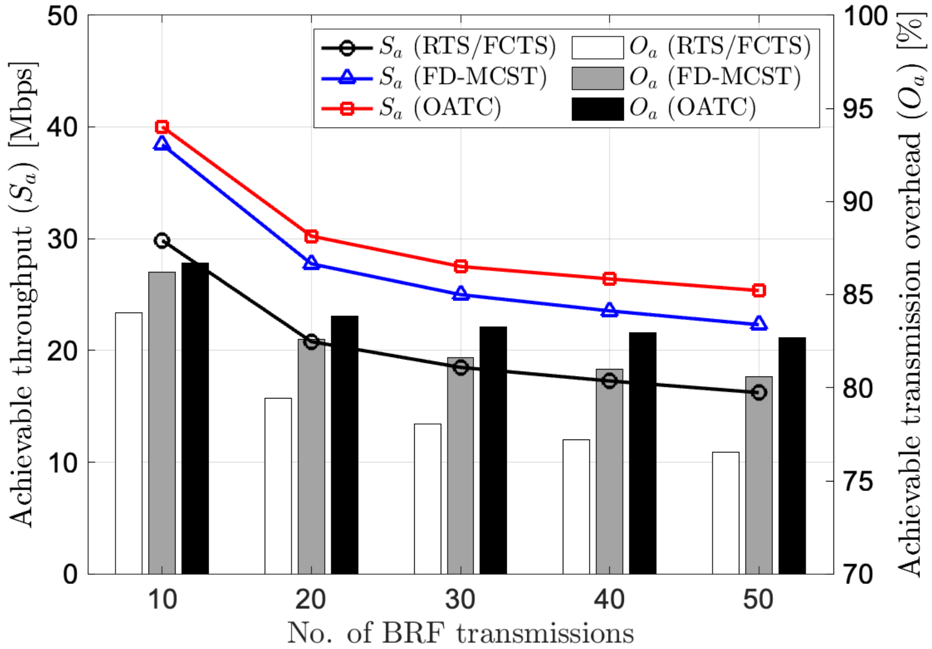

Figure 4.4: Performance comparison of achievable throughput and achievable transmission overhead with the influence of network density

SINR constraint of the transmission. As a result, OATC converges the transmission rate of all concurrent transmissions and increases the number of successful transmissions. The figure depicts that the achievable throughput decreases as the number of BRF transmissions increases. This is because, in the coverage area of a fixed network, the distance from the transmitter to the receiver becomes shorter. However, OATC achieves the highest achievable throughput compared to the other two protocols regardless of the number of BRF transmissions. The figure also shows that as the number of BRF transmissions increases, the achievable transmission overhead of OATC is much higher than that of the two referenced protocols. Specifically, when the number of BRF transmissions is 50, OATC gives an achievable overhead ratio of 83%, while RTS/FCTS and FD-MCST give 77% and 81%, respectively. This is because the higher transmission rate given by OATC results in a shorter successful transmission time to complete a transmission.

Finally, Table 4.4 presents the simulation results and describes the performance analysis of the operating transmission scheme in the OATC scheme. Depending on the scenarios and results of numerical simulation, an increase in the number of BRF transmissions leads to the network becoming denser and an increase in the total interference power. As can be

Table 4.4: Performance analysis of OATC scheme in selecting CT as operational transmission scheme

No. of BRF transmissions	**Ratio of CT in OATC**	**Interference reduction [dBm]**	C_a **gain**	S_a **gain**
10	0.11	0.53 (3%)	36%	34%
20	0.06	0.62 (8%)	41%	45%
30	0.05	0.61 (22%)	44%	49%
40	0.04	0.54 (61%)	46%	53%
50	0.03	0.60 (17%)	48%	56%

seen from the table, the ratio of the CT scheme that works as the transmission scheme in the OATC scheme is decreasing to reduce the interference caused by the concurrent transmission. Therefore, reducing CT in the OATC scheme increases the achievable network capacity and achievable throughput gain and reduces interference when the number of BRF transmissions increases. However, when the number of BRF transmissions is 50, the total interference power reduction decreases because the distance between the source and destination node is shorter for the selection of BRF transmission. In summary, in comparison with FD MAC protocols using RTS/FCTS and FD-MCST, the proposed OATC scheme has advantages in terms of total interference power, achievable network capacity, and achievable throughput.

4.4 Summary

In this chapter, an OATC scheme to optimize the capacity as the power management module is proposed in the FD wireless networks. Compared to the MAC protocol of RTS/FCTS and FD-MCST, the performance of OATC is evaluated. The simulation result reveals that the CT and the MCST scheme alone cannot guarantee the optimum transmission capacity in the FD system. Therefore, it is important to apply the ST and TPC for network interference. Taking into account the tradeoff between the interference power and received power, the OATC outperforms the RTS/FCTS and FD-MCST with around 56% and 14% achievable throughput improvement, respectively.

Chapter 5

Channel Interference Balancing Allocation Scheme

In this chapter, the CIBA scheme is designed as the resource management module in multi-channel multihop wireless networks. The proposed CIBA is designed to consider minimizing interference as the important factor in optimizing BRF transmission capacity over multi-channel multihop wireless networks. Different from the previous chapters, CIBA optimizes the transmission capacity by considering the effect of total interference power on the sub-channels and allocating the concurrent transmissions to balance the interference among different sub-channels.

This chapter is structured with six main sections. First, the research background and related works in the area of channel allocation are reviewed. Second, the system model and assumptions of the research work are described. Third, the research discussion of the channel allocation management framework is provided. Fourth, the designed CIBA scheme is discussed in detail. The fifth section discusses the performance analysis of the proposed CIBA scheme through numerical simulations. Then, the sixth section draws the summary of the chapter.

5.1 Research Background

Beyond the realization of the simultaneous transmission of the FD system, capacity optimization becomes a challenge in wireless networks considering the tradeoff between interference power (i.e., SI and IUI) and the network capacity gain in the wireless networks. In this regard, transmission resource management and scheduling approaches were seen as promising opportunities to increase the network capacity. The user scheduling and resource allocation algorithm was presented to avoid the high interference effect from the concurrent transmission in [128]. Unlikely, Tehrani et al. introduced channel allocation and power allocation to optimize uplink and downlink transmission capacity, affecting overall network capacity [129].

This research investigates the performance of the channel allocation scheme in the multi-channel multihop wireless networks to optimize transmission capacity in total interference power and achievable capacity in the FD wireless networks. The multi-channel multihop wireless network refers to the wireless network with different transmission channels, and a wireless node is equipped with multiple radios [130]. Different from the current studies of interference mitigation schemes, TPC, and user scheduling algorithms, this research the method of allocating the nearby transmission into the other sub-channel to mitigate the interference power. Mitigating the interference power improves the transmission capacity and increases the capacity of the entire network. Therefore, the objectives of this chapter are to study how the channel allocation schemes affect the performance of the transmission capacity with total interference power. This chapter proposes the CIBA scheme as an allocation management module for exploiting the multi-channel channel allocation scheme applicability in terms of interference power in the FD wireless networks.

5.1.1 Related Works

The basic transmission with relaying strategy can be divided into single relaying and multiple relaying transmissions according to the number of relay nodes in the transmission flow. In addition, according to the communication system, it can be categorized as relay HD (RHD) and relay FD (RFD) transmission modes [131]. Since there are no research works supporting the quality of service requirements of RHD and RFD transmission modes, Cheng et al. presented a resource allocation scheme to solve the CCI problems in the relaying networks [132]. In the proposed scheme, a new cancellation coefficient parameter is introduced to analyze the performance of the RFD mode. In the research, the authors also conducted the performance evaluation of the allocation scheme for the hybrid RHD and RFD transmission modes and concluded that the capacity gain of the RFD over RHD is more than twice.

In a similar work on RFD, the authors in [133] designed the IUI estimation and cancellation protocol for unidirectional FD transmission. The authors also designed the scheduling and power resource allocation approach to maximize the achievable spectral efficiency. Their simulation results reveal that the proposed protocol consistently outperforms the FD MAC protocol and the spectral efficiency gain in high-interference environments is significant. Similarly, Li et al. designed a user scheduling scheme to reduce the IUI from uplink to downlink transmission in the FD infrastructure-based network [134]. Then, similar research was conducted at [135], which considers TPC for capacity optimization and interference mitigation in ad hoc networks.

In recent years, the research direction to consider the challenges associated with resource allocation and capacity optimization in multi-channel multihop wireless networks has gotten attention. The resource allocation problem has been approached from different angles, starting with analysis and protocol-oriented solutions. A channel allocation and scheduling algorithm is proposed in [136] for congestion control in the multi-channel multihop wireless network. In the research, the optimization algorithms to maximize the network traffic utilization are designed by considering the intensity of incoming traffic, channel loads, available channels, and transmission scheduling. Diakonikolas and Zussman described analytical results of FD transmission in the single-channel and multi-channel wireless network [137]. In the research, the authors argued that it is essential to propose and evaluate the FD system performance through the scheduling, channel allocation, and TPC in multi-channel wireless networks.

Therefore, channel allocation management is worth studying as a research approach aiming at the algorithm design level based on a solid theoretical background. It is also interesting to observe changes in network capacity through the simulation approach that can be demonstrated analytically to ensure some performance improvements. The purpose of this chapter is to provide a simple framework to investigate the performance of the multi-channel and multihop wireless network as a function of the number of nodes with different transmission modes (HD and FD), single relaying transmission, and channel allocation algorithms.

5.1.2 Motivation

Current research on the multi-channel allocation scheme has mainly been studied in HD wireless networks. Therefore, the motivation is to consider the capacity maximization problem through multi-channel allocation in the FD wireless networks. Since FD systems are getting more attention with the spectral efficiency benefit than HD, it is worth considering the effect of applying an interference-based balancing approach on the multi-channel allocation scheme in the FD wireless networks. Furthermore, this research motivates us to investigate further how to apply the multi-channel allocation scheme to future wireless communications.

5.2 System Model

This chapter assumes that the wireless network is a multi-channel and multihop wireless network with multi-channel transmission. The network assumes that the wireless node is equipped with multiple radios. Therefore, the spectrum is divided into K sub-channels, each with the same bandwidth B. Let $\mathbb{K} = \{1, \cdots, \mathsf{k}, \cdots, \mathsf{K}\}$ denotes the set of sub-channels and a different sub-channel, k where $\mathsf{k} \in \mathbb{K}$, is allocated to each source node and/or relay node, on the other way, SR transmission and/or RD transmission, respectively, without loss of generality. Supporting that a source node and/or a relay node is being allocated a single sub-channel, then its channel allocation indicator is given as n_{k} where $n \in \mathbb{N}$.

5.2.1 Channel Model

The available spectrum is assumed to be organized in K separate sub-channels. For the kth sub-channel, the signal attenuation of the transmission link over a communication channel depends on the log-distance pathloss model with ITU recommendation [138]. Then, the channel gain in the unit of dB from node i to node j, where $i, j \in \mathbb{N}$, is given as

$$PL_{ij}^{\mathsf{k}} = PL_0^{\mathsf{k}} + 10 \cdot \alpha \cdot \log_{10}(\frac{d_{ij}}{d_0}) + PL_{\mathrm{F}} - W_{ij} + X_\sigma \tag{5.1}$$

where $PL_0^{\mathsf{k}} = 20 \cdot \log_{10}(\mathrm{F}) - 28$ and F is the frequency of transmission in the unit of MHz. $PL_{\mathrm{F}} = 15 + 4(\kappa - 1)$ is the floor penetration loss factor with κ floors between the transmitter and the receiver and $\kappa = 0$. This pathloss model is also considering instantaneous fading as a Gaussian random variable (X_σ) with zero mean and standard deviation of σ.

5.2.2 Interference and SINR Model

The existing researches use the concept of a receiver-oriented interference model, the Physical Model [60] and Protocol Model [139], to represent interference of ongoing transmission. Since this research does not consider the interference between different channels, the Physical Model, which is dependent on the interference at the kth sub-channel, is assumed.

The Physical Model assumes that all wireless nodes access the transmission medium without previously checking transmissions from neighboring wireless nodes. Then, the effect of interference on the transmission is evaluated against the channel gain. The concept of *interference distance* is introduced to obtain a better parameter to quantify the effect of interfering nodes at different distances from the interfering node to the receiving node.

Definition 1 (Interference Distance)**.** *An interference distance D_{kj} concerning a receiving node j is the total of all distances powered by pathloss exponent, α, over a summation of k simultaneous transmissions result in the signal reception at node j.*

Lemma 1. *Assuming that a node i transmits to another node j at distance d_{ij}. Then, other active nodes, K are performing k simultaneous transmissions, $k \in \{1, \ldots, K\}$. Therefore, the interference distance to the intended receiving node j is*

$$D_{kj} = \sum_{k \in K, k \neq i} \frac{1}{d_{kj}^{\alpha}} \tag{5.2}$$

where d_{kj} is the distance from interfering node k to the receiving node j.

Proof 1. *With the assumption that all the nodes have similar receiver characteristics, such as omnidirectional antenna, same sub-channel, same transmit power and thermal noise, and same physical configuration, the k simultaneous transmissions from other nodes will result in D_{kj}. However, (3.4) at the receiving node j will result the successful reception as long as*

$$SINR_{ij} \nleq \beta \tag{5.3}$$

and other active nodes, K, are located at distance greater than d_{ij} and vice versa. The notation D_{kj} is hereafter called interference distance.

5.3 Channel Allocation Management Framework

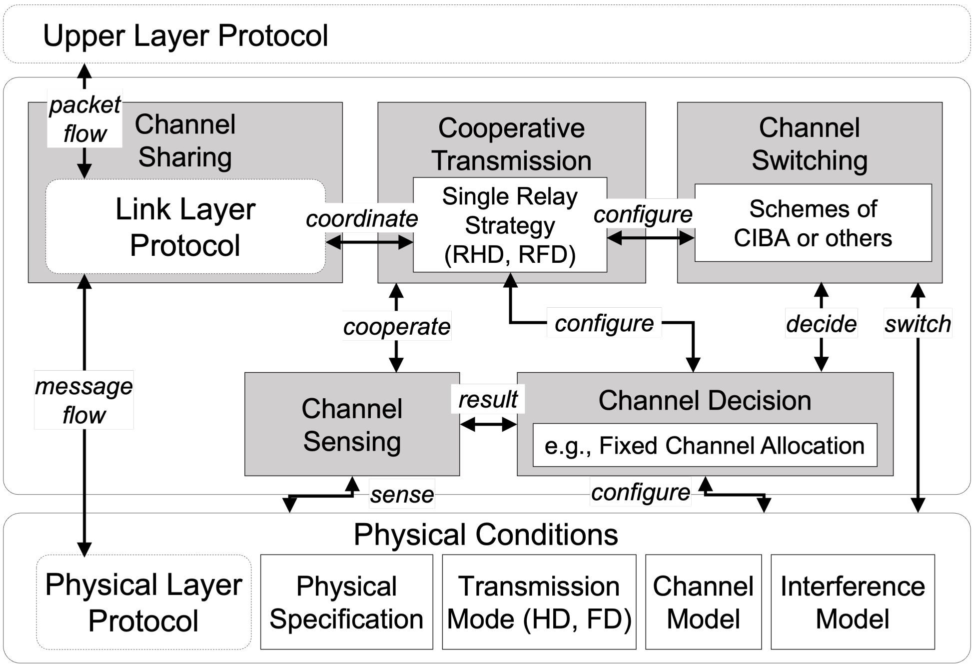

Figure 5.1: Multi-channel allocation management framework in wireless networks

A multi-channel allocation management framework is introduced in this section with four components: channel sensing, channel decision, channel switching, and channel sharing. Figure. 5.1 shows the multi-channel allocation management framework conceptualized regarding the cooperative transmission between the wireless nodes. In the framework, the wireless node performs cooperative transmission by involving any BRF transmission through the specified transmission mode (HD and FD transmission modes). The function and process of each component are as follows:

1. Channel Sensing: a wireless node captures and detects the channel condition of the ongoing transmission through its transmission mode

2. Channel Decision: a wireless node completes the channel selection based on a channel allocation algorithm and sets the assigned channel for data transfer

3. Channel Switching: the wireless node switches the pre-assigned channel allocation with an additional advanced algorithm to a new channel to improve a cooperative network performance

4. Channel Sharing: the wireless node shares the channel decision information through a shared wireless medium network with the link layer protocol

5.3.1 Channel Allocation Constraints

This research assumes a list of channel allocation constraints. First, it is assumed that a wireless node can occupy up to two channels. Second, for the relay node, only one channel can be assigned to the HD node at one timeslot. However, the FD node can use at one timeslot. Furthermore, all the transmitting nodes use one channel as a common channel for sharing their channel information with others.

Algorithm 5 Channel Allocation Algorithm

Definition: Assuming the total no. of sub-channel, $\mathsf{K} = 2$, N is total no. of nodes, n_{k} is node that being assigned as a sub-channel k

Input: N

Output: n_{k}

function FCA
  Set $\mathsf{k} = \mathsf{K}$ ▷ k is the index of sub-channel
  Set $F = N/3$ ▷ f is the index of BRF transmission
  for $f \leftarrow 1$ to F **do**
    Set n_{S}^{f}, n_{R}^{f}, $n_{\mathrm{D}}^{f} \leftarrow f$ ▷ n is the index of node
  end for
  function SPCA(N, K, n_{k})
  function STCA(N, K, n_{k})
  function SACA(N, K, n_{k})
  function CIBA(N, K, n_{k})
  Share $\forall n_{\mathsf{k}}$ **information**
end function

Algorithm 6 SR Pairing Channel Allocation Algorithm

```
function SPCA
    while ∀N is not assigned a sub-channel do
        for f ← 1 to F do
            if f ≤ K then
                for k ← f to K do
                    if SR^f, RD^f is NULL then
                        Assign SR^f, RD^f ← k
                        Set n_S^f, n_R^f as n_k ← k
                    end if
                end for
            else
                for k ← 1 to K do
                    if SR^f, RD^f is NULL then
                        Assign SR^f, RD^f ← k
                        Set n_S^f, n_R^f as n_k ← k
                    end if
                end for
            end if
        end for
    end while
end function
```

5.3.2 Channel Allocation Algorithms

As simplified in Algorithm 5, all transmitting nodes of the BRF transmission are assigned one channel according to a channel allocation algorithm. The algorithm can allocate the sub-channels to the SR transmission and RD transmission. In this research, three fixed channel allocation schemes are studied, and the algorithms are described below.

1. SR Pairing Channel Allocation (SPCA) algorithm: SPCA assigns the sub-channel by pairing the SR and RD transmissions of the BRF transmission. Algorithm 6 shows the channel allocation by SPCA.

2. SR Transmitting Channel Allocation (STCA) algorithm: STCA assigns the same

Algorithm 7 SR Transmitting Channel Allocation Algorithm

function STCA
  while $\forall N$ is not assigned a sub-channel **do**
    for $f \leftarrow 1$ to F **do**
      for $\mathsf{k} \leftarrow 1$ to $\mathsf{K} - 1$ **do**
        if SR^f, RD^f is NULL **then**
          Assign $\text{SR}^f \leftarrow \mathsf{k}$ and $\text{RD}^f \leftarrow \mathsf{k} + 1$
          Set n_{S}^f as $n_{\mathsf{k}} \leftarrow \mathsf{k}$ and n_{R}^f as $n_{\mathsf{k}} \leftarrow \mathsf{k} + 1$
        end if
      end for
    end for
  end while
end function

sub-channel to the same SR or RD transmissions of the BRF transmission. In particular, STCA assigns the first sub-channel to the SR transmission and the second sub-channel to the RD transmission as described in Algorithm 7.

3. SR Alternating Channel Allocation (SACA) algorithm: SACA assigns the sub-channel by alternating the sequence of SR and RD transmissions of the BRF transmission. Algorithm 8 shows how SACA works out the channel allocation.

5.4 CIBA Scheme

The main idea of CIBA scheme is to switch the existing channel allocation to balance the total interference power of two sub-channels over several concurrent transmissions. As the number of concurrent transmissions in the network increases, the total interference power also increases with the shared channel. The fixed channel allocation schemes assign the channel statically to the transmission according to the specific algorithm. CIBA scheme allocates the channel dynamically with the purpose of total interference mitigation by balancing the interference power of each sub-channel, in which the summation of interference power is based on the defined interference distance in the entire network. By balancing the total interference power between the two sub-channels in the network

Algorithm 8 SR Alternating Channel Allocation Algorithm

function SACA
  while $\forall N$ is not assigned a sub-channel **do**
    for $f \leftarrow 1$ to F **do**
      for $\mathsf{k} \leftarrow 1$ to $\mathsf{K} - 1$ **do**
        if $f \pmod 2 = 1$ **then**
          if SR^f, RD^f is NULL **then**
            Assign $\text{SR}^f \leftarrow \mathsf{k}$ and $\text{RD}^f \leftarrow \mathsf{k} + 1$
            Set n_{S}^f as $n_{\mathsf{k}} \leftarrow \mathsf{k}$ and n_{R}^f as $n_{\mathsf{k}} \leftarrow \mathsf{k} + 1$
          end if
        else
          if SR^f, RD^f is NULL **then**
            Assign $\text{SR}^f \leftarrow \mathsf{k} + 1$ and $\text{RD}^f \leftarrow \mathsf{k}$
            Set n_{S}^f as $n_{\mathsf{k}} \leftarrow \mathsf{k} + 1$ and n_{R}^f as $n_{\mathsf{k}} \leftarrow \mathsf{k}$
          end if
        end if
      end for
    end for
  end while
end function

using a multi-channel allocation scheme, CIBA could increase the achievable capacity of the whole network. According to the CIBA algorithm, CIBA computes the interference distance with a common channel and assigns the sub-channel based on the minimum difference in interference distance between two sub-channels. As explained in Algorithm 9, the CIBA algorithm is mainly divided into two main steps: balancing the interference and allocating the channel. The concept of the multi-channel allocation through the CIBA algorithm is as follows. First, a receiver obtains the interference distance from the other concurrent transmissions and shares the distance with other receivers. Second, the receiver collects the interference distances from other receivers. Third, the receiver computes and balances the total interference power of the two sub-channels. Last, the receiver allocates the sub-channel according to the algorithm.

Algorithm 9 Channel Interference Balancing Allocation Algorithm

function CIBA
  Compute $\forall D^f_{k\mathrm{R}}, D^f_{k\mathrm{D}}$ of SR^f, RD^f
  while $min\{diff(\mathbb{G}_1, \mathbb{G}_2)\}$ **do**
    while $\forall(D^f_{k\mathrm{R}}, D^f_{k\mathrm{D}})$ is not assigned into a group **do**
      Set $\mathbb{G}_1 = rand(D^f_{k\mathrm{R}}, D^f_{k\mathrm{D}})$
      Set $\mathbb{G}_2 = rand(D^f_{k\mathrm{R}}, D^f_{k\mathrm{D}})$
    end while
  end while
  while $\forall N$ is not assigned a sub-channel **do**
    for $f \leftarrow 1$ to F **do**
      if SR^f, RD^f is NULL **then**
        if SR^f is belonging to $\mathbb{G}_1$ **then**
          Assign $\mathrm{SR}^f \leftarrow \mathsf{k}$
          Set n^f_{S} as $n_{\mathsf{k}} \leftarrow \mathsf{k}$
        else
          Assign $\mathrm{SR}^f \leftarrow \mathsf{k}+1$
          Set n^f_{S} as $n_{\mathsf{k}} \leftarrow \mathsf{k}+1$
        end if
        if RD^f is belonging to $\mathbb{G}_1$ **then**
          Assign $\mathrm{RD}^f \leftarrow \mathsf{k}$
          Set n^f_{R} as $n_{\mathsf{k}} \leftarrow \mathsf{k}$
        else
          Assign $\mathrm{RD}^f \leftarrow \mathsf{k}+1$
          Set n^f_{R} as $n_{\mathsf{k}} \leftarrow \mathsf{k}+1$
        end if
      end if
    end for
  end while
end function

5.5 Numerical Simulations

In this section, the performance of the CIBA scheme is evaluated through numerical simulations. The discussion is carried out using the different transmission modes, (for example, HD and FD) in both single-channel and multi-channel in multihop wireless network environments.

Table 5.1: Simulation parameters for evaluation of CIBA scheme

Parameter	**Value**
Network coverage size	100 m × 100 m
Number of nodes	9, 12, 15, 30, 60, 90, 120, 150
Transmit power	20 dBm
Channel model	Log-distance pathloss model with ITU recommendation
Attenuation constant (α)	3
Wall attenuation (W_{ij})	0 dB
Shadowing parameter (X_σ)	8 dB
Noise level (η)	-174 dBm
Channel bandwidth (B)	20 MHz
Number of sub-channels (K)	2
Frequency of sub-channels (F)	5.18 and 5.32 GHz
Number of simulations	10,000 times

5.5.1 Simulation Scenarios and Settings

The simulation program is written using MATLAB R2021a and verified according to section 2.5.1. This research includes three simulation scenarios: (i) the analysis of different transmission modes in the multihop wireless with single-channel and multi-channel; (ii) the performance difference between fixed channel allocation schemes for multi-channel and multihop wireless networks with FD transmission mode; and (iii) the performance of the proposed CIBA scheme. Table 5.1 describes the simulation parameters and setting according to the standard specification of IEEE 802.11ac [104]. Besides, Figure 5.2 also shows the numerical simulation block diagram for the proposed CIBA scheme. As in the

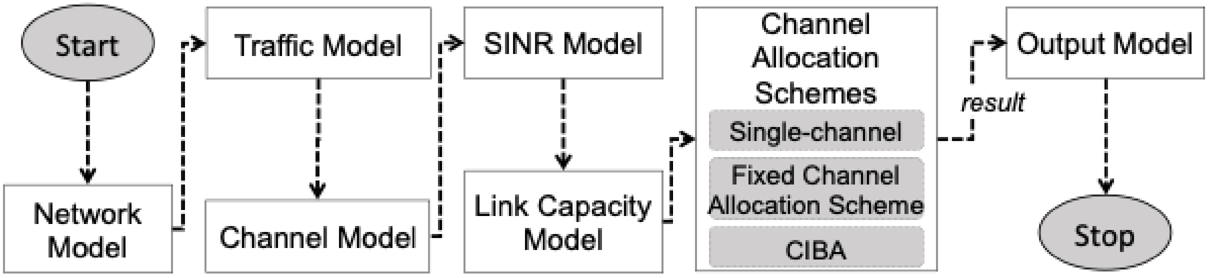

Figure 5.2: Block diagram of numerical analysis for CIBA scheme

previous chapter, the wireless nodes are uniformly distributed in the network. In a homogeneous network, all the wireless nodes have similar transmit power, channel bandwidth, and the number of equipped channels. In the traffic model, the selection of node combinations that form a BRF transmission is random. However, the channel model in this chapter is assumed as the log-distance pathloss model with ITU recommendation. The transmission rate is based on the SINR model and link capacity model. After performing the numerical simulation for three simulation scenarios, the matrices of total interference power and achievable network capacity are mainly looked into for performance investigation. The simulation results are the average of the 10,000 different experiments.

5.5.2 Simulation Results and Discussion

The performance analysis of the channel allocation schemes is evaluated as the following.

Performance Analysis of Different Transmission Modes

Figure 5.3 describes the performance comparison between HD and FD transmission modes considering the single-channel allocation and SPCA as a multi-channel allocation in multihop wireless networks. It can be seen from the figure that the average total interference of the HD transmission mode is lower than that of the FD in both single-channel and multi-channel multihop wireless networks. Using SPCA as a multi-channel allocation algorithm, FD transmission provides lower total interference than single-channel HD transmission. The reason is that the SPCA can allocate the channel for the total interference power mitigation and gives benefits even over single-channel HD transmission. For example, if the number of BRF transmissions in the network is 10, the total interference power is -67.66 dBm in single-channel HD transmission mode, but the interference power can be reduced

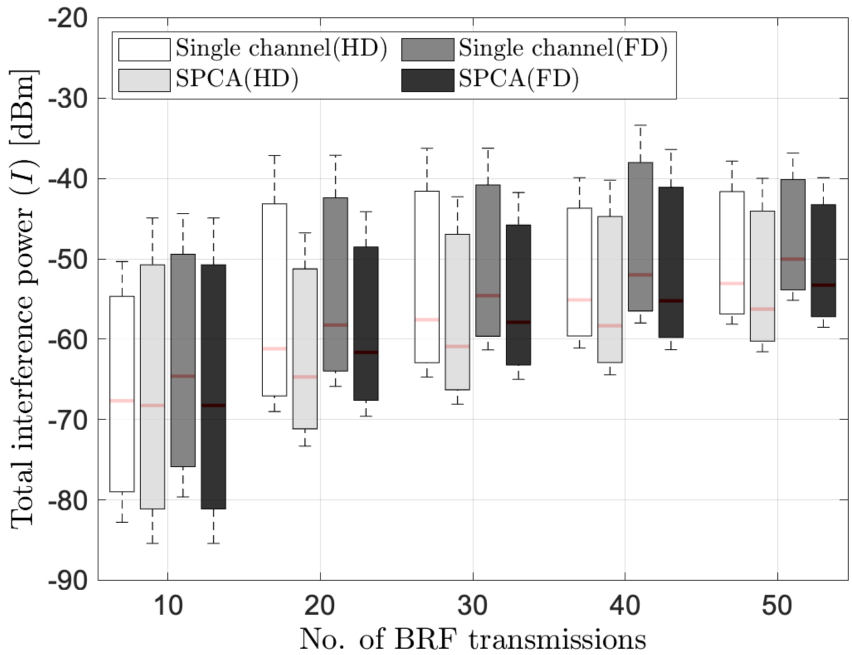

Figure 5.3: Performance analysis of transmission modes in total interference power

from -64.60 to -68.24 dBm (around 56%) compared to single-channel FD transmission by the multi-channel allocation. When the number of BRF transmissions is 50, multi-channel FD transmission can reduce the interference from -50.04 dBm to -53.27 dBm (6.4%) lower than the single-channel FD transmission and 0.4% reduction than -53.07 dBm of the single-channel HD transmission. The simulation results also describe that the total interference power of both HD and FD transmission modes increases with the number of BRF transmissions; that is, the network has a high node density. Regardless of the number of BRF transmissions, the total FD interference power caused by FD transmission in the single-channel network is higher than that of the HD transmission, but the FD transmission mode can help reduce the total interference power via a multi-channel allocation algorithm.

Figure 5.4 shows the achievable network capacity performance of HD and FD transmission modes when treating single-channel allocation and SPCA as multi-channel allocation algorithms. Regardless of the number of BRF transmissions, the multi-channel FD transmission mode using SPCA represents the achievable network capacity improvement over single-channel FD and HD transmission modes. Compared to the single-channel HD transmission, the single-channel FD transmission can increase the achievable network

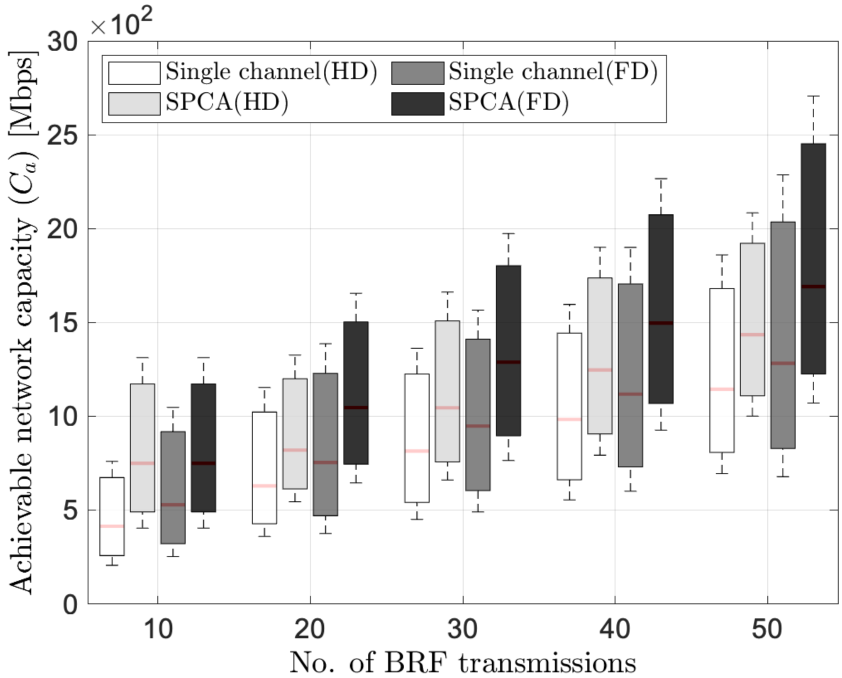

Figure 5.4: Performance analysis of transmission modes in achievable network capacity

capacity despite higher total interference power. However, since the single-channel FD transmission gives a higher total interference power than the multi-channel HD transmission, the HD transmission adopting the ST strategy can achieve better achievable network capacity in the multi-channel multihop wireless network. Furthermore, another interesting observation is that the increase in achievable network capacity can be obtained by the multi-channel FD transmission. Comparing the FD and HD transmission modes in a single-channel environment, the achievable network capacity in multi-channel FD transmission in the ten BRF transmissions network increases by approximately 1.4 times and 1.8 times, respectively. In addition, when the number of BRF transmissions is 50, the multi-channel FD transmission is 1.3 times and 1.5 times that of single-channel FD and HD transmission, respectively. The FD transmission produces a higher total interference than the HD transmission in the single-channel and multihop wireless networks, but the FD transmission can provide a better network capacity via a multi-channel allocation algorithm regardless of the number of BRF transmissions.

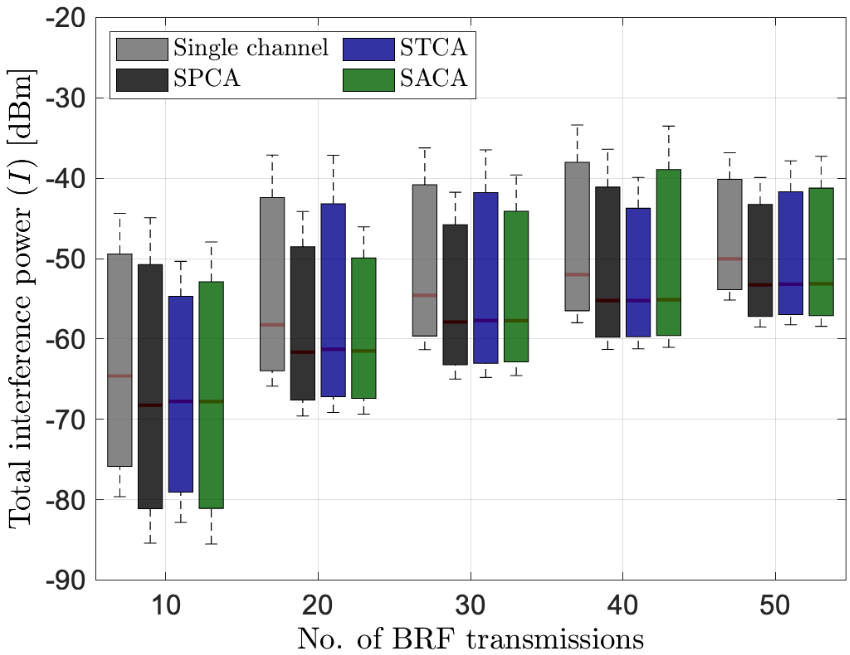

Figure 5.5: Performance analysis of fixed channel allocation schemes for FD system in total interference power

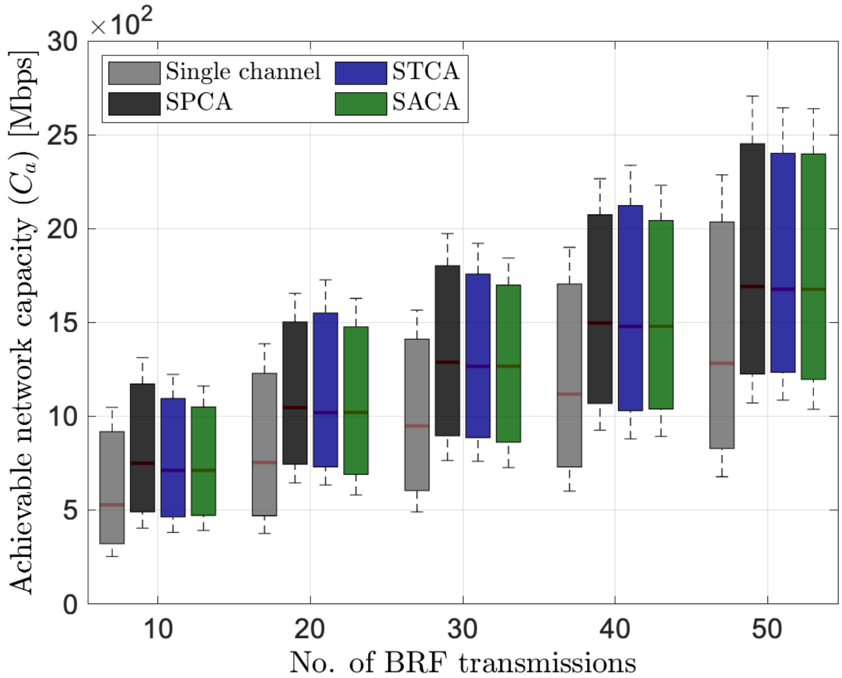

Figure 5.6: Performance analysis of fixed channel allocation schemes for FD system in achievable network capacity

Performance Analysis of Fixed Channel Allocation Schemes

Figure 5.5 and 5.6 show the performance of various fixed channel allocation schemes in the multi-channel multihop wireless network considering only FD transmission. As shown in the figures, the three channel allocation algorithms of multi-channel allocation, namely SPCA, STCA, and SACA, have advantages over the transmission single-channel transmission. Among the three different channel allocation algorithms, Figure 5.5 describes that SPCA achieves a higher network capacity than others, especially in the network with low node density. Quantitatively, if the number of BRF transmissions is 10 in the network, the network capacity increases from 712.17 Mbps to 749.08 Mbps, around 5.2%. For two sub-channels, the first sub-channel is assigned to the SR transmission and the second sub-channel is to the RD transmission of the BRF transmission in STCA. Alternating the allocation sequence of SR transmission and RD transmission in SACA. The simulation results illustrate that the STCA and SACA algorithms give almost similar interference power and achievable network capacity. In other words, assigning adjacent BRF transmissions into different sub-channels provides many advantages over STCA and SACA. This is because the effect of interference and interference distance to the desired receiving node can be shortened.

Performance Analysis of CIBA Scheme

Figure 5.7 and 5.8 compare the performance of the proposed CIBA scheme with the three fixed channel allocation schemes (SPCA, STCA, and SACA). The simulation results show that the total interference power can be suppressed by balancing the interference power using the CIBA scheme. By balancing the total interference power among the two sub-channels of a multihop wireless network, the total interference power through the network can be reduced. Table 5.2 compares CIBA and other fixed channel allocation schemes' total interference power for the network with three BRF transmissions. As shown in the table, compared to other fixed-channel allocation schemes, the CIBA can minimize the total interference power in the multi-channel and multihop wireless network. Based on the principle of minimizing interference distance difference, CIBA balances the total interference power between the sub-channel and performs the channel allocation. Therefore, compared to other fixed-channel allocations, CIBA produces less total interference power

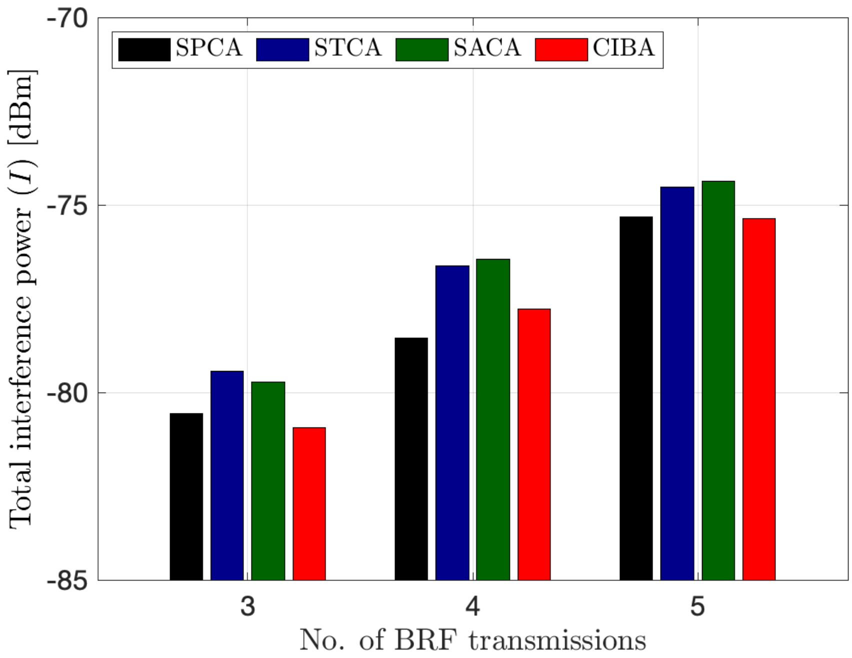

Figure 5.7: Performance comparison of multi-channel allocation schemes for FD system in total interference power

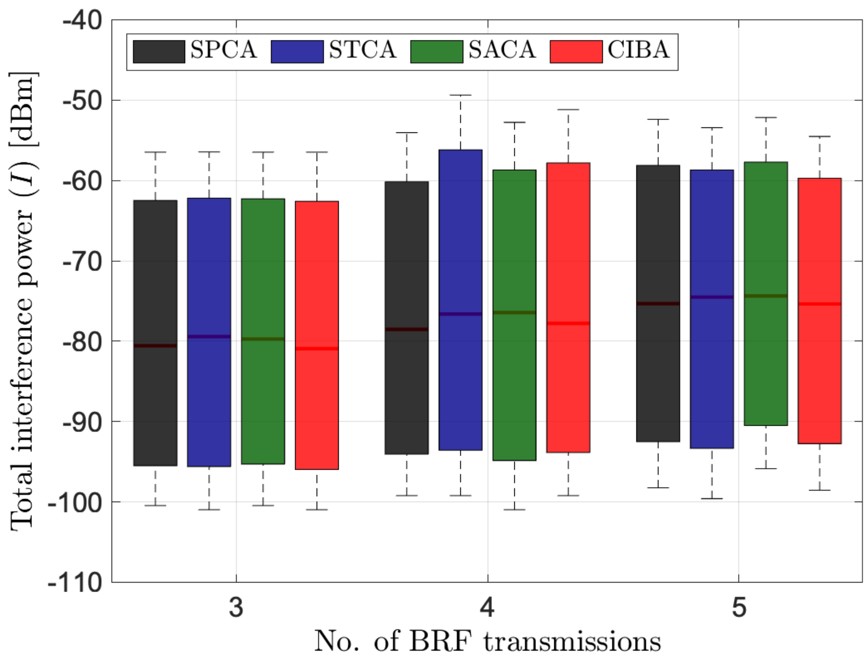

Figure 5.8: Performance analysis of multi-channel allocation schemes for FD system in total interference power

in the entire network.

Table 5.2: Performance comparison of multi-channel allocation schemes in total interference power for 15-node FD network

Algorithms	**Sub-channel 5.18 GHz**	**Sub-channel 5.32 GHz**	**Whole Network**
SPCA	-76.61	-81.21	-75.32
STCA	0.0	-74.51	-74.51
SACA	-81.0	-75.41	-74.36
CIBA	-78.56	-78.19	-75.36

Notes: All the values is in the unit of dBm.

In addition, as shown in Figure 5.9 and 5.10, CIBA gives the advantages of achievable network capacity Compared to STCA and SACA, the simulation results show that CIBA always provides a higher achievable network capacity. If the number of BRF transmissions is 3 and 5 in the network, the achievable network capacity improvement that CIBA

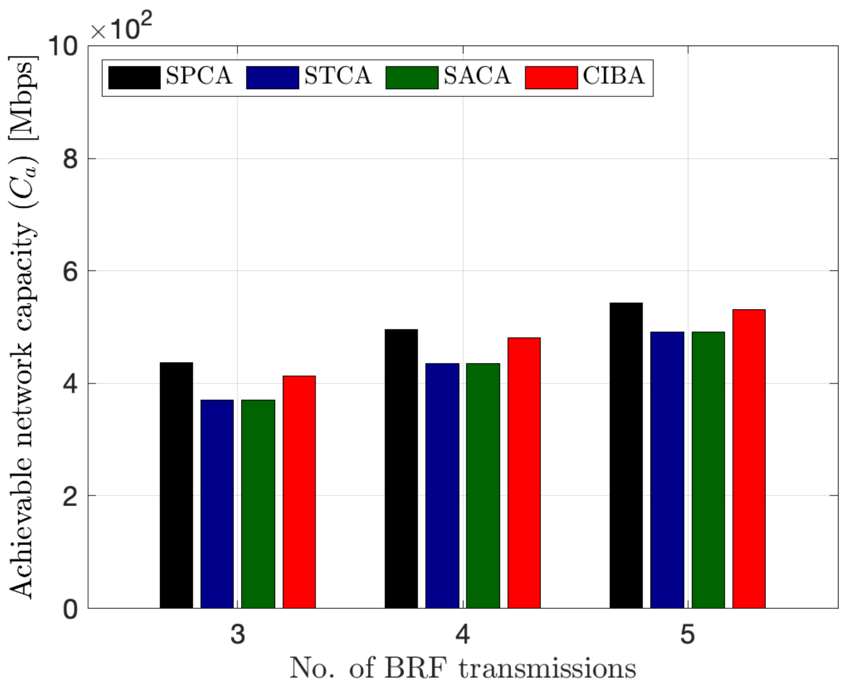

Figure 5.9: Performance comparison of multi-channel allocation schemes for FD system in achievable network capacity

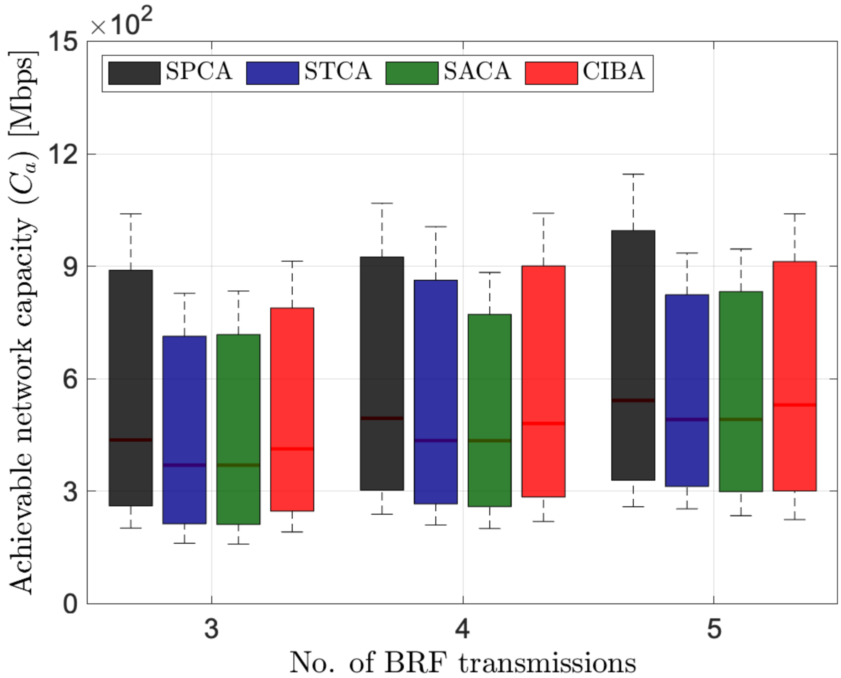

Figure 5.10: Performance analysis of multi-channel allocation schemes for FD system in achievable network capacity

can achieve is approximately 1.2% and 7.9%, respectively. However, in some network scenarios, such as network topology with five BRF transmissions, CIBA is not superior to the SPCA algorithm. This is because the CIBA allocation of the channel is primarily focused on balancing the total interference power of the two sub-channels in the network. CIBA does not consider the balance between the total interference and capacity gain of each BRF transmission. Therefore, one possible attempt to optimize CIBA performance is to balance the interference power of BRF transmissions instead of two sub-channels in the network. Although SPCA provides a higher achievable network capacity than CIBA, CIBA outperforms SPCA when considering the tradeoff between the total interference power and capacity gain per BRF transmission.

Assuming that only two sub-channels are considered as preliminary research studies for channel allocation in the multi-channel and multihop wireless network, the design of CIBA with numerical studies is only focused on in this chapter. To consider the time complexity of the channel allocation algorithms, SPCA, STCA, and SACA are linear time algorithms, while CIBA is a non-linear time algorithm. Through numerical simulations, compared to SPCA, CIBA has high time complexity and lower total interference power with moderate achievable network capacity, while SPCA has low time complexity with higher achievable network capacity and moderate total interference power. Due to the time complexity, when the number of BRF transmissions is very large, CIBA is expected to achieve higher network capacity than SPCA. In conclusion, the proposed CIBA has the advantage of achievable network capacity and total interference power as the number of BRF transmissions increases in the network.

5.6 Summary

In this chapter, the channel allocation schemes are reviewed in the single-channel and multi-channel multihop wireless. By applying the interference distance in balancing total interference power, the CIBA scheme is proposed in multi-channel multihop wireless networks. Simulation results show that multi-channel allocation schemes allow the FD systems to reduce the total interference power and increase the capacity in the network. In particular, when the number of nodes in the network is reduced, the performance of FD systems is almost double those of HD systems.

Chapter 6

Conclusion

In the future development of the 6G mobile communication system, the research attention on capacity optimization is being conducted continuously. A lot of research has been done on the FD system in the aspects of capacity optimization, interference mitigation, and so on through designing MAC protocol, resource management, i.e., TPC and user scheduling approaches, and hybrid-duplex system with and without the relaying strategy. This research focuses on the transmission capacity optimization of wireless communication in FD wireless networks. To deal with the growing interference problem in the FD systems and to ensure the optimum transmission and achievable network capacity, a coreMAC framework develops three schemes: a mixture of concurrent and sequential transmission (MCST) scheme, optimal achievable transmission capacity (OATC) scheme and channel interference balancing allocation (CIBA) scheme. Our approach is mainly on integrating concurrent transmission and sequential transmission without considering the current hardware specification.

In chapter 3, the FD-MCST protocol was proposed to support the MCST scheme for capacity optimization to address the inefficient capacity management issue in the FD wireless networks. MCST is the first cooperative transmission scheme that allows both concurrent and sequential transmissions in a single timeslot. Through numerical simulations, the proposed FD-MCST performs very satisfactorily in terms of achievable network capacity and throughput, especially when the number of basic relaying flow (BRF) transmissions increases. Quantitatively, the proposed FD-MCST increases the achievable network capacity by about 1.7 times and about two times of achievable throughput, compared to the existing FD MAC. In addition, the numerical simulation results show that MCST can be utilized in the LoRa network and can give the benefits of low latency, low energy consumption and high achievable throughput for low-power wireless systems. Therefore, the objective of capacity optimization through network capacity management is achieved.

Chapter 4 presented an OATC scheme to solve the inefficient transmission resource management. By considering the tradeoff between the interference power and capacity gain, OATC is designed with the temporal reuse mechanism via the transmission scheme and spatial reuse mechanism by the TPC technique. The simulation results show that the proposed OATC scheme performs well in interference mitigation and greatly increases the achievable network capacity and throughput regardless of the number of BRF transmissions and DATA length. Compared to RTS/FCTS and FD-MCST, the achievable throughput is improved up to 62% and 14%, respectively. In this way, OATC achieves the objective of capacity optimization and interference mitigation through the power management module.

In chapter 5, the CIBA scheme was proposed as an allocation management module to give low interference power in the FD multi-channel wireless networks. CIBA allocates adjacent transmissions to different sub-channel to reduce the interference and optimize the transmission capacity. Simulations show that the FD multi-channel transmission has better performance than the single-channel transmission in the FD wireless networks. In multi-channel transmission, the CIBA scheme has advantages over the other multi-channel allocation schemes in terms of total interference power and achievable capacity. Hence, CIBA accomplishes the objective of capacity optimization through the allocation management module.

In the coreMAC framework, the three schemes operate either individually or integrate each other according to the settings and network system requirements. For example, if the wireless nodes in the network can only support the static transmit power and static channel allocation ability, only the MCST scheme can be operated. Otherwise, the OATC scheme and CIBA scheme can be utilized for the purpose of achievable throughput optimization and interference mitigation through the TPC technique and dynamic channel allocation. In this dissertation, the principle feature of each scheme is presented and the performances are evaluated and discussed in each chapter. And, the consideration of the MCST scheme and OATC scheme with the multi-channel multihop wireless networks remains the additional research work in this dissertation.

The findings throughout this dissertation show that the proposed coreMAC framework is suitable for highly dynamic environments of future wireless networks such as vehicular communication systems such as auto-driving cars and UAV systems. Nowadays, the vehicular communication system is a trend in the new technology field, and high transmission capacity is required for cooperative communication with the surrounding vehicles dynamically according to the operating environment. With the assumed system model, simulation parameters and settings, the proposed MCST scheme benefits the low latency, which influences the throughput performance of the application. Then, the proposed OATC scheme maximizes the achievable throughput by controlling the transmit power and benefits for low-power wireless systems like drone communication systems. Besides, the CIBA scheme can give the benefit of interference mitigation that could aid the latency reduction through the multi-channel multihop wireless networks. Therefore, the FD-MCST, the OATC scheme, and the CIBA scheme can be applied to optimize the performance of the FD-enabled vehicular communication system in future wireless networks through cooperative communication strategies.

6.1 Contributions

This research work contributes to wireless communication by integrating communication strategies of transmission strategy, relaying strategy, and allocation strategy, and utilizing the benefits of the FD system as the coreMAC framework. As the research impact, the proposed coreMAC framework poses breakthroughs with the transmission scheme, power management scheme, and resource management scheme via the design of the FD MAC protocol and algorithms, which benefits the spectral efficiency of the transmission.

The main contributions of this dissertation are as the followings.

- The BRF transmission is designed by considering the relaying strategy in the FD system and enabling the concurrent and sequential transmissions in a single timeslot.

- It is necessary to consider the sequential transmission even in the FD system due to interference, especially in a dense network environment. Therefore, by integrating the advantages of concurrent and sequential transmissions, the FD-MCST protocol that utilizes an MCST scheme is designed and proposed to optimize the transmission capacity in FD wireless networks.

- It has been found that using CT and MCST schemes alone does not always provide the highest achievable network capacity, even using the TPC technique in the FD wireless networks. Therefore, the OATC scheme combines these two schemes to achieve optimum transmission capacity by using the tradeoff threshold that considers both interference power and received power of the transmission. From the simulation results, the OATC scheme uses a high ratio of CT scheme to achieve optimal achievable network capacity when the network is not dense and uses a small ratio of CT scheme to reduce total interference power when the network is dense.

- The quantitative analysis of HD and FD systems is performed using a multi-channel allocation scheme in the multihop wireless network environment in addition to the single-channel wireless networks. The discussion of the different channel allocation schemes shows the different performances over the existing multihop wireless networks. The proposed CIBA scheme shows the possible way to mitigate the interference by sharing information on the overall interference power balance of the entire network between the nodes.

The framework was proposed in the host-to-network layer in the TCP/IP model and the resulting lower transmission latency and higher achievable throughput affect the transport layer protocol performance that will benefit the quality of service for the specified applications such as the auto-driving cars and UAVs. The contributions of this research can provide only a small portion compared to the demands of the future wireless network, especially to the extremely massive-scale communication system like 6G. However, among the several potential technologies, this research work can be classified into efficient and effective communication through the FD system, D2D communications, and cooperative transmission approaches.

6.2 Concluding Remarks

The wireless network plays a key role in today's communication system, and new forms of it will become central to emerging technologies, including robots, drones, self-driving vehicles, and IoT devices. Based on the current situation and prospects of future wireless communication, this research combines cooperative communication strategies, i.e., transmission strategy, relaying strategy and allocation strategy, and FD system that has a high potential for the next-generation mobile communication system. The knowledge gained from this research is intended to be useful in developing the new Super-smart Society 5.0 and the metaverse applications with high capacity demands.

However, to realize this research and utilize the proposed framework, it is required to realize the FD system and the hardware in the network should be able to provide the FD capability. It means that the world would require changing the communication system from a conventional HD system to an FD system, which is a big challenge for the whole wireless community.

6.3 Future Research Works

Some future extensions of this research work could be categorized into three groups:

- As one of the research works in the FD system era, this research lacks consideration of the influence of self-interference and the influence of time synchronization issues on simultaneous transmission. The research can be easily extended by considering the main issues of SI and time synchronization in the FD system.

- The current work is only based on the single relaying transmission flow with a relay node. Another interesting research extension is considering multiple relay nodes and the relay node selection for capacity optimization. Besides, future work should investigate the performance of the proposed framework with both bidirectional FD transmission and unidirectional FD transmission in the network.

- Regarding channel allocation management, future work will investigate the performance of the CIBA scheme with an increased number of sub-channels and extend the study of throughput analysis to design the MAC protocol using the Markov

Chain approach in the presence of the hidden terminal problem. Besides, the allocation for the CIBA scheme should also consider both minimizing interference and increasing capacity gain. Additionally, the dynamic channel allocation should be further considered when the nodes move around in the network.

Bibliography

[1] Cisco. Cisco annual internet report (2018-2023) white paper. `https://www.cisco.com/c/en/us/solutions/collateral/executive-perspectives/annual-internet-report/white-paper-c11-741490.pdf`, 2020. (Last accessed: 23 January 2023).

[2] M. Z. Chowdhury, M. Shahjalal, S. Ahmed, and Y. M. Jang. 6G wireless communication systems: Applications, requirements, technologies, challenges, and research directions. *IEEE Open Journal of the Communications Society*, 1:957–975, 2020.

[3] Y. Shiroishi, K. Uchiyama, and N. Suzuki. Society 5.0: For human security and well-being. *Computer*, 51(7):91–95, 2018.

[4] Y. Nagasato, T. Yoshimura, and R. Shinozaki. Realizing society 5.0 expectations from Japanese business. *Journal of Information and Management*, 38(1):3–8, 2018.

[5] S. Henry, A. Alsohaily, and E. S. Sousa. 5G is real: Evaluating the compliance of the 3GPP 5G new radio system with the ITU IMT-2020 requirements. *IEEE Access*, 8:42828–42840, 2020.

[6] M. Maier. 6G as if people mattered: From Industry 4.0 toward Society 5.0. In *International Conference on Computer Communications and Networks (ICCCN)*, pages 1–10. IEEE, 2021.

[7] P. Yang, Y. Xiao, M. Xiao, and S. Li. 6G wireless communications: Vision and potential techniques. *IEEE Network*, 33(4):70–75, 2019.

[8] Y. Zhao, W. Zhai, J. Zhao, T. Zhang, S. Sun, D. Niyato, and K. Y. Lam. A comprehensive survey of 6G wireless communications. *arXiv preprint arXiv:2101.03889*, pages 1–34, 2020.

[9] H. Peng, P. C. Chen, P. H. Chen, Y. S. Yang, C. C. Hsia, and L. C. Wang. 6G toward metaverse: Technologies, applications, and challenges. In *VTS Asia Pacific Wireless Communications Symposium (APWCS)*, pages 6–10. IEEE, 2022.

[10] N. Kato, B. Mao, F. Tang, Y. Kawamoto, and J. Liu. Ten challenges in advancing machine learning technologies toward 6G. *IEEE Wireless Communications*, 27(3):96–103, 2020.

[11] Y. Zhao, J. Zhao, W. Zhai, S. Sun, D. Niyato, and K. Lam. A survey of 6G wireless communications: Emerging technologies. In *Future of Information and Communication Conference*, pages 150–170, 2021.

[12] H. Tataria, M. Shafi, M. Dohler, and S. Sun. Six critical challenges for 6G wireless systems: A summary and some solutions. *IEEE Vehicular Technology Magazine*, 17(1):16–26, 2022.

[13] T. Nakamura. 5G evolution and 6G. In *Symposium on VLSI Technology*, pages 1–5. IEEE, 2020.

[14] M. Alsabah, M. A. Naser, B. M. Mahmmod, S. H. Abdulhussain, M. R. Eissa, A. Al-Baidhani, N. K. Noordin, S. M. Sait, K. A. Al-Utaibi, and F. Hashim. 6G wireless communications networks: A comprehensive survey. *IEEE Access*, 9:148191–148243, 2021.

[15] T. Fujii and K. Umebayashi. Smart spectrum for future wireless world. *IEICE Transactions on Communications*, 100(9):1661–1673, 2017.

[16] X. Lin. An overview of 5G advanced evolution in 3GPP release 18. *IEEE Communications Standards Magazine*, 6(3):77–83, 2022.

[17] M. Sue. Why full duplex technology is suddenly hot in 5G. `https://www.lightreading.com/opticalip/why-full-duplex-technology-is-suddenly-hot-in-5g/d/d-id/765522`, 2020. (Last accessed: 01 June 2023).

[18] D. Shumeye Lakew, U. Sa'ad, N. N. Dao, W. Na, and S. Cho. Routing in flying Ad Hoc networks: A comprehensive survey. *IEEE Communications Surveys & Tutorials*, 22(2):1071–1120, 2020.

[19] W. Gao, B. Lin, and G. Chuai. Service-and interference-aware dynamic TDD design in 5G ultra-dense network scenario. *EURASIP Journal on Wireless Communications and Networking*, 2017(1):1–10, 2017.

[20] V. Singh, A. Gadre, and S. Kumar. Full duplex radios: Are we there yet? In *19th ACM Workshop on Hot Topics in Networks*, pages 117–124, 2020.

[21] A. Sabharwal, P. Schniter, D. Guo, D. W. Bliss, S. Rangarajan, and R. Wichman. In-band full-duplex wireless: Challenges and opportunities. *IEEE Journal on Selected Areas in Communications*, 32(9):1637–1652, 2014.

[22] K. E. Kolodziej, B. T. Perry, and J. S. Herd. In-band full-duplex technology: Techniques and systems survey. *IEEE Transactions on Microwave Theory and Techniques*, 67(7):3025–3041, 2019.

[23] M. R. Amin, M. S. Hossain, and M. Atiquzzaman. In-band full duplex wireless LANs: Medium access control protocols, design issues and their challenges. *Information*, 11(4):216–242, 2020.

[24] X. Zhang, W. Cheng, and H. Zhang. Full-duplex transmission in PHY and MAC layers for 5G mobile wireless networks. *IEEE Wireless Communications*, 22(5):112–121, 2015.

[25] C. Chen, S. Hou, and S. Wu. Saturation throughput analysis of an asymmetric full-duplex MAC protocol in WLANs with hidden terminals. *IEEE Access*, 6:69948–69960, 2018.

[26] L. Shi, Z. Li, X. Bi, L. Liao, and J. Xu. Full-duplex multi-hop wireless networks optimization with successive interference cancellation. *Sensors*, 18(12):4301–4315, 2018.

[27] E. Everett, A. Sahai, and A. Sabharwal. Passive self-interference suppression for full-duplex infrastructure nodes. *IEEE Transactions on Wireless Communications*, 13(2):680–694, 2014.

[28] L. Laughlin, C. Zhang, M. A. Beach, K. A. Morris, and J. Haine. A widely tunable full duplex transceiver combining electrical balance isolation and active analog cancellation. In *81st Vehicular Technology Conference (VTC Spring)*, pages 1–5. IEEE, 2015.

[29] K. E. Kolodziej, J. G. McMichael, and B. T. Perry. Multitap RF canceller for in-band full-duplex wireless communications. *IEEE Transactions on Wireless Communications*, 15(6):4321–4334, 2016.

[30] C. D. Nwankwo, L. Zhang, A. Quddus, M. A. Imran, and R. Tafazolli. A survey of self-interference management techniques for single frequency full duplex systems. *IEEE Access*, 6:30242–30268, 2017.

[31] D. Korpi, M. Heino, C. Icheln, K. Haneda, and M. Valkama. Compact in-band full-duplex relays with beyond 100 dB self-interference suppression: Enabling techniques and field measurements. *IEEE Transactions on Antennas and Propagation*, 65(2):960–965, 2017.

[32] S. Wu, H. Guo, J. Xu, S. Zhu, and H. Wang. In-band full duplex wireless communications and networking for IoT devices: Progress, challenges and opportunities. *Future Generation Computer Systems*, 92:705–714, 2019.

[33] A. Masmoudi and T. Le-Ngoc. Channel estimation and self-interference cancellation in full-duplex communication systems. *IEEE Transactions on Vehicular Technology*, 66(1):321–334, 2016.

[34] N. Panwar, S. Sharma, and A. K. Singh. A survey on 5G: The next generation of mobile communication. *Physical Communication*, 18:64–84, 2016.

[35] Y. A. Adediran, H. Lasisi, and O. B. Okedere. Interference management techniques in cellular networks: A review. *Cogent Engineering*, 4(1):1–10, 2017.

[36] X. Wang, H. Huang, and T. Hwang. On the capacity gain from full duplex communications in a large scale wireless network. *IEEE Transactions on Mobile Computing*, 15(9):2290–2303, 2016.

[37] Z. Zhang, K. Long, A. V. Vasilakos, and L. Hanzo. Full-duplex wireless communications: Challenges, solutions, and future research directions. *Proceedings of the IEEE*, 104(7):1369–1409, 2016.

[38] Y. Yao, B. Li, C. Li, C. Yang, and B. Xia. Downlink performance analysis of the full-duplex networks with interference cancellation. *IEEE Transactions on Communications*, 68(4):2324–2338, 2020.

[39] S. Goyal, P. Liu, and S. S. Panwar. User selection and power allocation in full-duplex multicell networks. *IEEE Transactions on Vehicular Technology*, 66(3):2408–2422, 2016.

[40] F. Wu, X. Pu, M. Zhang, S. Li, and W. Ma. An interuser interference suppression approach in full-duplex wireless communications. *Transactions on Emerging Telecommunications Technologies*, 29(3):1–17, 2018.

[41] A. H. Gazestani, S. A. Ghorashi, B. Mousavinasab, and M. Shikh-Bahaei. A survey on implementation and applications of full duplex wireless communications. *Physical Communication*, 34:121–134, 2019.

[42] J. Y. Kim, O. Mashayekhi, H. Qu, M. Kazandjieva, and P. Levis. Janus: A novel MAC protocol for full duplex radio. *CSTR*, 2(7):1–12, 2013.

[43] S. Goyal, P. Liu, O. Gurbuz, E. Erkip, and S. Panwar. A distributed MAC protocol for full duplex radio. In *Asilomar Conference on Signals, Systems and Computers*, pages 788–792, 2013.

[44] T. Febrianto, J. Hou, and M. Shikh-Bahaei. Cooperative full-duplex physical and MAC layer design in asynchronous cognitive networks. *Wireless Communications and Mobile Computing*, pages 1–14, 2017.

[45] K. Tamaki, Y. Sugiyama, M. Bandai, S. Saruwatari, T. Watanabe, et al. Full duplex media access control for wireless multi-hop networks. In *77th Vehicular Technology Conference (VTC Spring)*, pages 1–5. IEEE, 2013.

[46] A. Maloo and P. K. Sharma. Full duplex wireless communication with dynamic buffer aided MAC protocol. *AEU-International Journal of Electronics and Communications*, 128:153488–153494, 2021.

[47] D. Nguyen, L. N. Tran, P. Pirinen, and M. Latva-aho. On the spectral efficiency of full-duplex small cell wireless systems. *IEEE Transactions on wireless communications*, 13(9):4896–4910, 2014.

[48] A. Marczak. Overview of cooperative communication methods. *Maritime Technical Journal*, 210(3):77–86, 2017.

[49] J. Sykora, V. Bota, Y. Zhang, and S. Ruiz. *Cooperative Radio Communications for Green Smart Environments*, chapter Cooperative Strategies and Networks, pages 271–304. River Publishers, 2016.

[50] H. Adam, W. Elmenreich, C. Bettstetter, and S. M. Senouci. CoRe-MAC: A MAC-protocol for cooperative relaying in wireless networks. In *Global Communications Conference (GLOBECOM)*, pages 1–6. IEEE, 2009.

[51] M. F. Kader, S. Y. Shin, and V. C. Leung. Full-duplex non-orthogonal multiple access in cooperative relay sharing for 5G systems. *IEEE Transactions on Vehicular Technology*, 67(7):5831–5840, 2018.

[52] B. Yu, L. Yang, X. Cheng, and R. Cao. Power and location optimization for full-duplex decode-and-forward relaying. *IEEE Transactions on Communications*, 63(12):4743–4753, 2015.

[53] Y. Li, N. Li, M. Peng, and W. Wang. Relay power control for two-way full-duplex amplify-and-forward relay networks. *IEEE Signal Processing Letters*, 23(2):292–296, 2016.

[54] L. Weizheng and T. Xiumei. Throughput analysis of full-duplex network coding in two-way relay channel. In *17th International Conference on Communication Technology (ICCT)*, pages 85–90. IEEE, 2017.

[55] E. E. B. Olivo, D. P. M. Osorio, H. Alves, J. C. S. Santos Filho, and M. Latva-Aho. Cognitive full-duplex decode-and-forward relaying networks with usable direct link and transmit-power constraints. *IEEE Access*, 6:24983–24995, 2018.

[56] J. Yu and W. C. Wong. A network resource management framework for wireless mesh networks. *Wireless Personal Communications*, 95(3):3433–3457, 2017.

[57] E. Moridi, M. Haghparast, M. Hosseinzadeh, and S. Jafarali Jassbi. Novel fault management framework using markov chain in wireless sensor networks: FMMC. *Wireless Personal Communications*, 114:583–608, 2020.

[58] S. K. M. Ataelmanan and M. A. H. Ali. Developing a framework for data communication in a wireless network using machine learning technique. *International Journal of Advanced Computer Science and Applications*, 12(3), 2021.

[59] I. F. Akyildiz, W. Y. Lee, and K. R. Chowdhury. CRAHNs: Cognitive radio ad hoc networks. *Ad Hoc Networks*, 7(5):810–836, 2009.

[60] P. Gupta and P.R. Kumar. The capacity of wireless networks. *IEEE Transactions on Information Theory*, 46(2):388–404, 2000.

[61] S. Toumpis and A.J. Goldsmith. Capacity regions for wireless ad hoc networks. *IEEE Transactions on Wireless Communications*, 2(4):736–748, 2003.

[62] Y. Yu, S. Shah, Y. Tan, and Y. Lim. End-to-end throughput evaluation of consensus TPC algorithm in multihop wireless networks. In *International Wireless Communications and Mobile Computing Conference (IWCMC)*, pages 941–946. IEEE, 2015.

[63] P. Li. Capacity of wireless ad hoc networks. *Encyclopedia of Wireless Networks*, pages 160–164, 2020.

[64] W. Cheng, X. Zhang, and H. Zhang. RTS/FCTS mechanism based full-duplex MAC protocol for wireless networks. In *Global Communications Conference (GLOBECOM)*, pages 5017–5022. IEEE, 2013.

[65] Y. Liao, K. Bian, L. Song, and Z Han. Full-duplex MAC protocol design and analysis. *IEEE Communications Letters*, 19(7):1185–1188, 2015.

[66] R. Doost-Mohammady, M. Y. Naderi, and K. R. Chowdhury. Performance analysis of CSMA/CA based medium access in full duplex wireless communications. *IEEE Transactions on Mobile Computing*, 15(6):1457–1470, 2016.

[67] Y. Song, W. Qi, W. Zhao, and W. Cheng. Full-duplex MAC protocol for CSMA/CA-based single-hop wireless networks. *Sensors*, 19(10):2413–2427, 2019.

[68] H. Zuo, Y. Sun, S. Li, Q. Ni, X. Wang, and X. Zhang. A medium access control mechanism for distributed in-band full-duplex wireless networks. *KSII Transactions on Internet and Information Systems (TIIS)*, 11(11):5338–5359, 2017.

[69] J. K. Kim, W. J. Lee, C. B. Chae, and J. H. Kim. Performance analysis of fair medium access control protocol for asymmetric full duplex in WLAN. *IEEE Access*, 8:140546–140557, 2020.

[70] W. Choi, I. S. Jang, and T. Kim. Antenna allocation scheme for full-duplex communication in IEEE 802.11ac WLAN. In *International Conference on Consumer Electronics (ICCE)*, pages 120–121. IEEE, 2017.

[71] W. K. Kim, J. K. Kim, and J. H. Kim. Centralized MAC protocol for wireless full duplex networks considering D2D communications. In *International Conference on Information and Communication Technology Convergence (ICTC)*, pages 730–732. IEEE, 2016.

[72] A. Khokar, R. Bajpai, and N. Gupta. Best user selection for NOMA-aided full-duplex cooperative D2D communication system. In *27th International Conference on Telecommunications (ICT)*, pages 1–5. IEEE, 2020.

[73] A. Yadav, G. I. Tsiropoulos, and O. A. Dobre. Full-duplex communications: Performance in ultra-dense small-cell wireless networks. *arXiv preprint arXiv:1803.00473*, pages 1–7, 2018.

[74] L. Anttila, V. Lampu, S. A. Hassani, P. P. Campo, D. Korpi, M. Turunen, S. Pollin, and M. Valkama. Full-duplexing with SDR devices: Algorithms, FPGA imple-

mentation, and real-time results. *IEEE Transactions on Wireless Communications*, 20(4):2205–2220, 2020.

[75] H. Ji, Y. Kim, T. Kim, K. Muhammad, C. Tarver, M. Tonnemacher, J. Oh, B. Yu, and G. Xu. Enabling advanced duplex in 6G. In *International Conference on Communications Workshops (ICC Workshops)*, pages 1–6. IEEE, 2021.

[76] H. Na and C. Lee. An inter user interference cancellation scheme for two users in full-duplex MIMO system. *EURASIP Journal on Wireless Communications and Networking*, 2018(1):1–9, 2018.

[77] L. Han, J. Mu, Y. Wang, and J. Gao. Performance analysis of multi-hop full-duplex decode-and-forward relaying. *Ad Hoc Networks*, 58:247–254, 2017.

[78] X. Yang, Y. Mao, Y. Gong, and T. Zhang. Uplink/downlink initiated based MAC protocol for asymmetric full duplex radio to improve throughput. In *International Wireless Communications and Mobile Computing (IWCMC)*, pages 1075–1078. IEEE, 2021.

[79] B. C. Nguyen and X. N. Tran. Performance analysis of full-duplex amplify-and-forward relay system with hardware impairments and imperfect self-interference cancellation. *Wireless Communications and Mobile Computing*, pages 1–10, 2019.

[80] Y. Song, W. Qi, and W. Cheng. Energy efficient MAC protocol for wireless full-duplex networks. *China Communications*, 15(1):35–44, 2018.

[81] Y. Liu, Y. Shen, D. Guo, and M. Z. Win. Network localization and synchronization using full-duplex radios. *IEEE Transactions on Signal Processing*, 66(3):714–728, 2017.

[82] C. Yao, L. Song, and Y. Li. X-Duplex radios: Flexible switching between full-duplex and half-duplex. *IEEE Wireless Communications Letters*, 7(1):94–97, 2017.

[83] W. Tang, S. Feng, Y. Liu, and Y. Ding. Hybrid duplex switching in heterogeneous networks. *IEEE Transactions on Wireless Communications*, 15(11):7419–7431, 2016.

[84] G. Liu, X. Chen, Z. Ding, Z. Ma, and F.R. Yu. Hybrid half-duplex/full-duplex cooperative non-orthogonal multiple access with transmit power adaptation. *IEEE Transactions on Wireless Communications*, 17(1):506–519, 2017.

[85] J. Huang, K. Qi, Z. Xu, and C. Yang. Hybrid full and half duplex networking. In *International Conference on Communications in China (ICCC)*, pages 1–6. IEEE, 2016.

[86] L. Han and J. Mu. Hybrid half-duplex/full-duplex multi-hop relaying schemes: outage performance and power optimization. *Ad Hoc Networks*, 58:54–61, 2017.

[87] H. Chen and F. Zhao. A hybrid half-duplex/full-duplex transmission scheme in relay-aided cellular networks. *EURASIP Journal on Wireless Communications and Networking*, 2017(1):1–10, 2017.

[88] Z. Cheng, H. Chen, and F. Zhao. Opportunistic half-duplex/full-duplex relaying mode selection criterion in cognitive relay networks. *EURASIP Journal on Wireless Communications and Networking*, 2018(1):1–14, 2018.

[89] C. Li, B. Xia, and Z. Chen. A new hybrid half-duplex/full-duplex relaying system with antenna diversity. In *85th Vehicular Technology Conference (VTC Spring)*, pages 1–5. IEEE, 2017.

[90] M. G. Khafagy, A. El Shafie, A. Sultan, and M. S. Alouini. Throughput maximization for buffer-aided hybrid half-/full-duplex relaying with self-interference. In *International Conference on Communications (ICC)*, pages 1926–1931. IEEE, 2015.

[91] K. Hocni and M. Yazid. Full duplex radio communications in high efficiency WLANs: Study and comparison of the main MAC protocols. *International Journal of Informatics and Applied Mathematics*, 3(1):1–21, 2020.

[92] K. Lee. ADAS: Adaptive switching between full-duplex and MU-MIMO for Wi-Fi networks. *Wireless Communications and Mobile Computing*, pages 1–10, 2019.

[93] J. K. Kim, W. J. Lee, and J. H. Kim. Full-duplex MAC protocol based on CSMA/CA for switching transmission mode. *Electronics*, 10(5):587–601, 2021.

[94] A. K. Gupta and T. G. Venkatesh. Design and analysis of IEEE 802.11 based full duplex WLAN MAC protocol. *Computer Networks*, 210, 2022.

[95] S. A. Hassani, L. Barend v., A. Bourdoux, F. Horlin, and S. Pollin. Adaptive filter design for simultaneous in-band full-duplex communication and radar. In *17th European Radar Conference (EuRAD)*, pages 5–8. IEEE, 2021.

[96] A. Bazzi, C. Campolo, B. M. Masini, A. Molinaro, A. Zanella, and A. O. Berthet. Enhancing cooperative driving in IEEE 802.11 vehicular networks through full-duplex radios. *IEEE Transactions on Wireless Communications*, 17(4):2402–2416, 2018.

[97] S. Biswas, A. Bishnu, F. A. Khan, and T. Ratnarajah. In-band full-duplex dynamic spectrum sharing in beyond 5G networks. *IEEE Communications Magazine*, 59(7):54–60, 2021.

[98] J. Lee and T. Q. S. Quek. Hybrid full-/half-duplex system analysis in heterogeneous wireless networks. *IEEE Transactions on Wireless Communications*, 14(5):2883–2895, 2015.

[99] D. Korpi, T. Riihonen, K. Haneda, K. Yamamoto, and M. Valkama. Achievable transmission rates and self-interference channel estimation in hybrid full-duplex/half-duplex MIMO relaying. In *82nd Vehicular Technology Conference (VTC2015-Fall)*, pages 1–5. IEEE, 2015.

[100] S. Goyal, P. Liu, S. Panwar, R. Yang, R. A. DiFazio, and E. Bala. Full duplex operation for small cells. *arXiv preprint arXiv:1412.8708*, pages 1–34, 2014.

[101] P. Cardieri. Modeling interference in wireless ad hoc networks. *IEEE Communications Surveys & Tutorials*, 12(4):551–572, 2010.

[102] A. Tsertou and D. I. Laurenson. Revisiting the hidden terminal problem in a CSMA/CA wireless network. *IEEE Transactions on Mobile Computing*, 7(7):817–831, 2008.

[103] M. D. Nguyen, Y. Lim, and Y. Tan. Performance analysis of mixture of half-duplex and full-duplex wireless networks using network coding. *IEICE Technical Committee on Ambient intelligence and Sensor Networks (ASN)*, 117(426):115–120, 2018.

[104] M. Murad and A. M. Eltawil. Performance analysis and enhancements for in-band full-duplex wireless local area networks. *IEEE Access*, 8:111636–111652, 2020.

[105] A. Augustin, J. Yi, T. Clausen, and W. M. Townsley. A study of LoRa: Long range & low power networks for the internet of things. *Sensors*, 16(9):1466–1484, 2016.

[106] L. Shan, T. Kagawa, R. Miura, F. Ono, H. B. Li, and F. Kojima. Demonstration experiment of inter-aircraft communication for location sharing of drone and helicopter. *IEICE Technical Report*, 118(344):211–216, 2018.

[107] M. Okennedy, T. Niesler, R. Wolhuter, and N. Mitton. Practical evaluation of carrier sensing for a LoRa wildlife monitoring network. In *IFIP Networking Conference (Networking)*, pages 614–618. IEEE, 2020.

[108] T. Polonelli, D. Brunelli, A. Marzocchi, and L. Benini. Slotted ALOHA on LoRaWAN-design, analysis, and deployment. *Sensors*, 19(4):838–857, 2019.

[109] S. Ahsan, S. A. Hassan, A. Adeel, and H. K. Qureshi. Improving channel utilization of LoRaWAN by using novel channel access mechanism. In *15th International Wireless Communications & Mobile Computing Conference (IWCMC)*, pages 1656–1661. IEEE, 2019.

[110] A. Gamage, J. C. Liando, C. Gu, R. Tan, and M. Li. LMAC: Efficient carrier-sense multiple access for LoRa. In *26th Annual International Conference on Mobile Computing and Networking*, pages 1–13, 2020.

[111] International Telecommunications Union. Propagation data and prediction methods for the planning of short-range outdoor radiocommunication systems and radio local area networks in the frequency range 300 MHz to 100 GHz. *Recommendation ITU-R P.1411-11*, pages 1–56, 2021. Last accessed: 13 February 2023.

[112] T. Bouguera, J. F. Diouris, J. J. Chaillout, R. Jaouadi, and G. Andrieux. Energy consumption model for sensor nodes based on LoRa and LoRaWAN. *Sensors*, 18(7):2104–2127, 2018.

[113] LoRa Alliance Technical Committee. LoRaWAN 1.1 specification. *LoRa Alliance*, pages 1–101, 2017.

[114] J. Padhye, V. Firoiu, D. Towsley, and J. Kurose. Modeling TCP throughput: A simple model and its empirical validation. In *ACM SIGCOMM Conference on Applications, Technologies, Architectures, and Protocols for Computer Communication*, pages 303–314, 1998.

[115] M. Dibaei and A. Ghaffari. Full-duplex medium access control protocols in wireless networks: A survey. *Wireless Networks*, 26(4):2825–2843, 2020.

[116] Y. Chen, Y. Sun, H. Zuo, S. Li, N. Lu, and Y. Wang. Rate selection based medium access control for full-duplex asymmetric transmission. *Wireless Networks*, 25(8):4873–4885, 2019.

[117] A. Tang, H. Huang, and X. Wang. Full duplex communications for next generation cellular networks: The capacity gain. *Journal of Shanghai Jiaotong University (Science)*, 23(1):11–19, 2018.

[118] Q. Qu, B. Li, M. Yang, and Z. Yan. Power control based multiuser full-duplex MAC protocol for the next generation wireless networks. *Mobile Networks and Applications*, 23(4):1008–1019, 2018.

[119] F. Liu, X. Hou, and Y. Liu. Capacity improvement for full duplex device-to-device communications underlaying cellular networks. *IEEE Access*, 6:68373–68383, 2018.

[120] C. Feng, Y. Zhong, T. Q. Quek, and G. Wu. Power control in full duplex networks: Area spectrum efficiency and energy efficiency. In *International Conference on Communications (ICC)*, pages 1–6. IEEE, 2017.

[121] H. H. Choi and J. R. Lee. Distributed transmit power control for maximizing end-to-end throughput in wireless multi-hop networks. *Wireless Personal Communications*, 74(3):1033–1044, 2014.

[122] R. Aslani and M. Rasti. Distributed power control schemes for in-band full-duplex energy harvesting wireless networks. *IEEE Transactions on Wireless Communications*, 16(8):5233–5243, 2017.

[123] L. Han, Y. Zhang, X. Zhang, and J. Mu. Power control for full-duplex D2D communications underlaying cellular networks. *IEEE Access*, 7:111858–111865, 2019.

[124] S. H. A. Samy, E. A. Maher, and A. El-Mahdy. Full-duplex decode and forward relay-aided device-to-device communication. In *Signal Processing: Algorithms, Architectures, Arrangements, and Applications (SPA)*, pages 131–136. IEEE, 2019.

[125] C. Kai, X. Zhang, X. Hu, and W. Huang. Optimal scheduling and power control for in-band full-duplex communication in WLANs. In *Global Communications Conference (GLOBECOM)*, pages 1–6. IEEE, 2020.

[126] M. R. Amin and M. S. Hossain. An RTS–CTS based medium access control protocol for full-duplex wireless local area networks. *Ad Hoc Networks*, 132:1–21, 2022.

[127] G. Liu, W. Feng, Z. Han, and W. Jiang. Performance analysis and optimization of cooperative full-duplex D2D communication underlaying cellular networks. *IEEE Transactions on Wireless Communications*, 18(11):5113–5127, 2019.

[128] G.C. Alexandropoulos, M. Kountouris, and I. Atzeni. User scheduling and optimal power allocation for full-duplex cellular networks. In *17th International Workshop on Signal Processing Advances in Wireless Communications (SPAWC)*, pages 1–6. IEEE, 2016.

[129] P. Tehrani, F. Lahouti, and M. Zorzi. Resource allocation in heterogenous full-duplex ofdma networks: Design and analysis. *arXiv preprint arXiv:1802.03012*, pages 1–30, 2018.

[130] T.J.M. Coenen, M. de Graaf, and R.J. Boucherie. An upper bound on multi-hop multi-channel wireless network performance. In *Proceedings of the International Conference on Mobile Technology, Applications, and Systems*, pages 1–6, 2008.

[131] T. Riihonen, S. Werner, and R. Wichman. Comparison of full-duplex and half-duplex modes with a fixed amplify-and-forward relay. In *Wireless Communications and Networking Conference (WCNC)*, pages 1–5. IEEE, 2009.

[132] W. Cheng, X. Zhang, and H. Zhang. Full/half duplex based resource allocations for statistical quality of service provisioning in wireless relay networks. In *Conference on Computer Communications (INFOCOM)*, pages 864–872. IEEE, 2012.

[133] E. Park, J. Bae, H. Ju, and Y. Han. Resource allocation for full-duplex systems with imperfect co-channel interference estimation. *IEEE Transactions on Wireless Communications*, 18(4):2388–2400, 2019.

[134] B. Li, C. Li, C. Yang, and B. Xia. User scheduling for full-duplex cellular networks. In *International Conference on Communications Workshops (ICC Workshops)*, pages 1–6. IEEE, 2019.

[135] K. Akçapınar, Ö. Gürbüz, and T. Ünlüyurt. Power allocation and routing for full-duplex multihop wireless networks under full interference. *Ad Hoc Networks*, 82:91–99, 2019.

[136] S. Merlin, N. Vaidya, and M. Zorzi. Resource allocation in multi-radio multi-channel multi-hop wireless networks. In *Conference on Computer Communications (INFOCOM)*, pages 610–618. IEEE, 2008.

[137] J. Diakonikolas and G. Zussman. On the rate regions of single-channel and multi-channel full-duplex links. *IEEE/ACM Transactions on Networking*, 26(1):47–60, 2018.

[138] International Telecommunications Union. Propagation data and prediction models for the planning of indoor radio communication systems and radio local area networks in the frequency range 900 MHz to 100 GHz. *Recommendation ITU-R P.1238-11*, 2021. Last accessed: 23 January 2023.

[139] M. Hui, H.M.K. Alazemi, and S. Roy. A stochastic model for optimizing physical carrier sensing and spatial reuse in wireless ad hoc networks. In *International Conference on Mobile Adhoc and Sensor Systems Conference*, pages 1–8. IEEE, 2005.

List of Publications

Journals

[1] **Aung Thura Phyo Khun**, Lin Shan, Yuto Lim, and Yasuo Tan, "MCST Scheme for UAV Systems over LoRa Networks," *Drones*, vol. 7, no. 6, pp. 371–387, 2023, DOI: 10.3390/drones7060371.

[2] **Aung Thura Phyo Khun**, Yuto Lim, and Yasuo Tan, "Optimal Achievable Transmission Capacity Scheme for Full-duplex Multihop Wireless Networks," *Sensors*, vol. 22, no. 20, pp. 7849–7868, 2022, DOI: 10.3390/s22207849.

[3] **Aung Thura Phyo Khun**, Yuto Lim, and Yasuo Tan, "FD-MCST Design and Analysis for Multihop Wireless Networks," *Ad Hoc Networks*, vol. 136, pp. 102977–102991, 2022, DOI: 10.1016/j.adhoc.2022.102977.

[4] **Aung Thura Phyo Khun**, Yuto Lim, and Stepan Kucera, "Capacity Performance for Full-duplex Multihop Wireless Networks Using Channel Interference Balancing Allocation Scheme," *Sensors*, vol. 22, no. 9, pp. 3554–3571, 2022, DOI: 10.3390/s22093554.

International Conference

[5] Zhihan Cui, **Aung Thura Phyo Khun**, Yuto Lim, and Yasuo Tan, "Factor Graph-based Deep Reinforcement Learning for Path Selection Scheme in Full-duplex Wireless Multihop Networks," *International Wireless Communications and Mobile Computing (IWCMC)*, Morocco, 2023. [Accepted]

[6] **Aung Thura Phyo Khun**, Yuto Lim, and Yasuo Tan, "MAC Protocol Design and Analysis of MCST Scheme in Full-duplex Wireless Multihop Networks," *International Wireless Communications and Mobile Computing (IWCMC)*, Croatia, pp. 1394–1399, 2022, DOI: 10.1109/IWCMC55113.2022.9824398.

[7] **Aung Thura Phyo Khun**, Yuto Lim, and Yasuo Tan, "Optimal Achievable Transmission Capacity Scheme with Transmit Power Control in Full-duplex Wireless Multihop Networks," *13rd International Conference on Mobile Computing and Ubiquitous Networking (ICMU)*, Japan, pp. 1–6, 2021, DOI: 10.23919/ICMU50196.2021.9638817.

[8] **Aung Thura Phyo Khun**, Hao Wang, Yuto Lim, and Yasuo Tan, "Consensus Transmit Power Control with Optimal Search Technique for Full-duplex Wireless Multihop Networks," *26th IEEE Asia-Pacific Conference on Communications (APCC)*, Malaysia, pp. 62–67, 2021, DOI: 10.1109/APCC49754.2021.9609849.

[9] **Aung Thura Phyo Khun**, Yuto Lim, and Yasuo Tan, "Capacity of Full-duplex Wireless Networks with Mixture of Concurrent and Sequential Transmission Scheme," *23rd International Symposium on Wireless Personal Multimedia Communications (WPMC)*, Japan, pp. 1–6, 2020, DOI: 10.1109/WPMC50192.2020.9309517.

[10] **Aung Thura Phyo Khun**, Yuto Lim, and Yasuo Tan, "Study of Temporally Coupled Framed Access Scheme in Slotted ALOHA," *3rd International Conference on Advanced Information Technologies (ICAIT)*, Myanmar, pp. 1–6, 2019, DOI: 10.1109/AITC.2019.8921187.

Domestic Conference

[11] **Aung Thura Phyo Khun**, Lin Shan, Yuto Lim, and Yasuo Tan, "Study of Network Capacity for Mixture of Concurrent and Sequential Transmission Scheme over LoRa Networks," *IEICE Technical Committee on Information Networks (IN)*, vol. 122, no. 407, IN2022-95, pp. 175–180, 2023.

[12] Zhihan Cui, **Aung Thura Phyo Khun**, Yuto Lim, and Yasuo Tan, "Study of Deep Reinforcement Learning for Wireless Multihop Networks," *IEICE Technical*

Committee on Sensor Network and Mobile Intelligence (SeMI), vol. 122, no. 309, SeMI2022-113, pp. 37–42, 2023.

[13] Zhihan Cui, **Aung Thura Phyo Khun**, Yuto Lim, and Yasuo Tan, "Study of Network Capacity in Wireless Multihop Networks with Nested Lattice and Factor Graph," *IEICE Technical Committee on Information Networks (IN)*, vol. 122, no. 233, IN2022-41, pp. 53–58, 2022.

[14] Zhihan Cui, **Aung Thura Phyo Khun**, Yuto Lim, and Yasuo Tan, "Study of Network Capacity in Wireless Multihop Networks with Factor Graph," *Joint Conference on Hokuriku Chapters of Electrical and Information Societies (JHES)*, 2022.

[15] **Aung Thura Phyo Khun**, Yuto Lim, and Yasuo Tan, "MAC Protocol Design and Analysis of MCST Scheme in Full-duplex Wireless Networks," *IEICE Technical Committee on Sensor Network and Mobile Intelligence (SeMI)*, vol. 121, no. 333, SeMI2021-78, pp. 103–108, 2022.

[16] **Aung Thura Phyo Khun**, Yuto Lim, and Yasuo Tan, "Consensus Transmit Power Control with Optimal Search Technique for Full-duplex Wireless Multihop Networks," *IEICE Technical Committee on Sensor Network and Mobile Intelligence (SeMI)*, vol. 121, no. 105, SeMI2021-20, pp. 39–44, 2021.